Neotectonic and Paleoseismic Onshore-Offshore integrated study of the Carboneras Fault (Eastern Betics, SE Iberia)

Estudio integrado tierra-mar de la Neotectonica y Paleosismología de la Falla de Carboneras (Béticas Orientales, SE Península Ibérica)

Ximena Moreno Mota

RISKNAT
Departament de Geodinàmica i Geofísica
Universitat de Barcelona

Barcelona Center for Subsurface Imaging
Unidad de tecnología Marina
Consejo Superior de Investigaciones Científicas

Neotectonic and Paleoseismic Onshore-Offshore integrated study of the Carboneras Fault (Eastern Betics, SE Iberia)

Estudio integrado tierra-mar de la Neotectonica y Paleosismología de la Falla de Carboneras (Béticas Orientales, SE Península Ibérica)

Memoria presentada por

Ximena Moreno Mota

para optar al grado de Doctora en Geología

Esta memoria se ha realizado dentro del programa de Ciències de la Terra (bienio 2005-2006) de la Universitat de Barcelona bajo la dirección de las Doctoras Eulàlia Masana Closa y Eulàlia Gràcia Mont

Barcelona, Julio de 2010

Part II: The Carboneras Fault onshore

Chapter 4: Geomorphological analysis of La Serrata section

4.1. Introduction

The onshore portion of the Carboneras Fault Zone (CFZ) runs for almost 50 km with a N045º-N050º orientation (Fig. 2.3a) across the province of Almería (SE Spain). The fault zone width varies between a few hundred metres and about 2 km and is formed by overstepping and "en-echelon" fault traces. After analyzing the whole length of the emerged fault with aerial photos and field survey, La Serrata, which is located in the central part (Fig. 4.1), was identified as the area with the strongest evidence of Quaternary tectonic activity.

La Serrata is a 14 km long and 1 km wide elongated range bounded by two parallel fault traces (Weijermars, 1991; Bell et al., 1997; Silva et al., 2003). It reaches up to 360 m high and is bounded by the Níjar Basin to the NW and by small basins of the volcanic Gata Province to the SE.

La Serrata is made up of Neogene deposits (volcanic and marine-sedimentary) and remnants of the *Alpujarride* (phyllites, quartzites and dolomites) and *Malaguide* (limestones, lutites and sandstones) nappe complexes of Paleozoic and Mesozoic age (e.g. Pineda et al., 1981; Boorsma, 1992; Fernández-Soler, 1996; Vera, 2000) (Fig. 4.1 and 4.2). The volcanic deposits in La Serrata are of the calcoalcaline-type, mainly massive dacites and andesites with amphiboles and their alterations such as breccias and conglomerates. Pyroclastic deposits of the same composition are also found (Fernández-Soler, 1996). Miocene marine-sedimentary deposits are represented by Messinian regressive phases. Lower Messinian units (MI) crop out locally as marls and white calcisiltites with good stratification to the NE of La Serrata. Upper Messinian units (MII) underwent the salinity crisis depositing, in the lower part, silexites, marls, calcareous turbidites with gypsy cement and, in the upper part, selenitic gypsum with interbedded gypsy turbidites. The marine transgression of Pliocene age generates a marked erosive phase and fills the existing basins discordantly with white and yellowish bioclastic calcarenites (PI). The Upper Pliocene (PII) is marked by a new marine regression forming thick units of quartz-rich conglomerates and sandstones with balanus and ostracodes fauna (Pineda et al., 1981). The Quaternary continental regime is characterized by the infill of the sub-aerial basins with large alluvial fans and fluvial terraces despite the presence of local pediment.

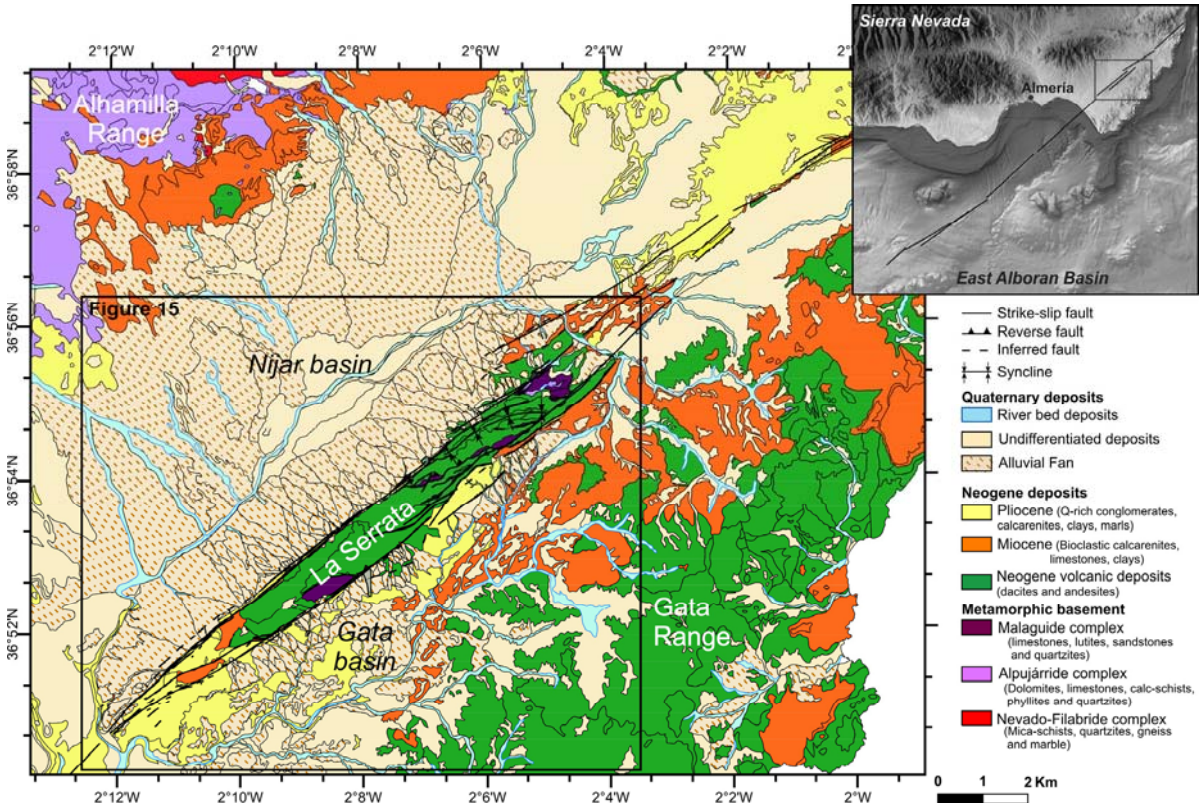

Figure 4.1. Simplified geological map of La Serrata area, central section of the emerged Carboneras Fault, modified from MAGNA 1:50.000 geological maps 1045 and 1046 (Voremans and Baena, 1977; Pineda et al., 1981). Rectangle locates Figure 4.2. Inset: Location of La Serrata in the Carboneras Fault onland and its prolongation to the Alboran Sea.

Despite being mainly a strike-slip structure, the CFZ shows evidence of vertical displacements at La Serrata. These vertical displacements are the result of compressive structures associated with strike-slip faults such as flower structures or restraining step-overs (Sylvester, 1988). The fault bounding La Serrata to the NW shows a discontinuous pressure-ridge where Pliocene rocks crop out (Fig 4.2) (Bell et al., 1997), providing evidence of an up-to-200 m wide fault zone with constant step-overs. In the field, decimetre-scale outcrops show the fractal character of this transpressive portion. The vertical component together with the presence of large Quaternary units resulting from the erosion of the uplifted areas along the fault zone indicates recent tectonic activity at La Serrata. Consequently, this constitutes a suitable area for paleoseismic studies.

Initial evidence of Quaternary tectonic activity is afforded by topographic maps and aerial photos. The most remarkable evidence consists of 1) a marked straightness of the fan-heads, 2) the aqbsence of gulfs in the apex zones (Goy and Zazo, 1983), and 3) a rectilinear mountain front with highly dipping fans and very incised valleys. Following the Mountain Front Sinuosity Index developed by Bull and McFadden (1977), Silva et

al. (1992a) considers this mountain front as type 1, which is an especially active mountain front. In detail, other evidence of tectonic activity includes, abundant outcrops of folded and faulted Quaternary deposits along gullies crossing the fault trace. On the basis of the evidence of active faulting, geomorphological, microtopographic, trenching and dating analyses were carried out with paleoseismic ends along La Serrata. Geomorphology is the key factor in investigating the long-term (Quaternary) behaviour of the fault and constitutes the first step towards selecting suitable paleoseismic sites. A geomorphological analysis of La Serrata is presented in this chapter.

4.2. Quaternary units

The record of recent faulting is preserved in the Quaternary sedimentary deposits that are formed at La Serrata by large alluvial fans and fluvial terraces (Fig. 4.2). Alluvial fans are deposited at the foot of the mountain front and four generations of fans can be distinguished. Each fan generation commonly overlies the preceding one, but when tectonic events occur, alluvial fans can be found overlying the older generations or the Neogene deposits (Fig. 4.3). Fluvial terraces are filling incisions in the alluvial fan-heads.

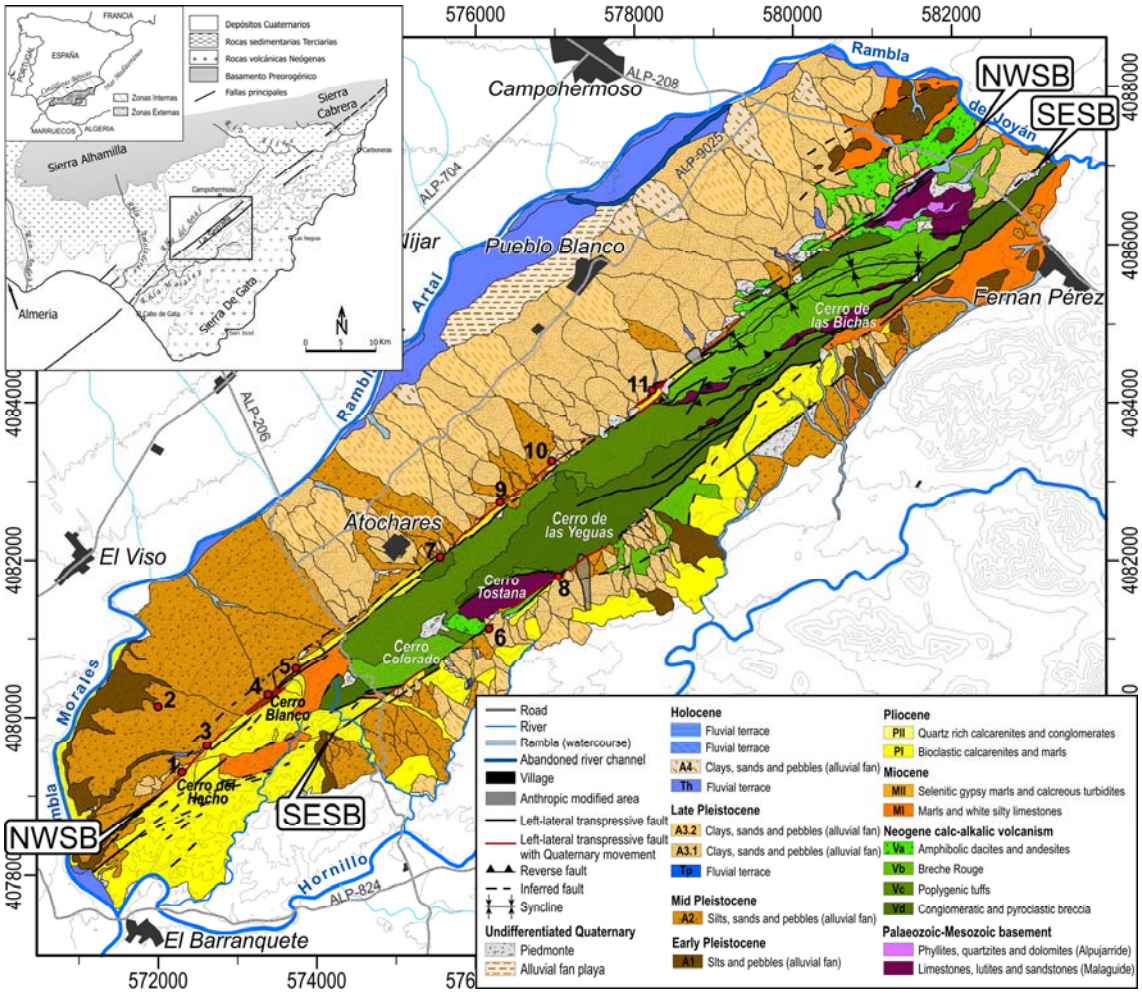

Figure 4.2. Geomorphological and geological map of La Serrata. Red points locate the geomorphological sites in this study: 1) El Hacho, 2) El Puntal, 3) El Hacho gully, 4) Big Pond, 5) Cerro Blanco, 6) Archidona Quarry, 7) Nuevo Rumbo, 8) El Hornillo, 9) Los Trances, 10) Pecho de los Cristos, 11) Cortijo del Parratero. NWSB: North West Serrata Boundary; SESB: South East Serrata Boundary.

These deposits, which are described below, are based on a) regional observations, and b) morphological and sedimentological descriptions performed at eleven sites where more detailed analyses were carried out. These sites are listed from

SW to NE (Fig. 4.2): (1) El Hacho, (2) El Puntal, (3) El Hacho Gully, (4) Big Pond, (5) Cerro Blanco, (6) Archidona Quarry, (7) Nuevo Rumbo, (8) El Hornillo, (9) Los Trances, (10) Pecho de los Cristos and (11) Cortijo el Parratero.

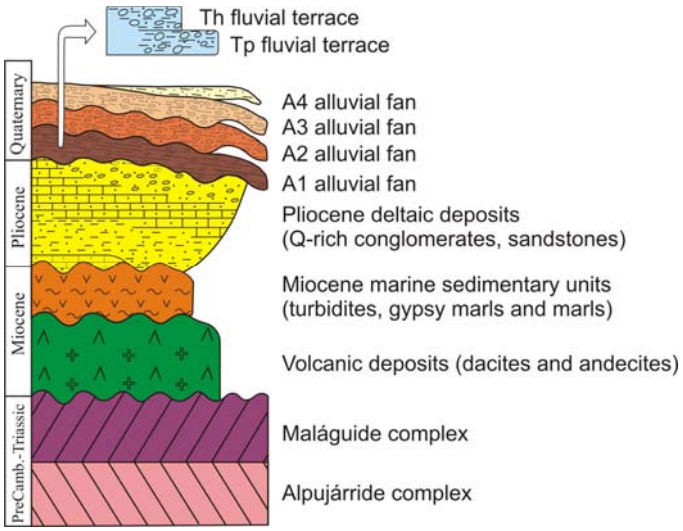

Figure 4.3. Schematic sedimentary sequence of the deposits of La Serrata and surrounding areas described in this chapter.

4.2.1. Alluvial fans

Alluvial fans predominate in the area, extending from the foot of La Serrata to the main fluvial system. On the basis of airphotography analysis and field observations, four generations of alluvial fans are distinguished according to their relative position and their geomorphological expression. From old to young the alluvial fans are named: A1, A2, A3 (subdivided locally as A3.1 and A3.2) and A4 (Fig. 4.2 and 4.3). Table 4.1 shows the correlation between these units and those proposed in previous studies.

Table 4.1: Correlation between the alluvial fan units defined in this chapter and the ones defined in previous works.

Pineda et al. (1981) (at La Serrata)	**Goy and Zazo (1983)** (at La Serrata)	**Silva et al, (1992b)** (Guadalentin depression, Murcia)	**Bell et al. (1997)** (along the Carboneras Fault)	**Harvey et al. (1999)** (at the Cabo de Gata ranges)	**This study (2011)** (at La Serrata)
Unit 79 (Holocene)	9th generation (Holocene)		Qfy (Late Holocene)	Qf5 (Holocene)	**A4**
Units 64 (Late Pleistocene)	6th generation (Late Pleistocene)	3rd depositional phase (Late Pleistocene)	Qf (Late Pleistocene, 35-100 ka)	Qf3 (ca. 85-10 ka) (Würm)	**A3.1**
Unit 70 and 75 (Late Pleistocene)	7th and 8th generation (Late Pleistocene)				**A3.2**
Units 55 and 59 (Mid Pleistocene)	4th and 5th generation (Mid Pleistocene)	2nd depositional phase (Mid Pleistocene)	Qfo (>100 ka)	Qf1 (> ca. 135 ka)(Riss and earlier age)	**A2**
Units 49 and 53 (Early Pleistocene)	1st, 2nd and 3rd generation (Plio-Pleistocene to Early Pleistocene)	1st depositional phase (Early Pleistocene)		Thin pediments forming alluvial fan-like accumulations	**A1**

Harvey's (1990) classification of alluvial fans was used to genetically interpret the alluvial fan units. Four main depositional processes are considered: debris flows, sheet-floods, stream-floods and hyperconcentrated flows (Harvey, 1984a). And the different texture and facies observed in the sediment are interpreted as products of different depositional processes. For instance: 1) matrix supported gravels are interpreted to be deposited as debris-flow, 2) clast-supported, structureless gravels as sheet-flood deposits, transitional debris-flow or hyperconcentrated flow deposits, 3) silt sheets as low energy distal sheet-flood deposits, and 4) stratified, locally cross-bedded, locally imbricate gravels as stream-flood deposits. Moreover, proximal-to-distal facies variations can be distinguished in alluvial fans, including down-fan diminution of clast size, but also a change in the relative importance of depositional environments, debris-flow being more common proximally and silt sheets distally (Harvey, 1990).

A1 alluvial fans

The morphology of the A1 alluvial fans is usually not very well preserved. A1 alluvial fans crop out locally in the SESB, whereas along the northern part of the Northwestern Serrata Boundary (NWSB) they crop out only in some topographic highs (Fig. 4.2). In the central and southern parts of the NWSB, A1 fans are largely overlain by younger deposits and only crop out at the bottom of channels because of the erosion of the upper units, especially close to the mountain front. On closer inspection, A1 alluvial fans overlie the Neogene basement.

Close to the range, the A1 alluvial fans show stratified and imbricated large pebbles and locally cross bedding, which indicate a stream-flood mode of deposition. Distally, clays and sands with interbedded thin channel-shaped layers of well rounded pebbles suggest intercalation of stream-flood and sheet-flood processes. Overlying A1 fans are soil textures very similar to the well developed *Red Mediterranean soil* (*Rhodoxeralfs*), which Schulte & Julià, (2001) identify in alluvial fans from the Vera Basin (located tens of kilometres to the north of the Carboneras fault) with leaching, rubefaction, clay formation and illuviation processes. The strongly calcified layers (~10 cm) interbedded within the A1 fans could have been caused by leaching and illuviation. Thick massive calcretes, some of them thicker than 1m, commonly cover the A1 alluvial fans in the proximal zones.

A2 alluvial fans

In the NWSB, large A2 alluvial fans, overlying A1 fans, extend from the foot of the range to the Rambla del Artal River (Fig. 4.2), except to the north where they are not observed. A2 fans are especially well preserved and roughly maintain their original shape in the southern part, where large younger deposits are absent. Farther north, this generation of fans is covered by younger alluvial fans but crops out along channels and

between younger units. Along the northwestern side of the range, A2 apexes are absent, resulting in a linear contact between A2 deposits and the mountain front. In the SESB, A2 alluvial fans are less extensive but still preserve their original morphology owing to the scarcity of younger units. There, they overlie either the A1 units or the Neogene basement.

In a proximal position these fans are composed of matrix supported sediments with poorly sorted coarse gravels of different lithologies, indicating debris-flow style deposition. Distally, the sediments are mostly clast-supported, they are well sorted and show imbricated fabrics indicating deposition by sheet and channel bodies (fluvial process). These alluvial fans are overlain by a soil that presents characteristics similar to those of the *Reddish Mediterranean soil* (Haploxeralfs), which Schulte & Julià (2001) identify in the fluvial terraces of the Vera Basin. Mature calcrete crust, up to 50 cm are developed from proximal to distal parts. Calcrete crusts can also be observed in intermediate levels, suggesting multiple incision and aggradation phases with short stabilization intervals.

A3 alluvial fans

This generation of alluvial fans shows well preserved morphologies. In contrast to older alluvial fans, A3 fan units are characterized by weak developed soil on top with thin (less than few millimetres) or absent calcrete crust.

Two subunits of A3 were defined, from bottom to top: A3.1 and A3.2. Stratigraphically, A3.1 fans are lower and they are usually larger, although small A3.1 fans are also observed when they are produced by small drainage areas. However, the main feature that differentiates these subunits is the apexes. Those of the A3.1 are located at the foot of the range whereas A3.2 apexes are located midway between the foot of the range and the Rambla del Artal. Internal structures, which were only observed in the proximal parts of A3.1 fans, show poorly sorted coarse gravels within a sandy-clay matrix or chaotic random pebbles in a fine matrix, indicating a debris-flow deposition.

A4 alluvial fans

A4 alluvial fans are thin, well-shaped and their apexes are located distally from La Serrata. Only four individual fans of this generation are observed in the NWSB, and none in the SESB. The A4 alluvial fans are dominantly loose fluvial sands and fine gravels, and no calcic soils are formed on top (Goy and Zazo, 1983; Harvey et al., 1999).

4.2.2. Fluvial terraces and paleo-channel at La Serrata

Up to 10 generations of Quaternary fluvial terraces have been described by other authors in the region (Schulte, 2002a; Santisteban and Schulte, 2007; Maher et al., 2007). These fluvial terraces were not observed along the Carboneras fault trace and no direct relationship was established between them and the local and small fluvial terraces along the channels draining La Serrata. These small fluvial terraces were grouped into two generations, in accordance with the stratigraphy, from old to young: Tp and Th (Fig-4.2). These terraces were used to define the most recent evolution of the fault.

Tp fluvial terrace

Tp fluvial terraces contain up to 4 metre high deposits that fill channels eroded in the A2 alluvial fans. Variation in the size of the pebbles is observed in these sediments, which is probably attributed to their distance from the range. Tp fluvial terraces were observed always deposited on top of the A2 alluvial fans (i.e. they are younger than A2 deposits). As well, at Los Trances site, they were observed stratigraphically below the A3 fans and at El Hacho Gully site they were observed stratigraphically below the th fluvial terrace (i.e. they are older than A3 and Th deposits).

At Los Trances, Tp is observed close to the range. Tp is made up of very well stratified channel-shaped lenses of alternating sands that are clast-supported and by very well sorted gravels containing volcanic clasts. The base of this deposit is dominated by large 10-15 cm clasts. At El Hacho gully outcrop, Tp is observed in a more distal position from the range and is composed of alternating continuous fine silts and clay layers and sandy to gravely layers. Abundant very fine snail shells are observed in selected layers.

Th fluvial terrace

Th fluvial terraces are observed along the northwestern edge of La Serrata and were analyzed at the El Hacho, Cerro Blanco and Pecho de los Cristos sites. These deposits fill incised channels in the proximal part of the alluvial fans and preserved the terrace morphology. They commonly cover some square metres and are up to 1,5 m thick. Their internal structure is made up of well stratified gravels, sands and clays with abundant charcoal fragments and snail shells. Calcic soils are absent.

Paleo-channel at El Hacho

3D-trenching for paleoseismological purposes performed at El Hacho (Moreno et al., 2008) revealed the presence of a buried, very young paleo-channel that was offset by the fault. Despite being a very local feature it is described here because it provides evidence of the most recent tectonic activity. The paleo-channel, incised on top of an

A3.1 alluvial fan, is 1-4 m wide and up to 80 cm deep and is made up of organic-rich dark brown sands with sub-angular gravels. No stratigraphical relationship with the fluvial terraces was established because these two features were not observed in contact. However, radiometric dating (see section 4.3) suggests that the age of this paleo-channel is close to that of Th.

4.3. Dating the geomorphological units

All paleoseismological studies demand a precise dating of the geological units to constrain the timing of the deformation. Quaternary stratigraphic sequences were obtained from mapping and field observations, and an approximate age of the main units was obtained from calcrete crusts and soil development in line with other studies in the area. Finally, a more accurate radiometric dating approach of specific layers was carried out for paleoseismological purposes.

4.3.1. Geological constraints on the ages

The evolution of alluvial fans and river terraces in southeastern Iberian Peninsula has been the subject of numerous studies (e.g. Goy and Zazo, 1983; Harvey, 1990; Silva et al., 1992b; Schulte, 2002b; Harvey, 2002; Santisteban and Schulte, 2007; Maher and Harvey, 2008). Thus, in line with other authors, major development (aggradation) of alluvial fans occurs during dry Quaternary glacial stages, when vegetation cover is low, precipitation is heavy and soils are easily erodable. By contrast, stable or degradational phases of alluvial fans occur during warm interglacial phases. In periods of stabilization, soils are well developed and calcrete crusts are formed. Late degradational phases lead to fan dissection through cut and fill episodes, producing inset terraces within fan-head trenches (Harvey, 1990). Given this hypothesis, aggradation of A1, A2 and A3 alluvial fans corresponds to Quaternary dry glacial stages. Stable soil development on A1, A2 and A3 and the consequent formation of calcrete crusts below the surface, occurred during the early stages of stable phases (interglacials). The degradation of the alluvial deposits took place in the final stages of the interglacial periods with the resulting erosion of the upper layers of these deposits. This process left the calcrete crust directly on surface. Moreover, at the end of this degradational phase, small terraces (Tp and Th) were deposited, filling the gullies incised in the fan-head. Thereafter, at the onset of the new glacial stage, the following generation of alluvial fans was deposited directly on top of the calcrete crust of the previous generation.

The evolution of soil profiles reflect, among other variables, the exposure time. Schulte (2002a) defines a Quaternary paleosols chronosequence for the Vera and Sorbas basins (tens of kilometres to the north of the study area) and correlates the soil evolution with the age of the fluvial terraces, alluvial fans and glacis over which the soils were developed. According to this author, *Rhodoxeralfs* (Red Mediterranean soils) correspond to climatic fluctuations (high temperature and rainfall) of the Early Pleistocene. The absence of this type of soils in younger deposits suggests a climate change towards drier and colder conditions that occurred after the Mid Pleistocene. More recent *Haploxeralf* soils (reddish Mediterranean soils) were formed during the relatively humid MIS 5 period, and very weakly developed soils (e.g. *Haploxerolls*)

were formed after MIS 3 stage. At La Serrata, *Rhodoxeralfs* soils overlie the A1 alluvial fan generation, *Haploxeralfs* overlie the A2 fans and, current soils (*Haploxerolls*-like) are found on top of A3 and A4 alluvial fans. Following the classification of Schulte (2002a), A1 could have formed during the Early Pleistocene, A2 during the Mid Pleistocene and A3 and A4 during the Late Pleistocene-Holocene. This is consistent with the ages proposed in earlier studies (Table 4.1).

Alluvial fans of the area show rich calcic soils (caliches in an evolved stage). Some authors have proposed a chronology based on their level of development. Works by Dumas (1969), Harvey (1984b) and later Silva et al. (1992b) distinguish three degrees of development in Quaternary calcrete crusts in southeastern Spain and relate them to the time necessary for their formation. Accordingly, the ages of the soils may be summarized as follows: 1) weak calcrete crusts date back to the last glacial stage (MIS 4-2), 2) mature calcretes about 1 m thick to the penultimate or previous mid Pleistocene glacial stages (MIS 10-6), and 3) ancient calcrete crusts more than 1 metre thick date back to the Early Quaternary. These stages of evolution of calcrete crusts were observed At La Serrata and can thus be used to estimate the ages of the sedimentary bodies. The thick (>1m) calcrete crust overlying A1 suggests an Early Quaternary age for these deposits; the 0.2-1m thick calcrete crust overlying the A2 fans indicates a Mid Pleistocene (penultimate? glacial stage) age; and the weak to absent calcrete crust overlying the A3 fans suggests a Late Pleistocene (late glacial stage) age. These ages are consistent with those attributed to the alluvial fans based on the development of soils (Schulte and Julià, 2001; Schulte, 2002a).

4.3.2. Radiometric dating

Radiogenic dating of the defined geomorphological units were performed mainly by sampling along trench walls and also on road-sides and quarry outcrops. Figure 4.4 shows the position of these samples. The following section provides the main results and the limitations intrinsic to each dating method as well as the reasons for disregarding some dates.

4.3.2.1. U-series disequilibrium dating (U/Th)

4.3.2.1.a. Considerations concerning dating calcrete crusts

Calcic laminated soils (caliche or calcrete crusts) development can be a complex polygenetic process of calcium carbonate mobilization and deposition after the formation of the sedimentary body. Uranium series disequilibrium method was performed on laminar calcic soils at La Serrata in order to 1) constrain the age of the alluvial fan acting as a substratum and 2) constrain the age of the paleo-events

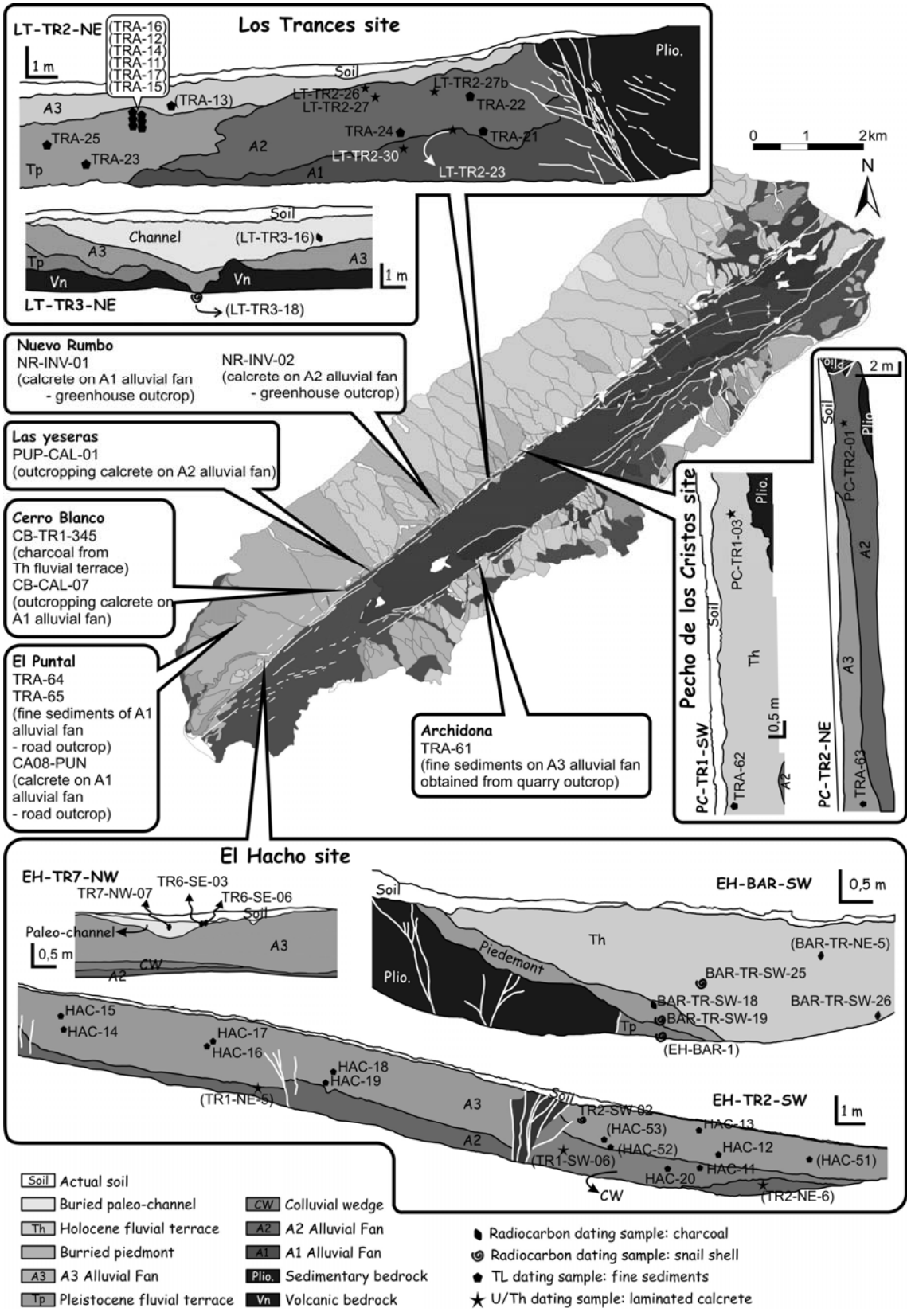

Figure 4.4. Location of radiometric dating samples and sites. Main trench walls show the relative stratigraphic position of the samples. Individual samples are listed by sites. For unit names of the La Serrata map, see figure 4.2.

evidenced by the faulting of these deposits. To obtain satisfactory results, the dating information must be used correctly.

The U/Th method provides the age of the calcification process after the development of the alluvial fans but does not yield a direct age of the substratum itself. Thus, when assigning the age of the deposit, the age of the calcrete crust must be considered as a minimum age. When assigning the time constraint of a seismic event, the age of a faulted calcrete crust must be considered as pre-dating the age of the seismic event regardless of the age of the fan substratum.

Calcrete crusts are initially formed on top of alluvial fans during the stabilization phase dominated by soil development (Alonso-Zarza et al., 1998) following the alluvial fan aggradational phase. After the first hard layer forms, successive calcrete development phases may take place, and multiple phases of soil formation, erosion and reworking occur (Alonso-Zarza et al., 1998). Given that the formation of calcrete crust in arid areas is not a continuous process and given that it begins to develop during stabilization phases, two types of calcrete crust are differentiated: primary and secondary. On a given alluvial fan generation, primary crusts are monogenic layers (although they are understood to be formed during a certain period of time) formed in the stabilization phase of this unit (following the aggradational phase). Secondary crusts are formed by calcic re-growth on top of the primary crust during further aggradation and stabilization phases of younger sedimentary units, resulting in a polygenic calcrete crust. Thus, if the primary calcrete crust is not overlain by younger sediments, no secondary calcrete will be formed.

At La Serrata, primary and secondary calcretes were distinguished in crusted alluvial units (A1 and A2) on the basis of stratigraphic observations and U/Th dating results. When the A2 crust is not overlain by the A3 fan, dating of the calcrete returns much older ages than those expected for the A3 fans by other dating techniques. When the A2 crust is overlain by the A3 fan the dating of the calcrete returns ages that are consistent with the expected A3 age, which is a much younger age than that expected for the A2 alluvial fan. When an A2 crust is not overlain by an A3 fan, the calcrete crust on top of A2 is considered to be primary or monogenic. When an A2 crust is overlain by and A3 fan, the calcrete crust is regarded as secondary. When dating a secondary calcrete, a mixing of primary and secondary crusts must be considered as they are not be visually distinguishable. If this mixing occurs, then intermediate ages will be obtained. Nevertheless, given that the sampling method adopted dismisses the laminated layer boundaries to avoid clastic elements, secondary calcrete dating results are most probably giving the age of subsequent calcic re-growth.

4.3.2.1.b. Dating the calcrete crusts at La Serrata

A total of 16 calcrete crust samples were dated with U/Th at La Serrata Table 4.2. Nominal dates were calculated using the daughter/parent ratio ($^{230}Th/^{234}U$) and assuming that all the ^{230}Th was formed by *in situ* decay of the ^{234}U. Nevertheless, the isotopic results provide evidence of some contamination of ^{232}Th during calcrete formation, leading to an overestimation of the sample age. Only two samples (LT-TR2-30 and NR-INV-01) have relatively acceptable 230Th/232Th ratio (230Th/232Th ratio >10) (Díaz-Hernández and Juliá, 2006). In order to bypass the detrital contamination effect, the isochron technique (Bischoff and Fitzpatrick, 1991) was applied (see section 3.2.3.2 for further details), and therefore, each sample analysis was, at least, triplicated. Samples from El Hacho (labelled TR-X) had enough weight to calculate separately each isochrone age (Table 4.2), but the sample weight was insufficient at the other sites. When the weight of a sample was not enough for the isochrone, groups of different samples with geological and numerical coherence were analyzed together in order to apply the isochron technique and obtain one age for each group of samples. Two groups of samples were determined (Table 4.2): the first group (LT-TR2-26 + LT-TR2-27 + LT-TR2-27b) is formed by apparently A2 secondary calcrete crusts, and the second group (LT-TR2-23b + LT-TR2-30 + CB-CAL-7 + NR-INV-01) is formed by apparently secondary A1 calcrete crusts. The resulting isochrone age obtained for each group will be used for further discussion. Nominal dates of samples NR-IN-02 and PC-TR2-01 are not corrected and thus will not be helpful for further analysis.

Moreover, at the El Hacho trenches, the thickness of the EH-TR2-06 calcrete sample allowed us to separate the lower (Inf.), middle (Med.) and upper (Sup.) sections (Table 4.2) and date them separately. Results are of the same age within the error bar. In sample EH-TR1-05, the lower (Inf.) and upper (Sup.) sections were also separated. The age of the upper part is slightly younger than the age of the lower part, suggesting a close-in-time re-growth of the calcrete crust.

4.3.2.2. Luminiscence dating

TL dating technique determines the time elapsed since a landform was last exposed to sunlight during transport (Quaternary-TL-Surveys, Web Page 2010). Two problems were encountered using TL dating of samples at La Serrata. The first problem concerns the possibility of too little exposure to sunlight before deposition. In such a case, it is possible that the sample has not been completely bleached, which results in an overestimation of the sedimentary age. For this reason, most of the 30 samples collected were selected when showing classification in the silty to gravel contents, suggesting surface water transport on the top of the alluvial fans. The second problem concerns the variations in calcite content within the sedimentary units and the time needed to form carbonatic cements. It is normally assumed that calcic cements are formed at an early

Table 4.2: U/Th dating results near La Serrata. Disregarded samples are in grey (see text for discussion).

Sample name	Lab code	Unit	U-238 (ppm)	Th-232 (ppm)	$^{234}U/^{238}U$	$^{230}Th/^{232}Th$	$^{234}U/^{232}Th$	$^{238}U/^{232}Th$	$^{230}Th/^{234}U$	Nominal Date (years BP)	Isochrone age (years BP)
TR1-NE-05-Sup.	1506	A2	1.09	0.81	1.11	2.024	4.634	4.169	0.1993	61,592 +/-1734	24053 +2732/-2667
TR1-NE-05-Inf.	2006	A2	1.28	0.36	1.09	4.621	12.056	11.043	0.3056	52,061 +/-1511	39384 +4854/-4651
TR2-NE-06-Sup.	1906	A2	1.03	0.61	1.09	2.882	5.709	5.22	0.3538	73,354 +/-2320	47099 +6054/-5743
TR2-NE-06-Med	1606	A2	1.03	0.55	1.09	3.231	6.363	5.823	0.3782	75,957 +/-2800	51217 +6736/-6352
TR2-NE-06-Inf.	1706	A2	0.91	0.79	1.14	2.324	4.066	3.57	0.3631	89,934 +/-3300	48650 +6308/-5969
LT-TR2-27b	2508	A2	1	0.47	1.27	6.216	8.359	6.596	0.74	137238 +6848/-6474	
LT-TR2-27	3308	A2	0.67	0.39	1.31	6.01	7.059	5.393	0.85	180396 +11216/-10263	80482 +29780/-23835
LT-TR2-26	2108	A2	0.53	0.37	1.22	4.642	5.357	4.408	0.87	194188 +16045/-14125	
LT-TR2-23	2008	A1	1.55	0.57	1.36	9.437	11.558	8.491	0.82	162304 +12769/-11557	
LT-TR2-30	2408	A1	1.29	0.22	1.42	18.91	25.539	17.992	0.74	132739 +6166/-5870	117740 +7621/-7167
CB-CAL-7	2308	A1	1.05	0.97	1.33	4.335	4.49	3.378	0.97	253756 +27248/-22311	
NR-INV-01	3908	A1	0.58	0.13	1.11	11.244	15.244	13.775	0.74	140270 +14202/-12617	
NR-INV-02	3708	A2	0.73	0.88	1.12	1.214	2.897	2.594	0.42	58268 +2219/-2176	-
PC-TR2-01	2208	A2	0.76	0.98	1.11	1.329	2.706	2.429	0.49	72285 +3123/-3039	-
CA08-PUN	3808	A2	0.13	0.16	1.27	4.052	3.191	2.511	1.27	>350000	-
PUP-CAL-01	3208	Plio.	0.18	0.49	1.24	1.571	1.422	1.15	1.1	>350000	-

stage in the history of the sediment, remaining at a constant level until the present. But in this area, circulation of calcite-rich underground waters during wet periods produces calcification of sediments long after deposition, which is demonstrated by the presence of secondary calcrete crusts. The new carbonate increases the total mass of the sediment and as a result the capacity of absorbing radiation. Therefore, the introduction of new carbonate into the system would produce a decrease in the dose-rate radiation, altering the luminescence signal. In such a case, the signal would be independent from the time elapsed since the sediment was exposed to sunlight, which would lead to an underestimation of the age of the sediment. Consequently, calcite-rich sediments were avoided, and the samples analysed were consistent with the rest of the data. These limitations of the method highlight the importance of elucidating the processes during and after deposition.

Interestingly, all the samples showing uncertainties in calcite content variations also present uncertainties in sunlight exposure before deposition. Problematic samples HAC-11, HAC-20, TRA-64 and TRA-65, TRA-13, TRA-21 and TRA-62 are discussed below (see table 4.3 for TL results) and are not considered for estimating the age of the deposit.

Samples HAC-11 and HAC-20 were collected from a buried and strongly calcified deposit exposed on a trench wall at the El Hacho site (Fig. 4.4). Since this deposit was interpreted to be a colluvial wedge, the TL results were disregarded because of the uncertainty of sunlight exposure (colluvial wedges can be formed rapidly) and probable calcite variation long after deposition (water circulation close to the fault zone).

Samples TRA-64 and TRA-65 were acquired from an A1 alluvial fan (Fig. 4.4). Although an Early Pleistocene age was expected for this unit, the TL dating was carried out to assign an old age to this unit before applying the ^{10}Be dating technique. Indeed, the TL dating results show ages beyond the limit of the method (150 ka). Moreover, this alluvial fan was thought to have undergone marked calcite variations, (most probably long after deposition), desregarding a consistent TL age.

Sample TRA-13 was acquired from a strongly calcified A3 deposit. This sample was dated as a test although the calcification was strong enough to alter the original internal texture and remove any possible evidence of sunlight exposure. Thereafter, the laboratory analyses of sample TRA-13 (Fig. 4.4) presented a remarkable diversity of the TL properties, causing large error bars and ruling out a consistent result.

Samples TRA21 were acquired from an A2 alluvial fan exposed in a trench wall (Fig. 4.4). The resulting TL age (89-133 ka BP) is younger than the upper TL results for the same unit. This was interpreted to be a result of the calcification related to the high energy water circulation evidenced by huge cobbles forming a large paleo-channel in

the lower part of the unit (and therefore lending support to the hypothesis of sun bleaching).

Sample TRA-62 was collected from a Th fluvial terrace (Fig. 4.4). TL age (10,2-7,8 ka BP) is considerably older than radiocarbon ages (720-560 yr BP). Although this fluvial terrace is similar to other Late Holocene fluvial terraces analysed along the range, the TL sample showed evidence of sunlight transport but not of calcification. Both dates are possible and thus this deposit can be only attributed to Holocene age.

Table 4.3:Thermoluminiscence (TL) dating results. Disregarded samples are in grey (see text for discussion).

Site	Sample name	Trench outcrop	Unit	TL age (ka BP)
Archidona	TRA-61	Quarry outcrop	A3	52.7 +7.1 / -5.7
El Hacho	HAC-11	EH-TR2	CW	55.4 +7.6 / -6.1
El Hacho	HAC-12	EH-TR2	A3.1	50.8 +6.2 / -5.0
El Hacho	HAC-13	EH-TR2	A3.1	29.2 +2.9 / -2.6
El Hacho	HAC-14	EH-TR2	A3.1	62.0 +9.6 / -7.4
El Hacho	HAC-15	EH-TR2	A3.1	29.3 +2.5 / -2.2
El Hacho	HAC-16	EH-TR2	A3.1	37.7 +3.8 / -3.3
El Hacho	HAC-17	EH-TR2	A3.1	28.7 +2.1 / -1.8
El Hacho	HAC-18	EH-TR2	A3.1	56.1 +7.0 / -5.6
El Hacho	HAC-19	EH-TR2	A3.1	53.5 +6.7 / -5.4
El Hacho	HAC-20	EH-TR2	CW	75.9 +12.5 / -9.1
El Hacho	HAC-51	EH-TR1	A3.1	44.9 +5.7/-4.8
El Hacho	HAC-52	EH-TR1	A3.1	55.5 +7.0/-5.6
El Hacho	HAC-53	EH-TR1	A3.1	52.9 +6.2/-5.0
El Puntal	TRA-64	Road-side outcrop	A1	> 150
El Puntal	TRA-65	Road-side outcrop	A1	> 150
Los Trances	TRA-11	LT-TR1	Tp	87.9 +22.4 / -14.8
Los Trances	TRA-12	LT-TR1	Tp	83.3 +21.0 / -14.2
Los Trances	TRA-13	LT-TR1	A3	83,3 +26.9 / -17.5
Los Trances	TRA-14	LT-TR1	Tp	70.2 +14.4 / -10.5
Los Trances	TRA-15	LT-TR1	Tp	69.8 +13.2 / - 9.8
Los Trances	TRA-16	LT-TR1	Tp	79.4 +16.6 / -11.7
Los Trances	TRA-17	LT-TR1	Tp	73.1 +19.4 / -13.6
Los Trances	TRA-21	LT-TR2	A2	106 +27 / -17
Los Trances	TRA-22	LT-TR2	A2	> 132
Los Trances	TRA-23	LT-TR2	Tp	87.7 +22.1 / -14.7
Los Trances	TRA-24	LT-TR2	A2	> 122
Los Trances	TRA-25	LT-TR2	Tp	89.3 +22.2 / -14.7
Pecho de los Cristos	TRA-62	PC-TR1	Th	9.02 +/-1.15
Pecho de los Cristos	TRA-63	PC-TR2	A3.1	41.6 +5.5 / -4.7

4.3.2.3. ^{14}C dating

Radiocarbon (^{14}C) dating was used in charcoal and snail shells (Table 4.4). Discrepancies were noted between young (Holocene) samples of shells and charcoal collected from the same stratigraphic layers at the same site (Fig. 4.4). This is probably due to the ingestion of old carbon from surrounding calcareous rock formation into the snail shells (Tamers, 1970), which is common at La Serrata. This results in ^{14}C deficiency carbon incorporation and leads to an overestimation of the age of the snail

shells up to 3000 years (Pigati et al., 2004). Moreover, if the sample corresponds to an old (>30 ka) snail shell, its age can be easily underestimated when the humic components of the surrounding soils (that can be much younger) have not been completely removed (Pigati et al., 2005).

Therefore, charcoal samples were considered as more reliable and snail shell radiocarbon dates were only used as a rough approximation in the absence of more reliable material.

Table 4.4: ^{14}C dating results

Sample	Sample type	Unit	Lab	$^{13}C/^{12}C$ (‰)	Conventional ^{14}C Age (yr BP)	2 σ Calibration (Cal yr BP)	2 σ Calibration (AD)
CB-TR1-345	Charcoal	Th	Beta Analytic	-23.5	1460 +/- 40	1420 - 1300	540 - 650
BAR-TR1-25	Sneil shell	Th	NOSAMS	-6,95	2030 +/- 35	1896-2109	-
EH-TR2-02	Sneil shell	A3.1	NOSAMS	-5,7	37200 +/- 1900*	40590 - 43974	-
BAR-TR1-26	Charcoal	Th	NOSAMS	-24,39	1220 + / -35	1061 - 1262	688 - 889
BAR-TR1-05	Charcoal	Th	NOSAMS	-22,73	905 +/- 30	742 - 911	1039 - 1208
EH-TR6-3	Charcoal	Paleoch.	NOSAMS	-22,56	1190 +/- 25	1013 - 1178	772 - 937
EH-TR6-6	Charcoal	Paleoch.	NOSAMS	-25,96	1130 +/- 70	926 - 1241	709 - 1024
EH-TR7-7	Vegetal	Paleoch.	NOSAMS	-25,07	1220 +/- 110	929 - 1313	637 - 1021
EH-BAR-1	Sneil shell	Tp	Beta Analytic	-6,1	44230 +/- 1140*	Out of range for calibration	
LT-TR3-18	Sneil shell	A3.1	Beta Analytic	-7,6	37240 +/- 520*	41861 - 42821	-
PC-TR1-03	Charcoal	Th	Beta Analytic	-22	660 +/- 50	720 - 560	1230 - 1390

4.3.2.4. ^{10}Be dating

When dating with cosmogenic isotopes, exposure ages and erosion rates of surfaces are calculated assuming no variation of the density of the material through time. However, in landforms made up of cemented sediments, models that do not consider the increase in density due to diagenetic processes are expected to significantly overestimate landform ages (Rodés et al., 2011).

The ^{10}Be technique was applied to date the top of a strongly cemented A1 alluvial fan located at El Puntal (Fig. 4.4). In this case, strong calcification (postdepositional process) of the alluvial fan surface may produce important density variations leading to significant inaccuracies. For this reason, Rodès et al. (2011) developed a model that considers not only uncertainties of bulk density measurements but also a linear density evolution through time. The model considers a mean bulk density of 2.0±0.3 g cm^{-3} at the time of formation and measures current bulk densities of 2.2±0.3 and 2.1±0.3 g cm^{-3} in each profile. Once the ^{10}Be inheritance is constrained by indirect estimation of erosion rates in the source area, ^{10}Be data modelling indicates that the El Puntal alluvial fan has an age ranging from 214 ka to *ca.* 1 Ma within 1 **σ** confidence level.

4.3.3. Discussion: Precise age of the Quaternary units at La Serrata

Each dating method has different implications for the age of the sedimentary units. In the study area, TL dates represent the time when the alluvial fan or fluvial terrace was deposited whereas ^{10}Be dates can help to assign a date to the exposure of the fan surface. ^{14}C estimates the time elapsed since the death of the organism (snail or vegetal) and U/Th ages represent the minimum estimate for the calcification. In this study, more than one dating method was used in the same unit to compare, corroborate or reject dating results, taking into account the geological context and significance of each sample.

Unit A1:

Unit A1 was sampled at El Puntal, for TL (alluvial fan sediments) and for U/Th (primary calcrete crusts) (Fig. 4.4) but both methods have their time limits (150 ka and 350 ka, respectively) over the age of A1 deposits (Tables 4.2 and 4.3). However, ^{10}Be cosmogenic isotope dating analyses were successful and provide an age ranging from 214 ka to *ca.* 1 Ma within 1 σ confidence level (Rodés et al., 2011). This large uncertainty in the age estimate can be partially reduced by the geological constrains according to calcrete and soil development (Dumas, 1969; Schulte and Julià, 2001), which suggests that soils and calcrete crusts formed on top of A1alluvial fans are of Early Quaternary age. This suggests that this alluvial fan may have formed during the final stages of the Early Quaternary period, although further analyses would be required for a better constraining.

Unit A2:

Calcrete crusts on top of A2 deposits were dated with U/Th dating at El Hacho and Los Trances (Fig. 4.4), and their isochrone age was calculated (Table 4.2). Fine sediments were sampled for TL in the trench walls at Los Trances site (Fig. 4.4 and Table 4.3). TL samples TRA-22 and TRA-24 are saturated and therefore exceed the lower range of the method. Nevertheless, they suggest an age older than 120 ka, probably during MIS 6 (penultimate glacial period) (Fig. 4.5). At Los Trances, the isochrone age has a large error range but according to the fan unit/climatic stages correlation, it is thought to be a primary calcrete formed in the last interglacial (MIS 5), during the stabilization period of the A2 alluvial fan. At El Hacho, where younger deposits covered the crust (Fig. 4.4), isochrone ages are slightly younger (last glacial, MIS4-2) (Table 4.2) and therefore are considered to be secondary calcretes (coinciding with the age of the upper A3 unit) (Fig. 4.5).

Although no numerical dates precisely constrain the age of the alluvial unit, a MIS 6 age is assigned to the aggradation period and a MIS 5 age to the stabilization phase (Fig. 4.5). This is consistent with the estimated age of non-calcic soils (Schulte

and Julià, 2001), which suggests a Mid Pleistocene age for soils formed on A2 deposits. However, the formation of mature calcrete crusts is assumed to have initiated in the Mid Pleistocene. Moreover, U/Th analyses of primary crust on top of A2 yields Late Pleistocene ages, ten to hundred thousand years before the expected age.

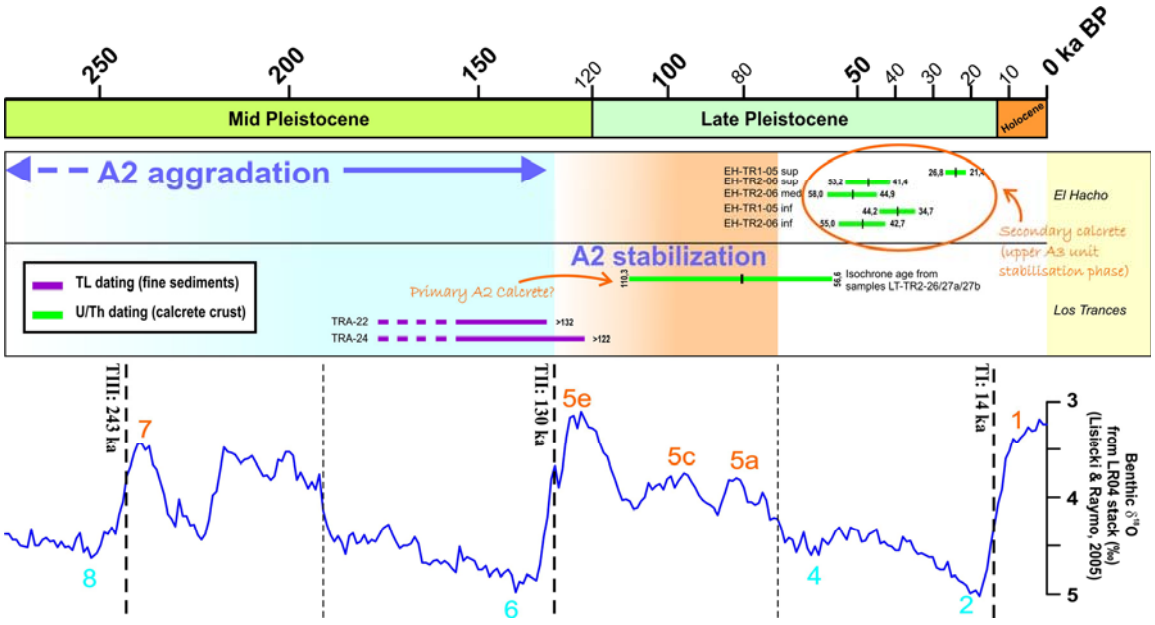

Figure 4.5. TL and U/Th ages from A2 top calcrete crust and A2 alluvial fan fine sediments, respectively. Separated by sites, in stratigraphic order.

Unit A3:

Only the A3.1 alluvial fan sub-generation was dated. TL was applied to silt, sand and fine gravels from trenches (El Hacho, Los Trances and Pecho de los Cristos) and quarry walls (Archidona Quarry) whereas snail shells from trench walls (El Hacho and Los Trances) and natural outcrops (El Hacho gully) were used for radiocarbon dating (Fig. 4.4).

All TL and ^{14}C dates are stratigraphically consistent (Fig. 4.6) and constrains the ages of the alluvial unit to the Late Pleistocene, which is in agreement with soil and calcrete crust development age estimates (Dumas, 1969; Harvey, 1990). This suggests that the A3.1 alluvial unit aggradation occurred during the MIS4-2 cold stage and the stabilization period during the current MIS-1 stage.

Unit A4:

No radiometric analysis was applied to A4 alluvial fans because of the absence of paleoseismic interest as they are located at a considerable distance from the fault in the centre of the Nijar basin. On the basis of references, A4 fans are estimated to be Holocene in age (Pineda et al., 1981). However, this age estimation does not match the

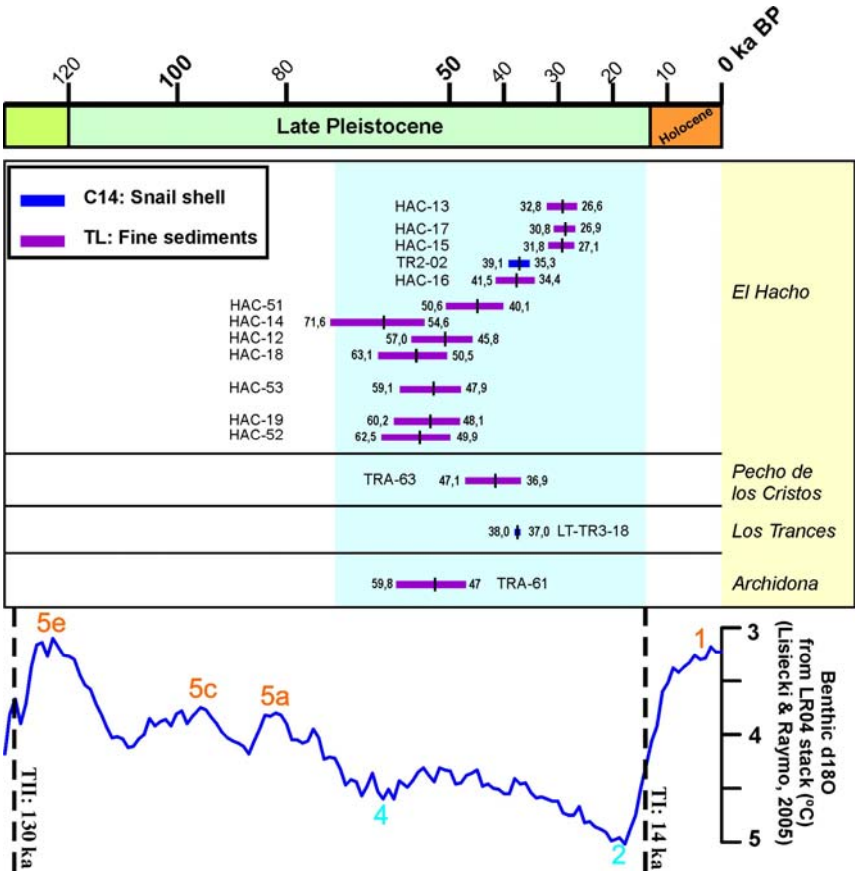

Figure 4.6. TL and ^{14}C ages from A3.1 alluvial fan fine sediments. Separated by sites, in stratigraphic order.

hypothesis of fan aggradation during cold stages. Further analysis is necessary to obtain the precise age of this unit.

Unit Tp:

Fine sands and gravels were dated by TL at Los Trances trenches and a thin snail shell collected from very fine sediments was dated by ^{14}C at the El Hacho river outcrop (Fig. 4.4). Both methods assigned a Late Pleistocene age to Tp terraces (Tables 4.3 and 4.4, Fig. 4.7). However, ^{14}C age yields a younger age than TL. According to uncertainties related to dating old shell samples (see section 4.3.2.3 of this thesis), this results is considered to provide only a weak idea of the age of the unit (late Pleistocene). Further dating of the El Hacho Tp fluvial terrace is needed to confirm whether it belongs to the same fluvial terrace generation as the one dated at Los Trances. Therefore, on the basis of fan generation/climatic relationships, TL dating suggests that the A3.1 fan aggradational phase occurred during the MIS5 warm stage.

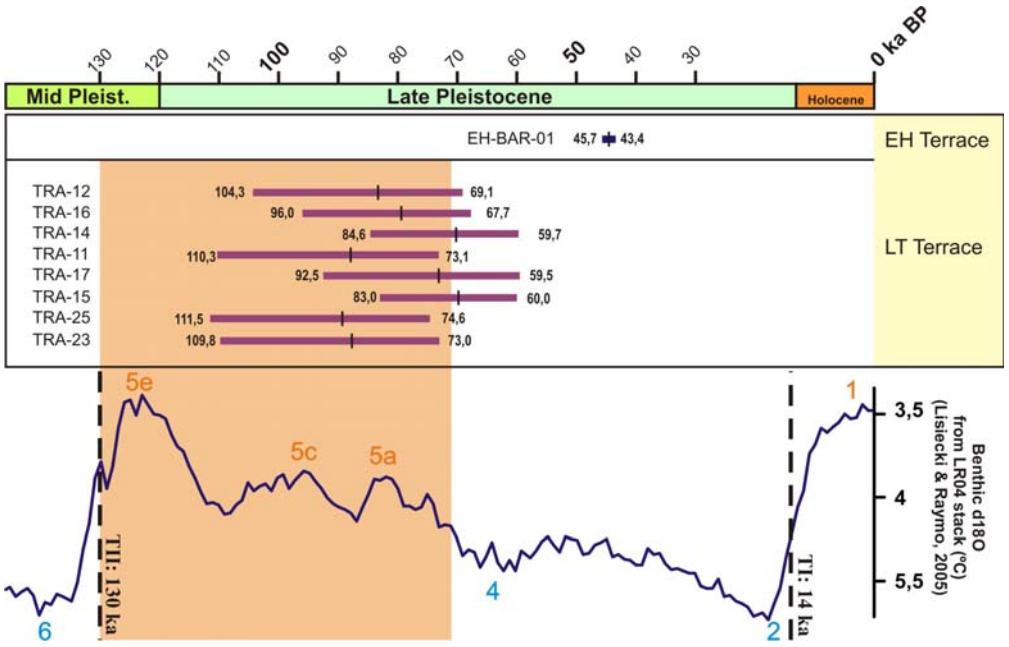

Figure 4.7. TL and ^{14}C ages from fine sediments from Tp fluvial terrace.

Unit Th and Paleo-channel:

Charcoal samples obtained from trenches dug in Th fluvial sediments at El Hacho, Cerro Blanco and Pecho de los Cristos (Fig. 4.4) were dated by ^{14}C AMS (Table 4.4). TL was also applied to a sample from Pecho de los Cristos (Table 4.3).

Radiocarbon results from charcoal samples suggest that these units are coeval (Fig. 4.8) and constrain the Th terraces between 0,56 - 1,42 ka BP and the paleo-channel observed in El Hacho trenches between 0,926 - 1,313 ka cal BP. However, no evidence was found to disregard the TL result at Pecho de los Cristos, and thus the age of this terrace remains uncertain within the Holocene.

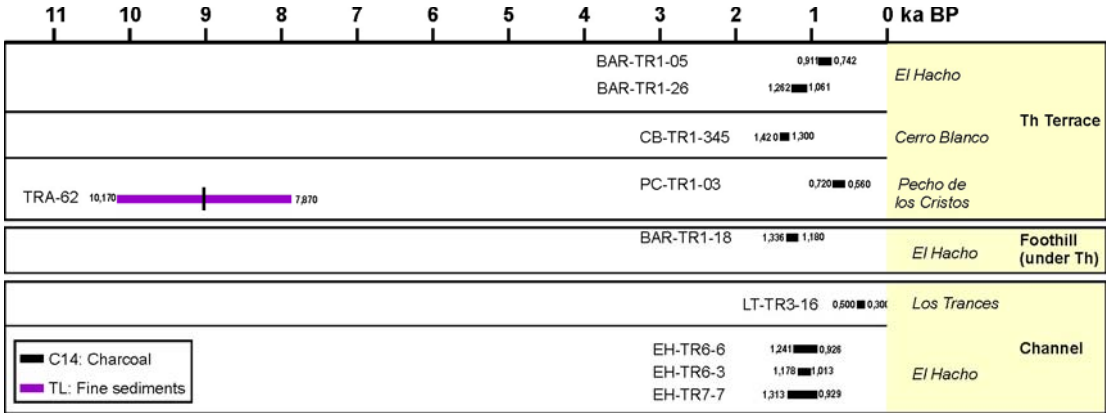

Figure 4.8. TL and ^{14}C ages from fine sediments of the Th fluvial terrace and paleo-channel from El Hacho.

4.4. Morphological evidence of Quaternary tectonic activity

The Quaternary activity of the Carboneras Fault at La Serrata is depicted by geomorphological features such as faulted and folded Quaternary deposits, deflected drainage, pressure ridges and the relative distribution of different generations of alluvial fans. All these features highlight the left-lateral and reverse nature of the fault, and reveal some measurable offsets which, together with the geomorphological dating, shed light on fault slip-rates during the Quaternary that have been unknown to date. These features are described and the geological implications are discussed. Some constraints on the slip-rates of the fault are also discussed.

4.4.1. Faulted and folded Quaternary units

Deformation of Quaternary units is exposed at several points at La Serrata. The oldest A1 fans are the most deformed Quaternary deposits, although evidence of deformation is observed in all the units up to Holocene age. However, in some cases, Holocene units are not affected along fault traces that deform Pleistocene units, probably because of a step over in the active strands of the CFZ.

In numerous outcrops, A1 alluvial fans are strongly faulted and deformed, confirming the high activity of the CFZ since the Early Pleistocene. A striking example of this deformation is located west of Cerro Blanco (site 5 in figure 4.2). It shows a band of well-stratified A1 sediments located between faults, forming a pressure-ridge (Fig. 4.9). This band is uplifted a minimum of 50 metres with respect to the top of A1 fans cropping out along nearby channel bottoms.

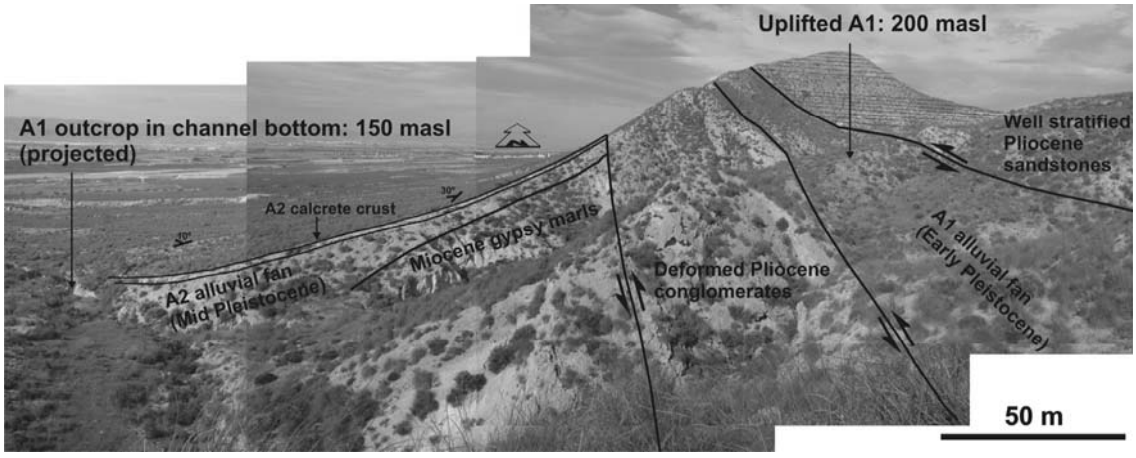

Figure 4.9. Landscape picture and overlying interpretation of the uplifted A1 alluvial fan close to the Cerro Blanco hill.

Another example of faulted Early Pleistocene deposits is located close to "El Cortijo del Parratero" (site 11 in Fig. 4.2) where a 170 metre-long lens of calcified and strongly deformed A1 material is confined within the fault zone between old Jurassic limestone and Pliocene bedrock (Fig. 4.10).

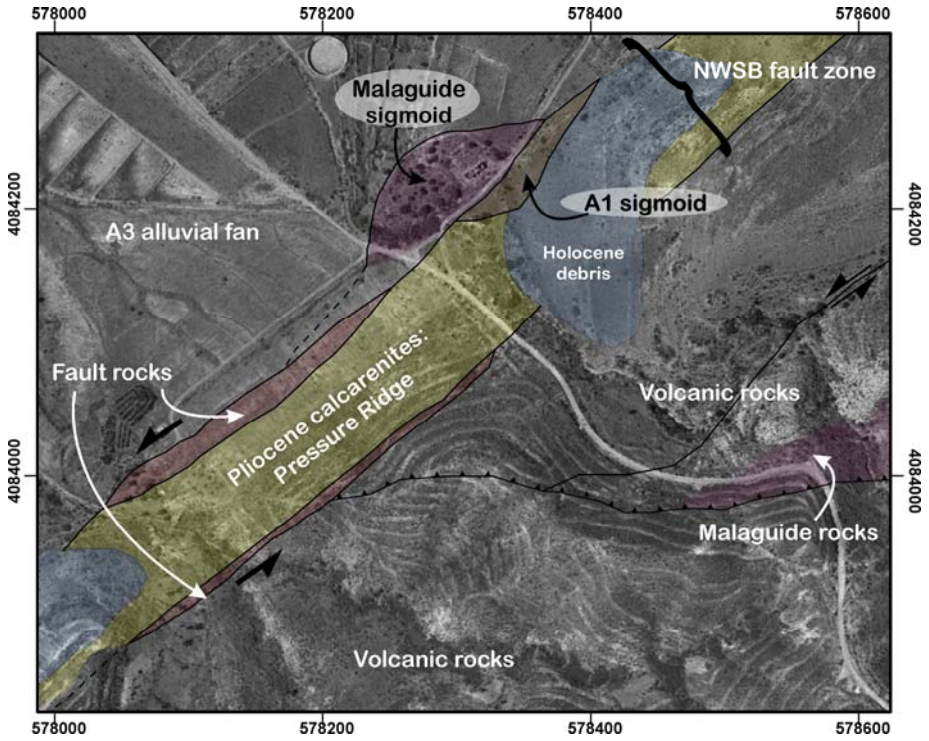

Figure 4.10. Orthophotomap of the A1 sigmoid in the fault zone next to a Malaguide basement rock sigmoid, close to El Cortijo del Parratero.

Generally, the straight linear contact between A2 alluvial fans and the mountain front (Fig. 4.2) provides evidence of considerable fault activity after A2 deposition. Several A2 alluvial fans at La Serrata do not have a drainage area large enough to account for their formation. Some others have been beheaded, losing their apex by offset, uplifting and erosion. In very few places, the apex is still preserved in the uplifted mountain front, such as the uplifted A2 apex (Fig. 4.11) close to El Hornillo (site 8 in figure 4.2) and south of the Collado de Naja Mountain. The fluvial network excavated the fan apex sides to counteract the high gradient produced by the mountain uplift (Fig. 4.11). The sediments resulting from the erosion formed a small and fine lobe (pediment-like) next to the uplifted apex and overlie an A3.1 alluvial fan. Moreover, the A3.1 alluvial fan is in straight contact with the A1 and A2 deposits located at the mountain front on the other side of the fault zone. There is therefore evidence of some tectonic activity after the age of A3.1 (Late Pleistocene). A trenching analysis would be necessary to ascertain whether the small lobe is also faulted, and thus, better constrain the age of the last fault activity in this area.

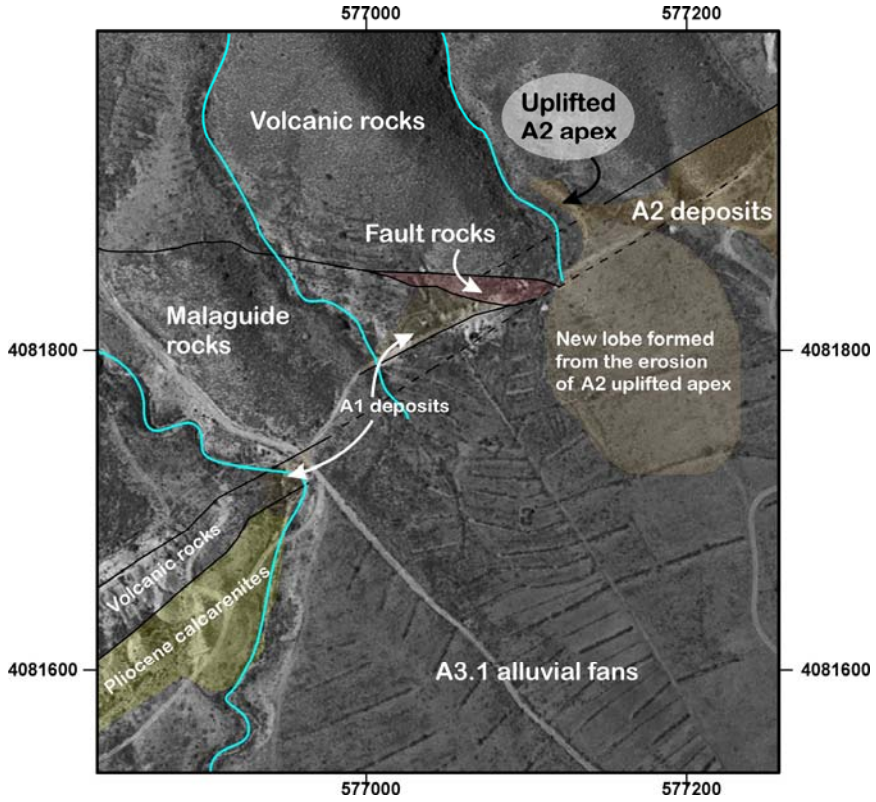

Figure 4.11. Orthophotomap of the A2 uplifted fan apex and the resulting downhill fine lobe located close to El Hornillo and south of the Collado de Naja Mountain.

Aerial images do not provide clear evidence of A3 faulted deposits, but trenches and artificial cuts reveal A3 units being faulted up to the surface (Fig. 4.4). At the Archidona quarry (site 6 in figure 4.2), east of the Cerro Colorado hill, the excavation exposes an A3 alluvial fan faulted up to the surface and incorporated into the fault zone (Fig. 4.12), confirming the Late Quaternary movement of the fault on the SE side of La Serrata.

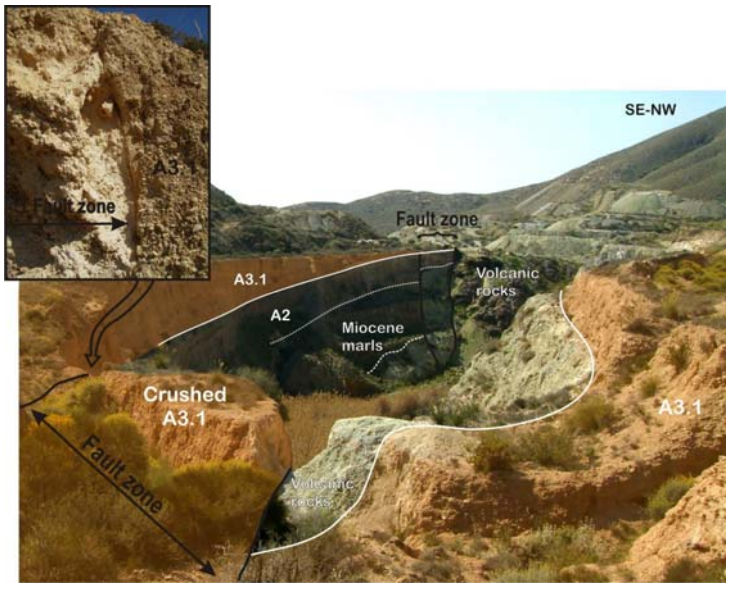

Figure 4.12. Artificial outcrop showing the fault contact between volcanic and Miocene rocks at depth and Pleistocene units faulted on top. A2 alluvial deposits are clearly faulted in the front wall and A3.1 deposits are faulted up to the surface and incorporated into the fault zone as observed in the zoom.

In trench walls, Late Pleistocene (Tp) and Holocene (paleo-channel) units are observed to be faulted, providing evidence of the very recent fault activity (Fig. 4.4 and 4.13b). In contrast, Holocene Th terraces do not appear to be faulted, which will be fully discussed in the following chapter. An apparently unaffected Th terrace is shown in the natural outcrop (Fig. 4.13a) overlaying a Tp terrace in fault contact with Pliocene microconglomerates. Further trenching analysis at El Hacho gully site will extend this discussion (site 3 in figure 4.2 and EH-BAR-SW sketch in figure 4.4).

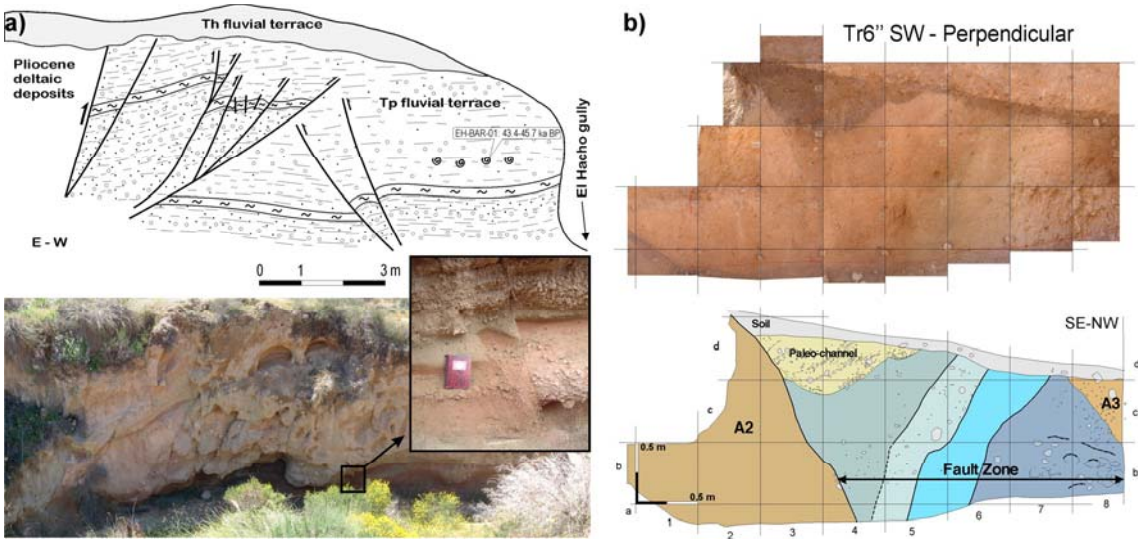

Figure 4.13. a) Field outcrop along the gully at El Hacho gully site showing the fault contact between Pliocene quartz-rich microconglomerates and Tp fluvial deposits. The fault zone is overlapped by apparently non-deformed Th fluvial deposits. The compressive flower structure character can be observed in the zoom. b) Faulted paleo-channel observed in trenches at El Hacho site. Photo-log above and interpretation below.

4.4.2. NWSB pressure ridges

A large pressure-ridge, which runs along the NWSB from Las Yeseras to La Pared Alta (Fig. 4.2), is the most compelling evidence for Quaternary deformation. This pressure-ridge is bounded by "en echelon" faults and strikes parallel to the main orientation of the CFZ at La Serrata (ca. N50). The deformation involves mainly Pliocene bedrock but also Early and Mid-Pleistocene alluvial fans. Pliocene bedrock is "sandwiched" between the Neogene basement forming La Serrata and the Quaternary alluvial fans deposited downstream (Fig. 4.2). Quaternary sediments were originally deposited on top of the Pliocene ridge with original gradients of around 3º (observed in nearby fan surfaces where no deformation exists at present) and were faulted and folded (topographic profile in Fig. 4.14) in subsequent deformation events. Close to the Cerro Blanco hill (site 5 in Fig. 4.2) the A1 alluvial fans are observed strongly faulted and tilted up to subvertical slopes (observed in natural outcrops near Las Yeseras), and A2

alluvial fans are folded and smoothly tilted to around 12º (although they can locally reach up to 35º). A maximum vertical offset of 20 m is obtained considering the vertical difference between the present-day 3º slope A2 (surface projected to the fault zone) and the A2 surface tilted at the pressure ridge.

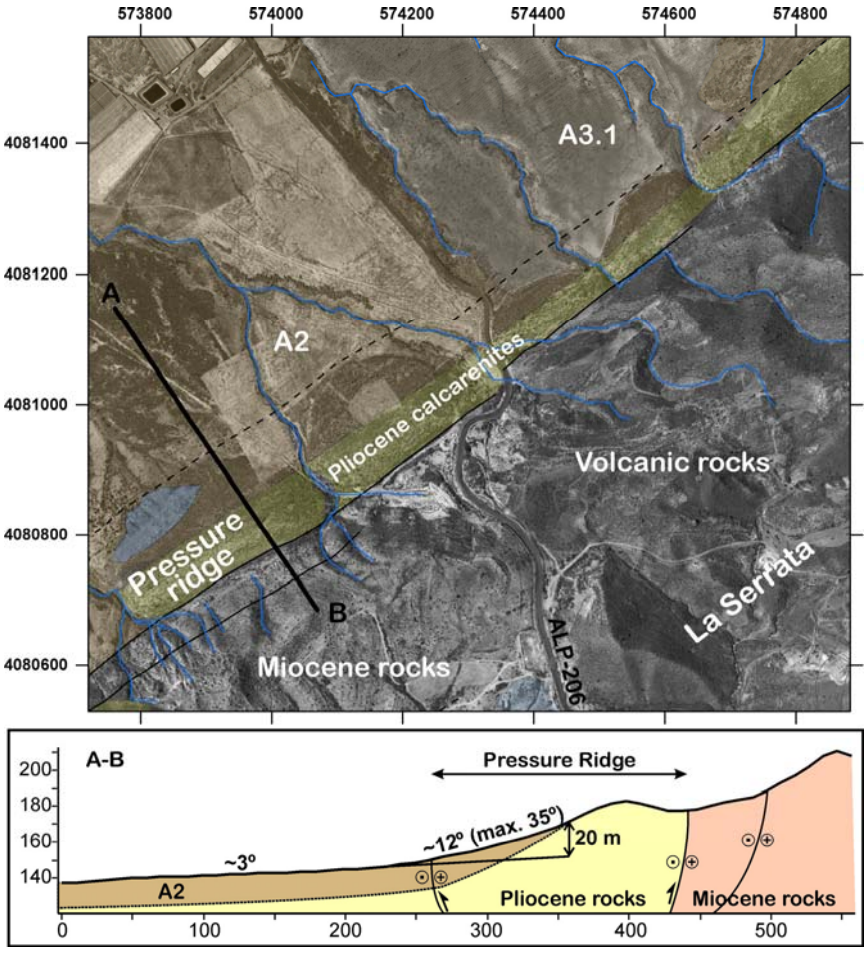

Figure 4.14. Orthophotomap showing part of the pressure ridge along the NWSB and topographic profile across the fault zone deZpicting the slope change in A2 unit at the pressure ridge.

4.4.3. Deflected drainage at La Serrata

A number of left-lateral deflected channels (bayonets) are observed along the La Serrata range. Some of these show clear evidence of tectonic offset in line with the consistent restitution of their deformation. The NWSB hosts numerous bayonets (Fig. 4.15a) with average offsets between 100-200 m.

At Pecho de los Cristos (site 10 in Fig. 4.2), the area around PC-TR2 trench (enlarged orthophotomap in Fig. 4.15a) is covered by an A3.1 alluvial fan, even though at present a source area capable of feeding this fan is absent. A trench shows that this alluvial unit is at least 2.2 m thick (trench sketch in Fig. 4.15a). Assuming a left lateral motion of the fault, the first source area capable of providing this amount of sediment is

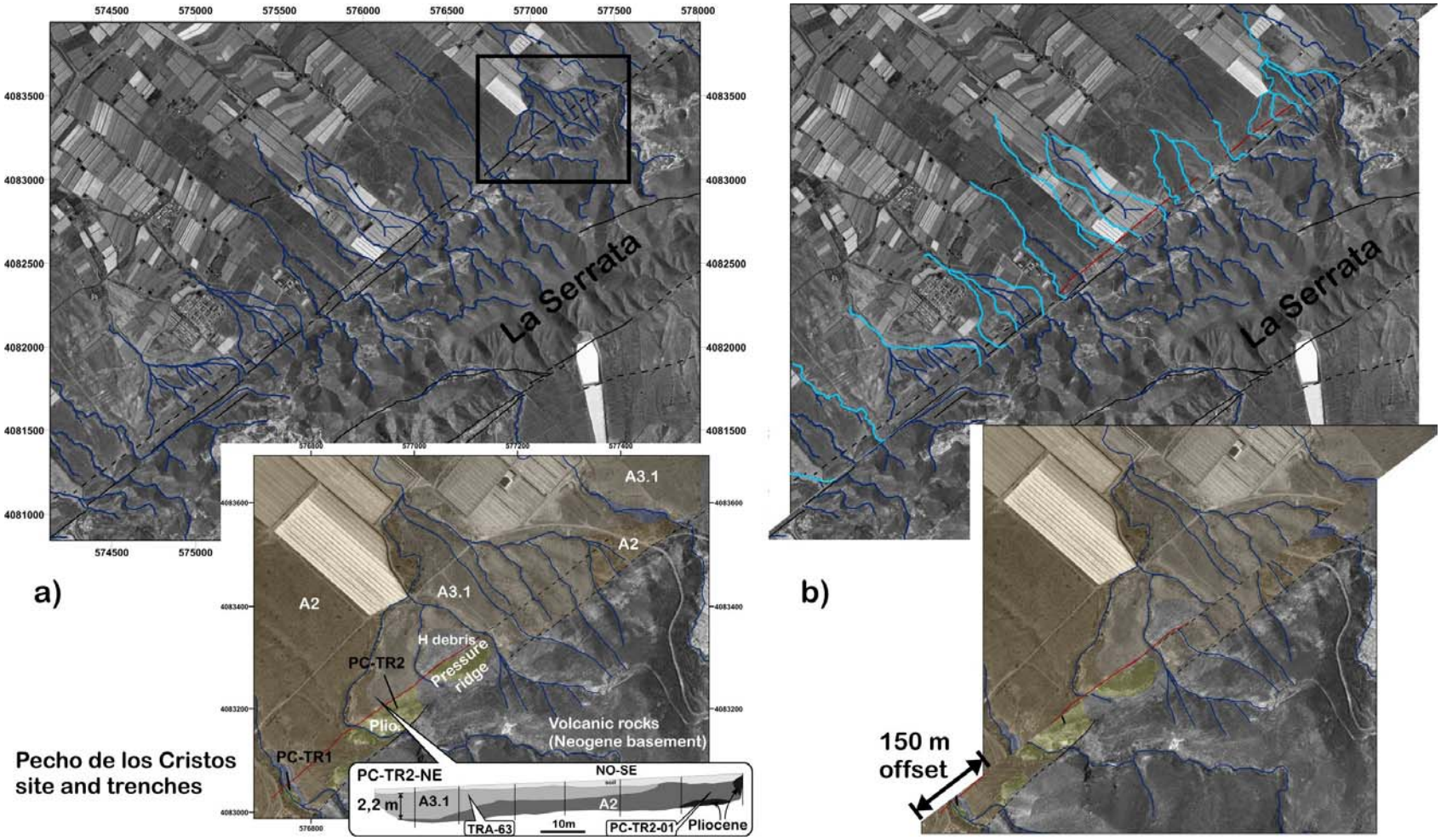

Figure 4.15. a) Orthophotomap showing offset gullies on the northwestern side of La Serrata at Los Trances and Pecho de los Cristos. The main gullies are outlined in dark blue. At the magnified Pecho de los Cristos orthophotomap, trenches are depicted in black, and the NE wall of PC-TR2 is sketched at the bottom of the figure. H debris: Holocene superficial debris; Plio.: Pliocene quartz-rich microconglomerates. b) Restored 150 m left-lateral offset along CF following piercing points from the connection of the main gullies (light blue) across the fault. See text for discussion.

located 150 m to the NE (magnified orthophotomap in Fig. 4.15b). When restoring this offset, other incised gullies match the correlative ones at the southern block. Furthermore, most of the deeply incised gullies on the A2 calcrete crust along the NWSB (Fig. 4.15a) also match the correlative ones in the southern block when extrapolating the 150 m offset at Pecho de los Cristos (light blue gullies in Fig. 4.15b).

At El Hacho (site 1 in Fig. 4.2), three fault zones were mapped (Fig. 4.16a): the southeastern one was observed in the field as a result of morphological evidence and trenches (these trenches will be discussed in the next chapter). The northwestern and central faults are inferred from the deflection along several gullies and were detected by geophysical techniques (see next chapter). These faults probably gave rise to the pressure ridge on the A2 deposits. Some gullies in the area are beheaded and abandoned, especially the ones preserved on the calcified surface of the A2 alluvial fans. For instance, the highly incised gully located at the south of the orthophotomap (Fig. 4.16a) is visibly deflected twice, first along the southeastern zone and then along the central one. Unfortunately, the original down-slope course of this gully has been obliterated by human activity. A left lateral offset of 145 m along the main fault zone is observed when restoring this gully (Fig. 4.16b). At the same time the abandoned and beheaded gullies match their respective gullies in the southern block. The same exercise was undertaken on the central fault trace, restoring 13.8 m of left-lateral offset gullies.

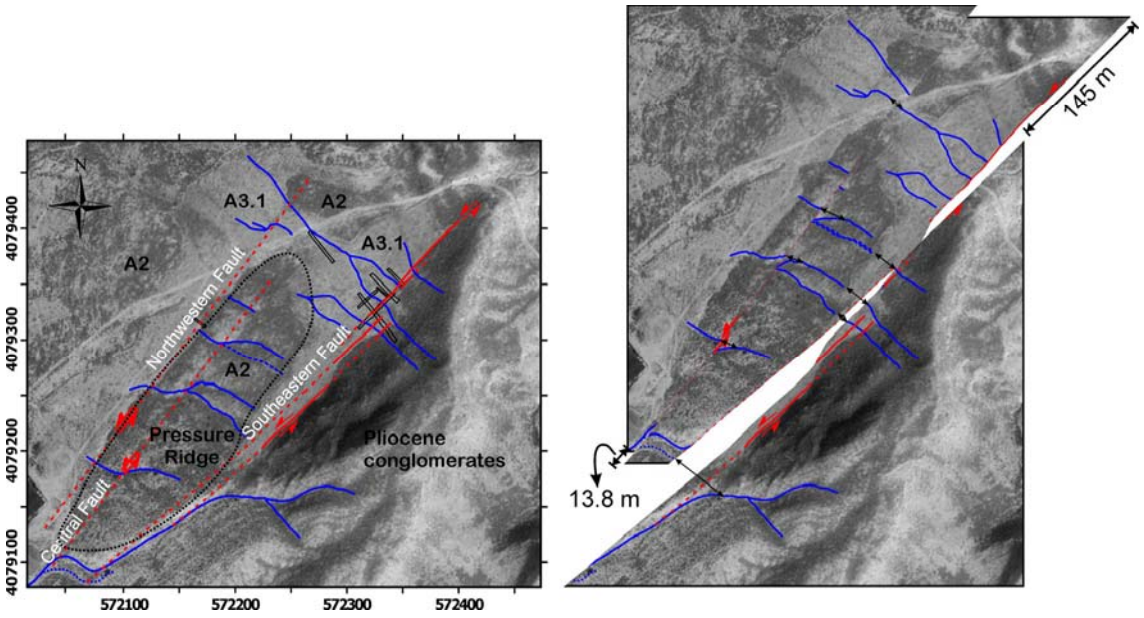

Figure 4.16. Orthophotomap with left-lateral offset gullies at El Hacho. Gullies and continuous fault lines were observed and mapped in the field with a Total Station. Dashed fault lines indicate inferred fault traces. Dashed gully was inferred from field observations (i.e. less incised), and dot line depicts an abandoned gully. Trenches at this site are depicted in black. b) Restored offset along faults following piercing points from the connection of gullies across the fault.

4.4.4. Relative distribution of alluvial fans

Alluvial fan generations are not equally distributed at the foot of La Serrata. Morphological differences of the same generation along the range indicate different regional processes. The apex position has been frequently used as an indicator of the mountain front uplift related to tectonic activity. The most striking observations at the NW foot of La Serrata (Fig. 4.2) are the absence of A3 fans in the southwest, the unshaped and elevated remnants of A1 between the Miocene sediments that crop out in the north, and the different apex position with respect to the mountain front between subsequent fan generations (A3.1 and A3.2). These indicators allow us to restore the NWSB tectonic evolution of the successive alluvial fans at the foot of La Serrata. This evolution may be summarized in five stages:

Stage I (Early Pleistocene?): Deposition of A1 alluvial fan generation at the foot of La Serrata Range (Fig. 4.17a).

Stage II (Mid Pleistocene): Patchy and elevated remnants of A1 alluvial fan in the northern part of La Serrata (Goy and Zazo, 1983) (Fig. 4.2) are interpreted as a result of a regional uplift in this area, leading to a lower base level and higher fluvial erosion (Fig. 4.17b). In parallel, extensive A2 fans covered the A1 fans to the south, suggesting a less pronounced uplift in this area.

Stage III (Late Pleistocene): A new regional uplift is thought to have occurred in the southern part of La Serrata, locally producing erosion and deep incisions in the fluvial network. This would produce erosion of the A2 calcrete crust, leaving A1 fans cropping out at the bottom of the gullies (Fig. 4.17c). At the same time, large A3.1 fans were deposited between the uplifted northern and southern areas of La Serrata.

Stage IV (Late Pleistocene): A decrease in the mountain front uplift produced a gradient stabilization of the channels feeding the alluvial fans, transferring the fan deposition a considerable distance from the mountain front. Thus, the apexes of the new fan units (A3.2) are located midway between the mountain front and the main river in the Nijar Basin (Fig. 4.17d). This decrease in the uplift of the mountain front can be interpreted either as a decline in the fault activity or as a change in the tectonic pattern, enhancing the strike-slip component of the fault.

Stage V (Holocene): The last generation of alluvial fans, A4, was deposited with their apexes even further downstream (Fig. 4.2), suggesting a stabilization of the gradient and a decrease in the mountain front uplift.

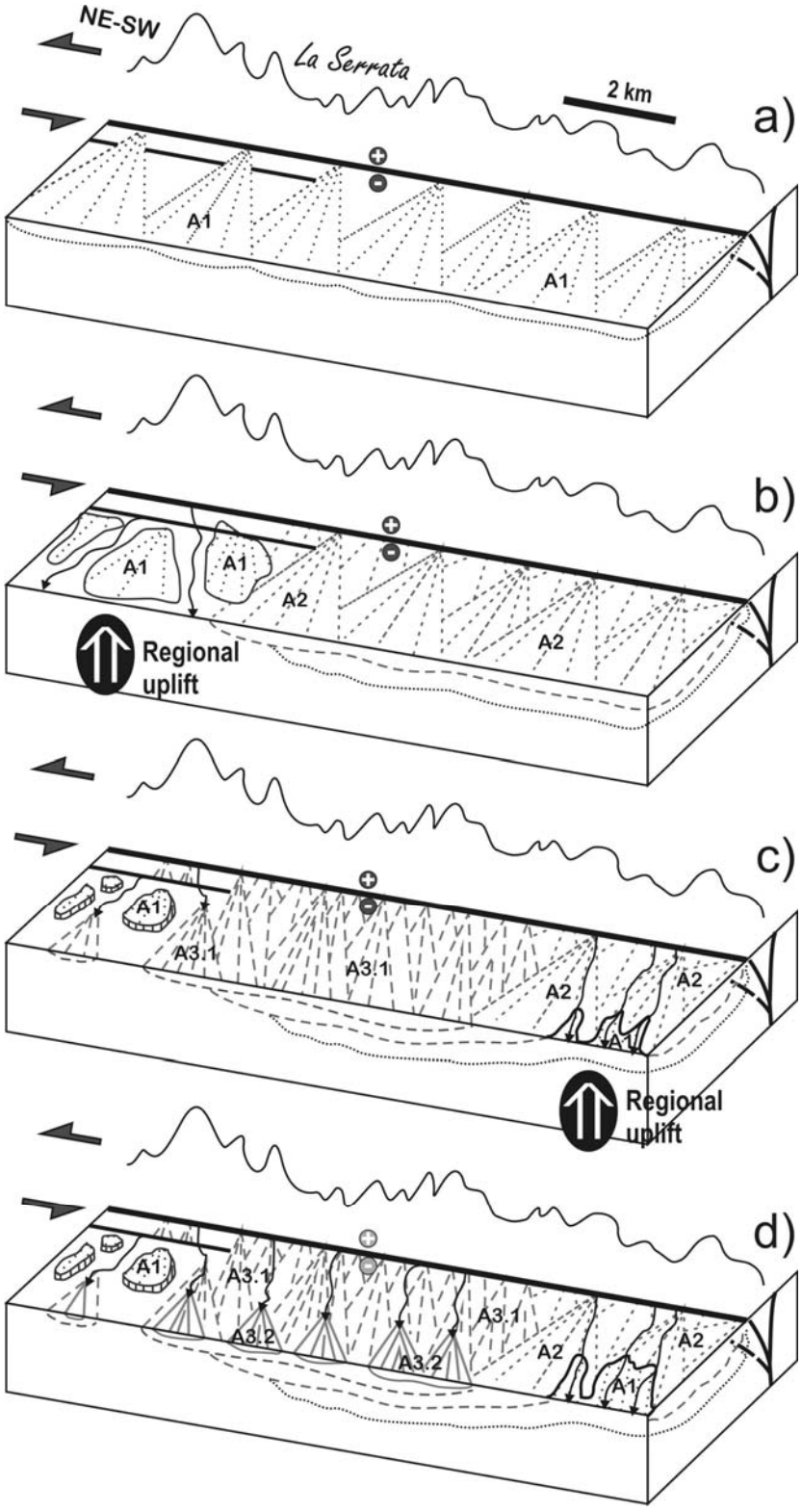

Figure 4.17. Sketch of the evolution of La Serrata Quaternary alluvial fans. Regional uplift occurs mainly in stages b and c in line with the relative distribution and geometry of alluvial bodies. A decrease in the uplift of La Serrata occurs in stage d in line with the lower position of the fan apex relative to the mountain front.

4.5. Discussion

Geomorphological analyses together with radiometric datings allow us to establish a chronology of the Quaternary units observed at La Serrata (Table 4.5). This age model is used to elucidate the tectonic evolution of the faults shaping La Serrata and to calculate some slip-rates for this active structure in order to determine some of the paleoseismic parameters of the Carboneras Fault Zone.

4.5.1. Chronology of the Quaternary units: Alluvial fans and climate changes

Once the Quaternary sub-aerial conditions were established in the area, the first alluvial fans were formed from the paleo-relief of La Serrata. Warm and wet Early Pleistocene conditions would have generated large and thick alluvial fans with internal characteristics (e.g. reddish colour, quick alternation between coarse and fine sediments), showing a slow aggradation mode in contrast to the Mid-to-Early Pleistocene conditions during which a marked distinction is produced between the aggradation and the dissection alluvial phases. ^{10}Be returns an age ranging between 0.214 and *ca.* 1 Ma for the top of this depositional A1 period (Table 4.5).

The transition between the Early to Mid Pleistocene is characterized by a major global climatic reorganization that marks the onset of successive major glaciations separated by pronounced interglacial periods. In line with the hypothesis of fan aggradation during cold stages, A2 alluvial fans could have been formed during the main glacial stages of the Mid Pleistocene (MIS 6-12), between 478-130 ka. The upper layers of A2 alluvial fans have TL ages (TRA-22 and TRA-24) with a lower age range in the final stages of the Mid Pleistocene, while primary calcretes are of Late Pleistocene, suggesting the upper layers of A2, which represented the last pulse of A2 aggradation, were deposited during the MIS 6: 130-191 ka.

Primary calcrete crusts were formed in A2 units during the following interglacial period: MIS 5 (Late Pleistocene), ranging from 130 to 71 ka BP. A progressive degradation and fan-head trenching pattern occurred during MIS 5, leaving A2 crust at the surface. Fluvial deposits (Tp) fill the gullies incised in A2 alluvial fans, and are dated in 111.5-59.5 ka BP at Los Trances (Table 4.5).

After MIS 5 the onset of Würm glaciations gave rise to heavy rainfall and to soil destabilization, favouring a new fan generation. A3.1 and A3.2 alluvial fans were formed during MIS 4-2, between 71-14 ka BP. Numerical results from A3.1 at El Hacho, Pecho de los Cristos, Los Trances and Archidona are consistent with this hypothesis and constrain the age of sediments placed there between 71.6 ka BP and 26.6 ka BP (Table 4.5). These results show a progressive aggradation of A3.1, suggesting that MIS 3 was not warm enough to stabilize the alluvial fan surface and to interrupt the aggradational phase. Thus, variation in the extension of the fans and variation in the

apex position of A3.2 units were not attributed to a climatic change but to a tectonic cause.

The current interglacial stage started at 14 ka BP (from LR04 stack, Lisiecki and Raymo, 2005) and hosted the degradation and fan-head incision of A3 units and the formation of the new fluvial terraces filling the incised channels. ^{14}C dating of Th deposits yields a late Holocene age (1420-560 ka BP) (Table 4.5). Their unconsolidated sediments denote the present-day warm conditions.

Primary calcretes formed on top of A1 and A2 units continued to grow during subsequent glacial and interglacial stages. This regrowth is probably due to water circulation along the crust, forming secondary calcrete crusts.

Table 4.5: Correlation between Marine Isotope Stages (MIS) and radiometric ages used for assigning an accurate age to the units at La Serrata. The age of MIS boundaries is obtained from Lisiecki and Raymo (2005).

Unit\Site	Correlation with Marine Isotope Stage	El Hacho	Los Trances	Pecho de los Cristos	Cerro Blanco	El Puntal	Archidona
Th	MIS 1: 14-0 ka	1.262-0.742 ka (^{14}C)		0.72-0.56 ka (^{14}C)	1.42-1.30 ka (^{14}C)		
Paleo-channel	MIS 1: 14-0 ka	1.313-0.926 ka (^{14}C)	0.5-0.3 ka (^{14}C)				
A3.1	MIS 4-2: 71-14 ka	71.6-26.6 ka (TL)		47.1-36.9 ka (TL)			59.8-47 ka (TL)
Tp	MIS 5: 130-71 ka		111.5-59.5 ka (TL)				
A2 primary calcrete	MIS 5: 130-71 ka		110.3-56.6 ka (U/Th)				
A2	MIS 12-6: 478-130 ka		>122 ka (TL)				
A1	Early/Mid Pleistocene					0.214-1 Ma (^{10}Be)	

4.5.2. Quaternary Tectonic evolution of La Serrata

After subtracting the morphological effect of climatic fluctuations, differences in the morphology of fan generations (i.e. size, slope, location, apex position) can still be observed because of tectonic factors. These observations together with the age of the Quaternary units of the area allow us to define the successive tectonic stages and temporal evolution of the Carboneras Fault.

The distribution of the Quaternary deposits at La Serrata range, entails two tectonic phenomena: 1) localized uplifts in the area during the Quaternary, and 2) changes in the vertical component of the fault since Late Pleistocene.

The oldest evidence of uplift took place in the northeastern area of La Serrata (Fig. 4.17b). This uplift occurred when A1 alluvial fans had already been formed but A2 had not yet been deposited. To constrain the age of this uplift, we can only use the lower

age of A1 given by ^{10}Be (1 Ma BP) and the upper age of A2 at La Serrata, which is assumed to be of MIS 6 age (130 ka BP). Thus, the age of the uplift would be constrained between 1 Ma and 130 ka BP.

The second uplift event inferred from fan distribution took place in the southwestern part of La Serrata (Fig. 4.17c). This uplift started when the calcrete crust of A2 was already formed, during MIS 5. Thus, the minimum age of this uplift would be < 130 ka BP.

The different position of the fan apex observed between A3.1 and A3.2 subunits suggests a change in the mountain front activity, which is interpreted as a decrease in the uplift of the mountain front during the Late Pleistocene. Since the A3.2 fans are not dated with numeric methods, the age of this change in the mountain front growth can only be constrained as younger than that of of A3.1, which would be < 71 ka BP, the start of MIS 4. As already stated, the decrease in the uplift of the mountain front can be attributed to 1) a decline in the activity of the Carboneras Fault, or to 2) a shift in the kinematics of the fault, from more dip-slip to more strike-slip.

A4 alluvial fans were not analysed in detail or dated in this study. However, their apexes are located at a considerable distance from the fault (Figure 4.2) with respect to those of the A3.2 fans. This suggests that the position of the fans was controlled by a tectonic factor (decrease in the uplift of La Serrata) during the Holocene.

The faulted and left-laterally offset paleo-channel at El Hacho provides compelling evidence of Holocene activity at the Carboneras Fault and of its predominant strike-slip kinematics. The age of the last movement of the fault in this segment is younger than 0.926-1.313 ka BP in accordance with the age of the sediments filling the offset channel. On the other hand, Holocene fluvial terraces (Th) showed undeformed deposits. Holocene paleochannel and Th fluvial deposits show overlapping ages when considering the σ1 probability for ^{14}C age distribution. There are two possible explanations for this: 1) Th terraces are slightly younger than the channel and post-date the last movement of the fault; and 2) their ages are coeval but Th does not appear faulted because of a fault trace migration to a parallel trace. The latter explanation demands that we should consider the whole fault zone and not only a specific fault trace when analysing the seismogenic potential of the source. Further trenching analysis will help to extend the discussion on the most recent tectonic activity of the fault.

4.5.3. Slip-rates deduced from geomorphological evidence

Faulted Quaternary deposits quantify Quaternary fault activity. The vertical and horizontal slip-rates of the Carboneras Fault may be estimated on the basis of mumerical ages.

Dip-slip rate inferred from the uplifted apex of A1 alluvial fan

At Cerro Blanco, the top of the A1 unit is observed at the bottom of the channel, but not in the "sandwiched" fault zone at the mountain front (Fig. 4.9). A minimum offset may therefore be inferred and a minimum dip-slip rate can be calculated. Thus, a minimum dip-slip rate of 0.05 mm/a since the Early Pleistocene is estimated from the minimum 50 m vertical offset measured in the field, and from the ^{10}Be ages of the A1 alluvial fan, ranging between 214 ka BP and ca. 1 Ma BP. Moreover, the apex of the alluvial fan that should be located in the range is absent. It may be assumed that the apex was uplifted more than 50 m and eroded, suggesting a considerably larger dip-slip rate.

The calcrete crust on top of the A2 alluvial fans is strongly folded and tilted in the pressure ridge zone (Fig. 4.14). A 20 m of vertical offset is inferred from the extrapolation of the normal inclination of the fan surface (around 3º). This vertical offset is produced after the calcrete crust formation. On the assumption that the calcrete crust was formed during the MIS 5 (130-71 ka), a minimum dip-slip rate of 0.15 mm/a since the Late Pleistocene is inferred.

Strike-slip rates from the deflected fluvial network

Offset gullies observed at Pecho de los Cristos (Fig. 4.15) and El Hacho (Fig. 4.16) suggest left-lateral offsets around 145-150 m. In both locations, the gullies are incised on the calcrete crust on top of A2 fans, facilitating the preservation of offset evidence. The calcrete crust predates the time of the movement. The primary crust was formed during the MIS 5 (130-71 ka), suggesting a minimum strike-slip rate of 1.1 mm/a since the Late Pleistocene.

The geomorphological evidence discussed in this section presents a minimum dip-slip rate of 0.15 mm/a and a minimum strike-slip rate of 1.1 mm/a, indicating a strike-slip rate one order of magnitude larger than the dip-slip rate in the long-term, which is expected in a transcurrent fault.

4.6. Conclusions

Four alluvial fan generations (A1, A2, A3 and A4) and two secondary channel fluvial terraces (Tp and Th) are the main Quaternary deposits at La Serrata. The ages of the sedimentary deposits at La Serrata were constrained by numerical dating analyses together with geomorphological observations and a correlation with climatic stages. From old to young, A1 alluvial fans are most likely of Early Pleistocene age although radiometric analysis return a wide age between 0.214 to *ca.* 1 Ma BP. A2 alluvial fans are interpreted as Mid Pleistocene deposits and are associated with the cold stages of MIS 12-6 (478-130 ka BP), the last pulse of this unit being related to MIS 6 (190-130 ka BP). Tp fluvial terraces were formed during the warm stage MIS 5 (130-71 ka BP) and yield ages constrained between 111.5 and 59.5 ka BP at Los Trances. A3 alluvial fans were formed during MIS 4-2, and A3.1 yields an age between 71.6 and 20.6 ka BP at El Hacho. The paleo-channel identified in the trenches at El Hacho has an age ranging between 1313 and 920 Cal yr BP. Th fluvial terraces are interpreted as having been formed during MIS 1 and different late Holocene ages were obtained as follows: 1262-742 yrs BP at El Hacho, 1420-1300 yrs BP at Cerro Blanco and 720-560 yrs BP at Pecho de los Cristos.

Primary and secondary phases of calcrete crust development were distinguished on top of the Early Pleistocene (A1) and Mid Pleistocene (A2) alluvial fans. Primary calcretes were formed in the first stabilization phase (warm stage) after the aggradation period (cold stage) of the fan. Secondary calcretes were formed during successive stages (cold and warm), probably by circulation of carbonatic ground-waters over primary calcretes.

Quaternary tectonic activity is evidenced by surface field studies and by faulted and folded Quaternary deposits (A1, A2, A3.1) observed in trenches along the boundaries of La Serrata. Moreover, the paleo-channel trenched at El Hacho reveals Holocene activity and constrains the age of a recent (last?) movement of this segment as younger than AD 637.

Th fluvial terraces do not show faulted deposits and have ages that overlap the faulted paleo-channel. There are two explanations for this: 1) Th terraces are slightly younger than the channel and postdate the last movement of the fault; and 2) the active fault trace has migrated to a parallel trace.

Slip-rates for this fault segment were calculated from field observations and dating results. Minimum dip-slip rates of 0.05 mm/a since 1 Ma, and 0.15 mm/a since 130 ka were obtained. A minimum left-lateral strike-slip rate of 1.1 mm/a since 130 ka is obtained on the basis of deflected drainage along the boundaries of La Serrata.

Regional distribution of Quaternary deposits at the foot of La Serrata suggest at least two episodes of regional uplift: the first one occurred between ca. 1 Ma BP and

130 ka BP in the northeastern part of La Serrata, and the second one took place after 71 ka BP in the soutwestern part of this range.

A down-stream gradual displacement of the apex position of the Late Pleistocene and Holocene deposits (A3.1, A3.2 and A4) is interpreted as the result from a decrease in the mountain front uplift activity at least after 71 ka BP. This could be due to 1) a decrease in the fault movement, or to 2) a change in the fault kinematics from dip-slip dominated to strike-slip.

Chapter 5: Paleoseismic study at La Serrata

5.1. Introduction

The NW boundary of La Serrata was identified as the segment with most evidence of Quaternary tectonic activity. It has the best conditions along the onshore fault trace for a detailed paleoseismic study. These are 1) large Quaternary deposits near and overlying the fault zone (some of them of Holocene age), 2) clear evidence of Lower to Mid Pleistocene deformed deposits and 3) an apparently good sedimentation-deformation ratio.

Five paleoseismic sites were selected to characterize the seismogenic activity of the Carboneras Fault Zone (CFZ) during the Quaternary. At these sites, the paleoseismic analysis including detailed near-fault geomorphological analyses based on microtopographic levelling, trenching and dating was carried out. Two sites, El Hacho and Los Trances, provided most of the paleoseismic results. At all the sites the location of the trenches was determined by an exhaustive geomorphological analysis and, at El Hacho, also by subsurface geophysical techniques (GPR and ERT).

The paleoseismic analysis was thus constrained to the NW boundary of La Serrata and the results are limited to this fault trace. A magnetotelluric profile was acquired across the La Serrata range to ascertain whether the different fault traces converge on depth.

5.2. El Hacho area

5.2.1. Geographic and geological setting

The El Hacho area, which includes, the El Hacho site and the El Hacho gully site, is located at the SW end of La Serrata between the villages of Atochares and Barranquete (Fig. 5.1). In this area, the SE fault trace bounding the range loses continuity, changes its orientation and seems to converge on the NW fault trace. Metamorphic or volcanic basement does not crop out in this part of the range, which is here composed of Miocene (MII) and Pliocene (PII) rocks, suggesting a smaller uplift than in the northern parts of the range. The fault zone is narrower here than to the NE, which favours the analysis as the deformation may be more easily quantifiable.

Most of the efforts were devoted to the El Hacho site *s.s.* (Fig. 5.1), an area of 350 x 250 m located at the foot of El Hacho hill, although an additional trenching analysis was performed at the El Hacho gully site (10 x 10 m) located 450 m to the NE along the fault trace.

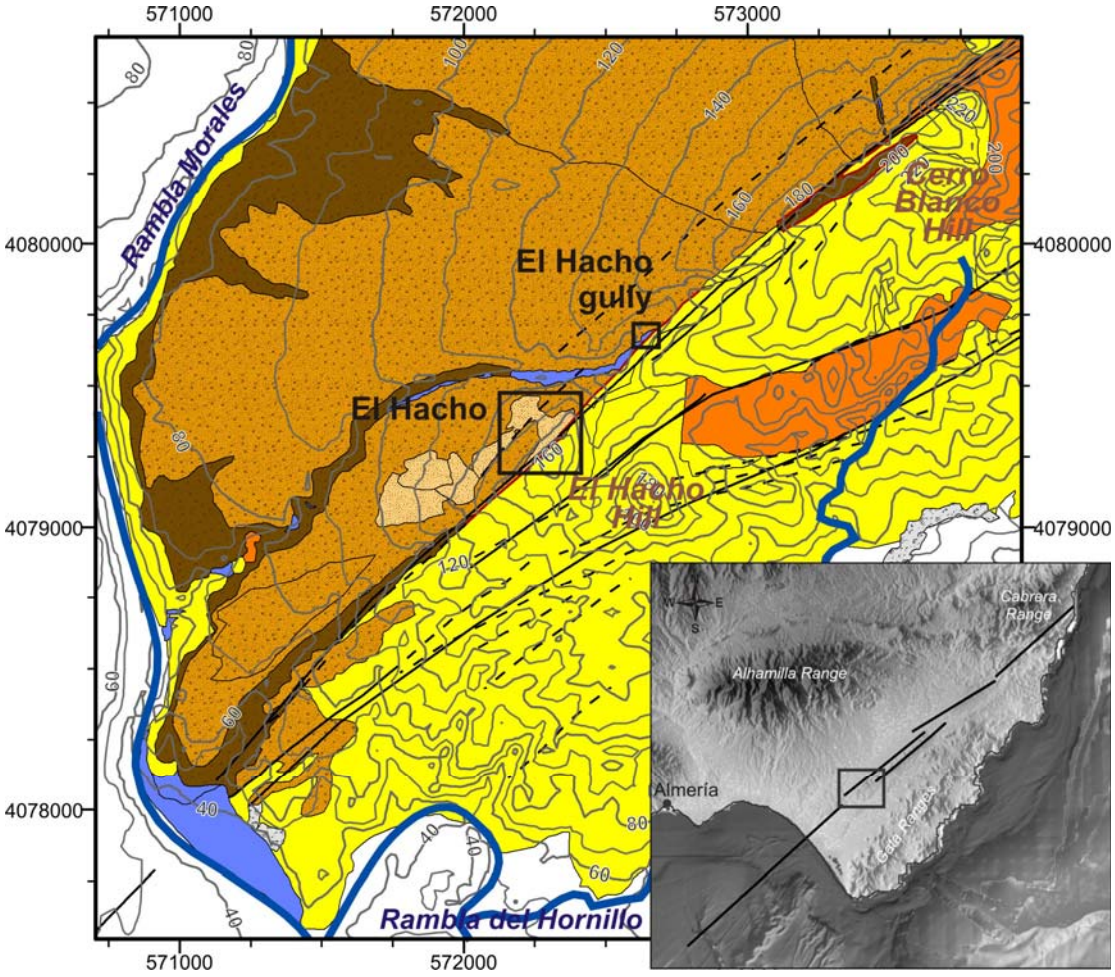

Figure 5.1. Detailed geomorphological map of the SE end of La Serrata and location of the El Hacho area and trenching sites. See caption in figure 4.2.

5.2.2. Overview

After selecting the site and prior to the paleoseismic study, a joint Ground Penetrating Radar (GPR) and an Electrical Resistivity Tomography (ERT) study were carried out at the El Hacho site to localize the most suitable areas for opening trenches. This initiative seeks to 1) assess the paleoseismic analysis by precisely localizing the fault trace in an area where the uppermost deposits appear not to be disturbed at surface, and 2) relate the geophysical signal to a specific geological unit that will be subsequently revealed by trenching.

After determining the precise location of the main fault zone and the main geomorphological units at the site, three trenches EH-TR1, TR2 and TR3 (Figure 5.2) were dug orthogonally to the fault to characterize the shallow fault architecture and its interaction with the associated deposits. In addition, two other trenches EH-TR4 and TR5, (Figure 5.2) were dug to locate secondary fault traces. The first trenches gave most of the information and the two last were imaged but not logged in detail as there was no clear evidence of Upper Pleistocene deformation.

To the northeast, at El Hacho gully site, the fault crosses a very recent fluvial terrace. The fault is clearly visible in the underlying Pleistocene deposits, but not clearly visible in the natural outcrop across the fluvial terrace sediment. A trench perpendicular to the fault trace was dug next to the gully outcrop in order to study the possible extend of the fault through the alluvial sediments.

The analysis of trenches across the fault allowed characterization of the fault zone and deformed Quaternary deposits, and some paleoseismic parameters were extracted from these observations. Nevertheless, given that the structure is considered to move mainly laterally, the strike-slip component must be obtained and this is not provided in the aforementioned analysis. For this reason, additional trenches were dug parallel to the fault to obtain the lateral offset of linear structures crossing the fault zone, such as gullies. This 3D trenching was planned with trench slides dug successively closer to the fault zone (EH-TR6, TR7 and successive slides in figure 5.2 and figure 5.9: TR6', TR6'', TR7', TR7'' and TR7''') in order to follow the trace of any buried channel and its approximation to the fault zone. Finally, four small trenches (TR6'p, TR6''p, TR7'p, TR7''p in figure 5.9) crossing the fault trace were used to provide detailed information on faulting evidence.

5.2.3. Near fault geomorphological analysis

In order to obtain a precise near-fault geomorphological map, a 0.25 m contour microtopographic map was levelled at the site (Fig. 5.2). This detailed geomorphology was also used to select the best location for trenching. The 25 m high El Hacho hill is located to the SE of the site. The hill is composed of well-rounded quartz conglomerates that contain *Balanus* (PII) of Pliocene age. Recent sediments resulting from the erosion

of the upper slopes have accumulated at the foot of the hill, whence the Quaternary alluvial fans extend to the NW. Two generations of alluvial fans are represented: A2 and A3. A3 fans overlie A2 fans. Moreover, two different lobes of A3 are differentiated. The stratigraphically lower one is locally termed A3*l*, which is more extensive than the upper one. A3*l* overlies A2 and has a sharp contact with the Pliocene hill. The upper lobe, which is termed locally A3u, is less extensive, overlies A3*l* and has well preserved fan morphologies. Chapter 4 describes two regional units in A3: A3.1 and A3.2. The el Hacho A3 fans overlying the A2 fans probably correspond to the A3.1 unit. The question is whether the upper lobe of this small fan (A3u) corresponds to the A3.2 generation or is still part of the A3.1. Owing to the local conditions of this area (small drainage area feeding the fan), A3.2 might differ from the rest of A3.2 at La Serrata. Further dating analysis should be done to confirm this. In any case, assigning a specific unit to this lobe is not relevant for the detailed paleoseismic study, and thus this differentiation is not taken into account for this local fan. Distinguishing the upper and lower lobe is relevant and is achieved by adding letters "*l*" (lower) and "u" (upper) to the A3 fan name.

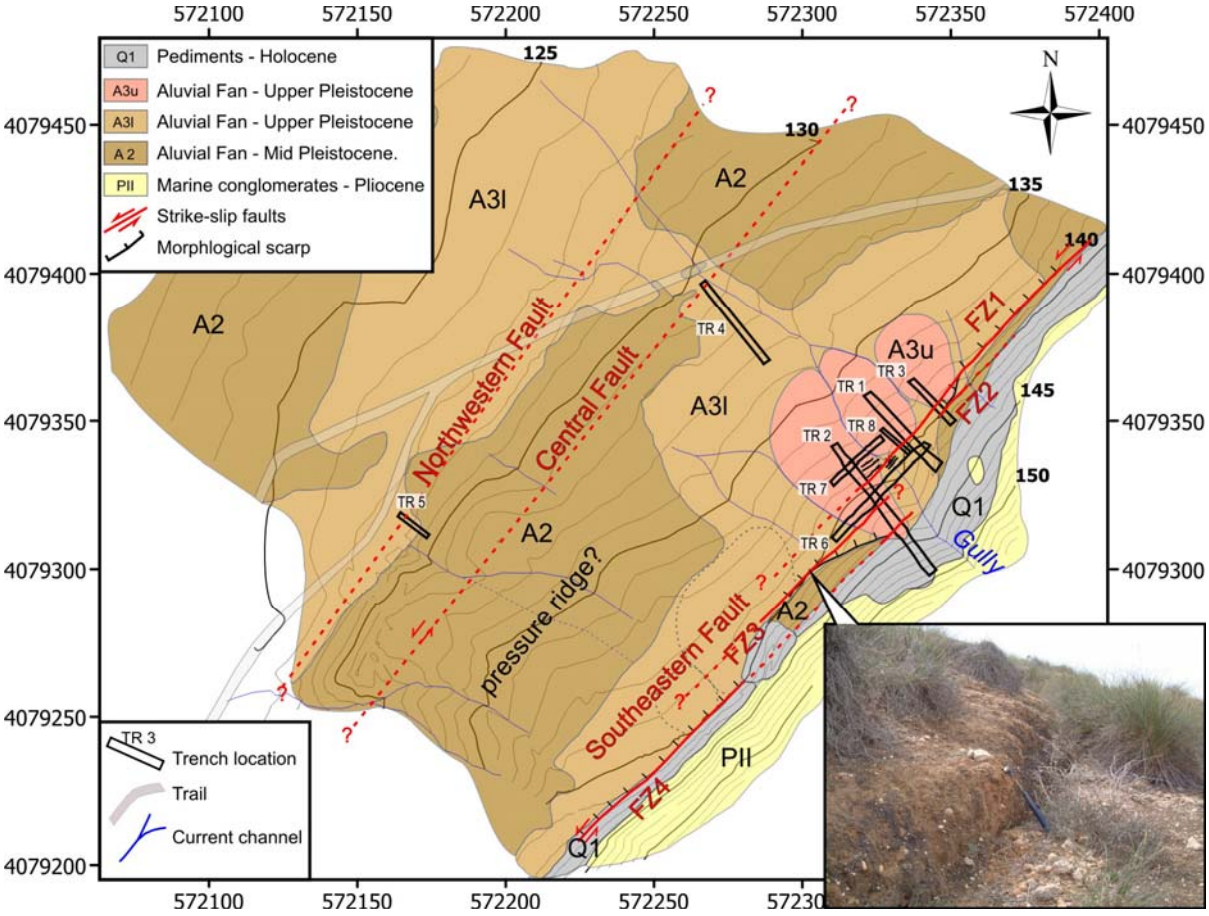

Figure 5.2. Near fault geomorphological map of the El Hacho site. Photograph shows the fault scarp in the Upper Pleistocene alluvial fan (hammer for scale).

Three fault traces were mapped in the area (Fig. 5.2): the southeastern fault, the central and the northwestern. The southeastern trace is the main fault trace of the site and is formed by an *en-échélon* fault zone whose successive fault traces are termed from NE to SW: FZ1, FZ2, FZ3 and FZ4 (Fig. 5.2). FZ1 and FZ4 fault traces are morphologically expressed on surface as a decimetre-high scarp (Fig. 5.2 detail picture) sharply delimiting the upper levels of the A3l deposit. Between FZ1 and FZ4, the releasing fault step-over produces a slight decrease in the topography, favouring the presence of channels draining the hill. The scarp is eroded there and changes its direction towards the hill. The northwestern and central fault traces (Fig. 5.2) are inferred from the deflected drainage and by the geophysical information. Moreover, these traces coincide with the presence of an elevated and apparently bounded strip of A2 alluvial fan interpreted as a pressure ridge. This elevated area is preserved thanks to the calcrete crust on top, and has generated along its NW limit a 3 m high rounded accumulative scarp probably produced by the northwestern fault trace.

Besides the incised channel descending the hill, the drainage is represented in the area by small incisions in the fan surfaces. These channels are beheaded and lack a drainage area, suggesting that they have been abandoned and offset from their original position, as discussed in Chapter 4 (section 4.4.3 and 4.5.3). The channels on top of unit A2 on the pressure ridge are more incised in the calcrete crust and are, therefore, well preserved, reflecting the uplift of the pressure ridge. It should also be noted that the apex of the small A3u lobes is not consistent with the present-day channels descending the hill, which suggests some offset after the formation of the lobe.

5.2.4. Subsurface structural analysis using geophysical techniques

5.2.4.1. Introduction

A large amount of information was obtained at the El Hacho site during two geophysical surveys. This dataset forms part of another thesis (M. Coll) and we shall only present here the results of the most significant profiles for further paleoseismic analysis.

The first survey took place prior to the first trenching and localized the areas most suitable for trenching. To this end, Ground Penetrating Radar (GPR) and Electrical Resistivity Tomography (ERT) methods were selected. Four different Ground Penetrating Radar (GRP) profiles (employing different frequency antennas: 25 MHz, 50 MHz, 100 MHz and 200 MHz) were acquired along 3 lines in order to: 1) obtain different resolution and penetration imaging, and 2) choose the best results for GPR facies and reflector characterization. All the GPR profiles were acquired in a continuous mode except the lower frequency antenna (25MHz), which was obtained in a step by step mode. ERT profiles were also acquired along the same GPR lines in order to combine the two methods. The array used for the ERT profiles was Wenner-

Schlumberger with electrodes spaced 2 m. GPR profiles obtained with four antennas and the ERT model (final model geoelectrical section obtained from inversion of ERT data) obtained along profile I (Fig. 5.3), which are perpendicular to the fault trace, are presented below.

A second GPR survey was developed in parallel to the 3D trenching survey in order to complete the information obtained from the trenches at the El Hacho site. Of the 17 profiles (Fig. 5.3) acquired with a shielded 270 MHz antenna, only the three profiles parallel to the fault zone (profiles K, L and M in Fig. 5.3) are shown here. These three profiles are located in the releasing fault step-over and were designed to identify linear features that were offset by the fault.

5.2.4.2. Imaging the sub-surface by Ground Penetrating Radar and Electrical Resistivity Tomography at the El Hacho site

The most fruitful information was obtained from the 50 MHz and 100 MHz GPR profiles that presented the best compromise between penetration depth and resolution. The 200 MHz profile (Fig. 5.3) shows low penetration (around 1.5 m) and a strong attenuation of the signal below the top reflections. The 25 MHz profile presents poor resolution and it was used only to corroborate information from the 50 MHz and 100 MHz profiles. In the ERT model, only the upper two meters of the profile should be considered given the poor resolution at the lower parts due to the resistence of electrical current flow of the upper units.

In the 50 MHz and 100 MHz GPR profiles (Fig. 5.3), three layered units were differentiated in accordance with the different frequency and the continuity of the reflections. The upper unit presents low frequency but good continuity reflectors. The intermediate unit presents some high frequency parallel reflectors with large undulations on top and a strong attenuation of the signal below it. The lower unit presents low continuity and low frequency reflections and is mostly characterized by the presence of small hyperbolas in the 100 MHz profile. Lateral disruptions of the reflectors are interpreted as faults. At the top of the ERT model, two zones of different resistivity can be distinguished. The SE half of the profile is characterized by a conductive (red) area and the NW half by a more resistive (blue) area.

Given the similar composition of the units at this site, little contrast is expected between them. However, strong reflections were observed in the GPR profiles and these are thought to be produced by the calcrete crust on top of the alluvial units. The upper unit identified in the GPR profiles is interpreted as the loose sediments of the A3 alluvial unit. The intermediate unit is interpreted as the A2 alluvial unit with the calcrete crust on top and loose sediments below it. The lower unit is interpreted as the thick calcrete crust overlying the A1 alluvial fan. This fan does not crop out in the area despite the fact that it is thought to be underlying the A2 fan.

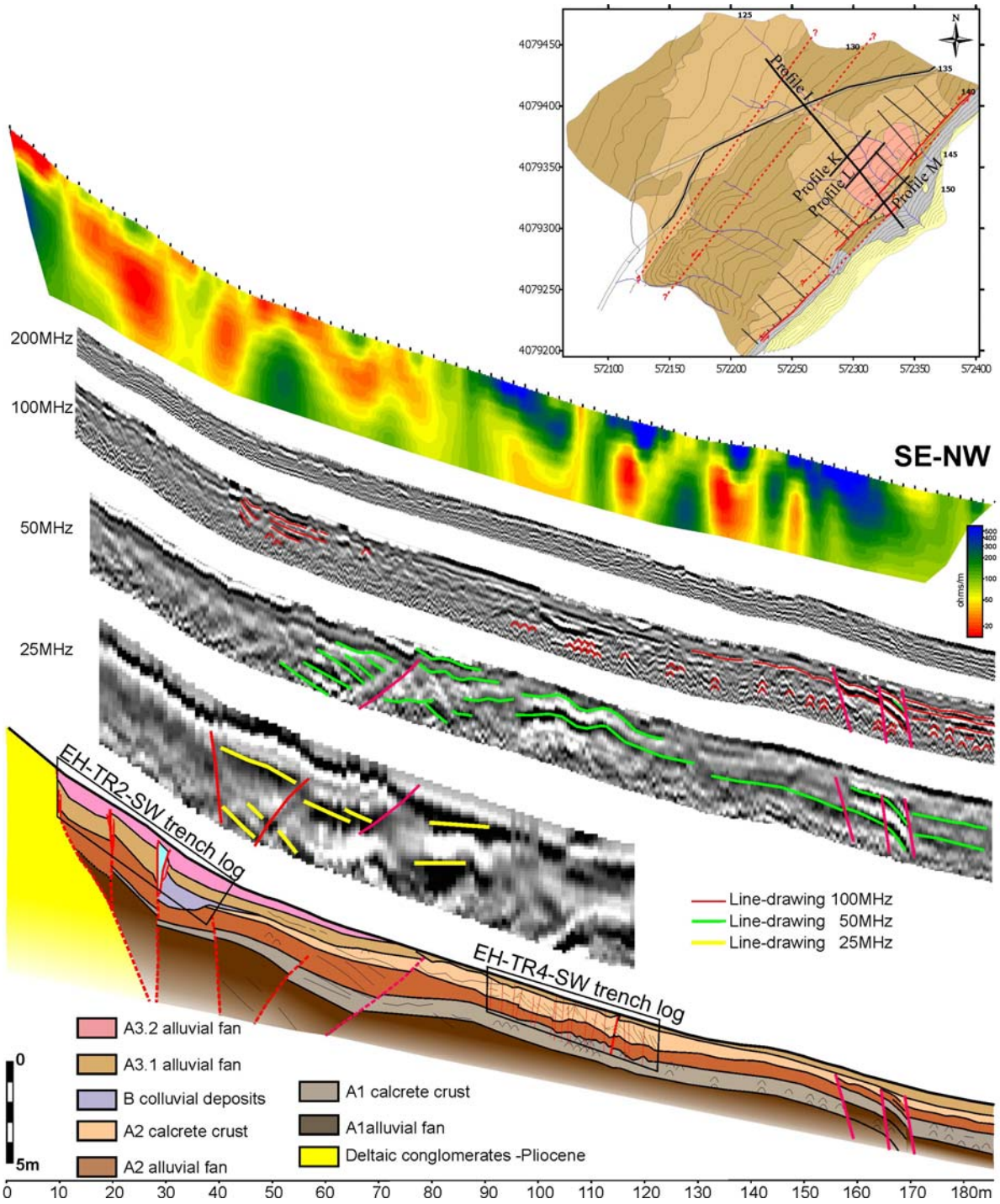

Figure 5.3. ERT model and GPR profiles acquired along profile I (location in the El Hacho microtopographic map above). GPR profile is presented with the four antennas used (25 MHz, 50 MHz, 100 MHz and 200 MHz). Below, a geological interpretation based on the geophysical profiles and further trenching observations. Trenches EH-TR2 and EH-TR4 will be presented and discussed below.

The strong attenuation of the ERT signal in very high resistivity zones is attributed to the presence of the thick calcrete crust. In the top of the model, the two zones of different resistivity are related to different sedimentary units. To the NW, the most conductive area is interpreted as the response of the A3 alluvial fan which is rich

in clays (high conductivity materials). To the NW, a more resistive area (blue) represents higher resistivity materials interpreted as a larger amount of calcrete crust close to the surface.

The integration of ERT, GPR and further trenching observations together with the geomorphological analysis of the area provided a geological interpretation of the subsurface at the El Hacho site (Fig. 5.3). The three-layered alluvial units are depicted and two fault zones identified. The fault zone located to the SE is a 70 m wide fault zone formed by diverging fault strands depicting a flower structure. The northwestern traces of this fault zone are represented on surface by the main fault zone of the area (the southeastern fault zone in Fig 5.2). The fault zone located to the NW is smaller, 1.5 m wide, and consists of three sub-vertical fault traces. This fault zone is represented on surface by the northwestern fault zone (Fig. 5.2) of the area. The central fault zone of the area is not clearly displayed by the GPR profiles, suggesting that its vertical component is probably small and that the reflections are not vertically displaced.

Profiles acquired during the second GPR survey show the same GPR units. Moreover, the three GPR profiles parallel to the fault zone show an approximately 1.5 m wide zone characterized by a sudden lateral change in the amplitude reflections (indicated by a red arrow in figure 5.4). This local unit is interpreted as the buried paleo-channel identified in the 3D trenching. Further analysis of the GPR profile will help to extend the unit observed at the trench wall to a wider area.

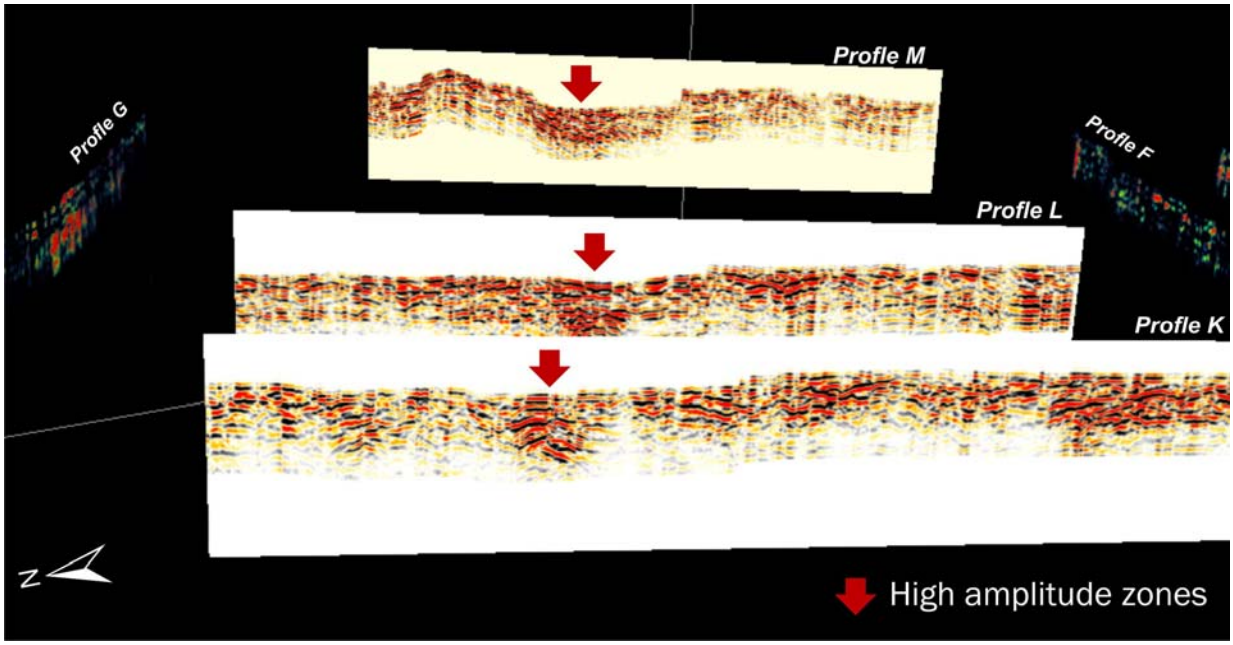

Figure 5.4. GPR profiles K, L and M running parallel to the fault trace. See location in the microtopographic map of Fig. 5.3.

5.2.4.3. Conclusions

GPR and ERT geophysical methods enabled us to conduct a rapid and relatively cheap survey of the study area before excavating the trenches. These methods increase the possibility of trenching across faults. Trenches allow the correlation of the sedimentary units with their geophysical GPR facies and resistivity areas, which can also be extrapolated to other profiles.

At the El Hacho site the interpretation of GPR profiles allowed the identification of different units and the interpretation of fractured zones, the 50 MHz and 100 MHz antennas being the most useful frequencies. At this site, the ERT models gave only information about the uppermost metres because of the specific lithologic characteristics.

5.2.5. Trenches perpendicular to the fault zone

5.2.5.1. Description of trenches

Trenches TR1, TR2 and TR3 at the El Hacho site were dug across the main fault trace (Fig. 5.5) and show Quaternary deposits affected by a main fault zone (FZ1 in Fig. 5.2) in the centre of the trench. Trench TR2 also shows two minor faults (FZ2 and FZ3) to the SE of the main fault zone. The block between FZ1 and FZ2 is uplifted. Besides the current soil, 5 Quaternary depositional units can be distinguished running sub-parallel to the ground surface (A2, B1, B2, A3ℓ, A3u). Three of these units correspond to the three alluvial units observed on surface (A2, A3ℓ, A3u) (Fig. 5.2). In a lower stratigraphic position, unit A2 crops out as brown silts, sands and quartz-rich pebbles commonly covered by a thick (up to 70 cm) white and reddish massive calcrete crust with angular carbonate concretion and interbedded laminate layers. Units A3ℓ and A3u are commonly placed on top of A2, and are formed by brown and reddish silts and sands slightly darker than unit A2, with well-rounded quartz pebbles and small angular carbonate pebbles. Unlike A2, Unit A3 lacks calcrete crust. Only incipient carbonatation processes are observed (sub-millimetric pisoliths levels). In both lobes of unit A3, several sub-units can be distinguished at the same time. Each sub-unit is usually formed by a cobble rich erosive base and a fining upward gradation. Texture and colour variations are also observed and small channels are found within the unit. These subunits are interpreted as corresponding to different phases of aggradation of the alluvial fan.

Besides the units observed on surface, two additional units are observed in the TR1 and TR2 trench walls, termed units B1 and B2 in figure 5.5. These wedge shaped units only appear next to the northwest side of the main fault zone and are made up of carbonate cobbles dispersed in a fine matrix. The matrix is brown to reddish with a slight fining upward sequence in each unit. B1 and B2 become completely white in the upper parts of each unit and close to the fault zone owing to a strong calcification. The

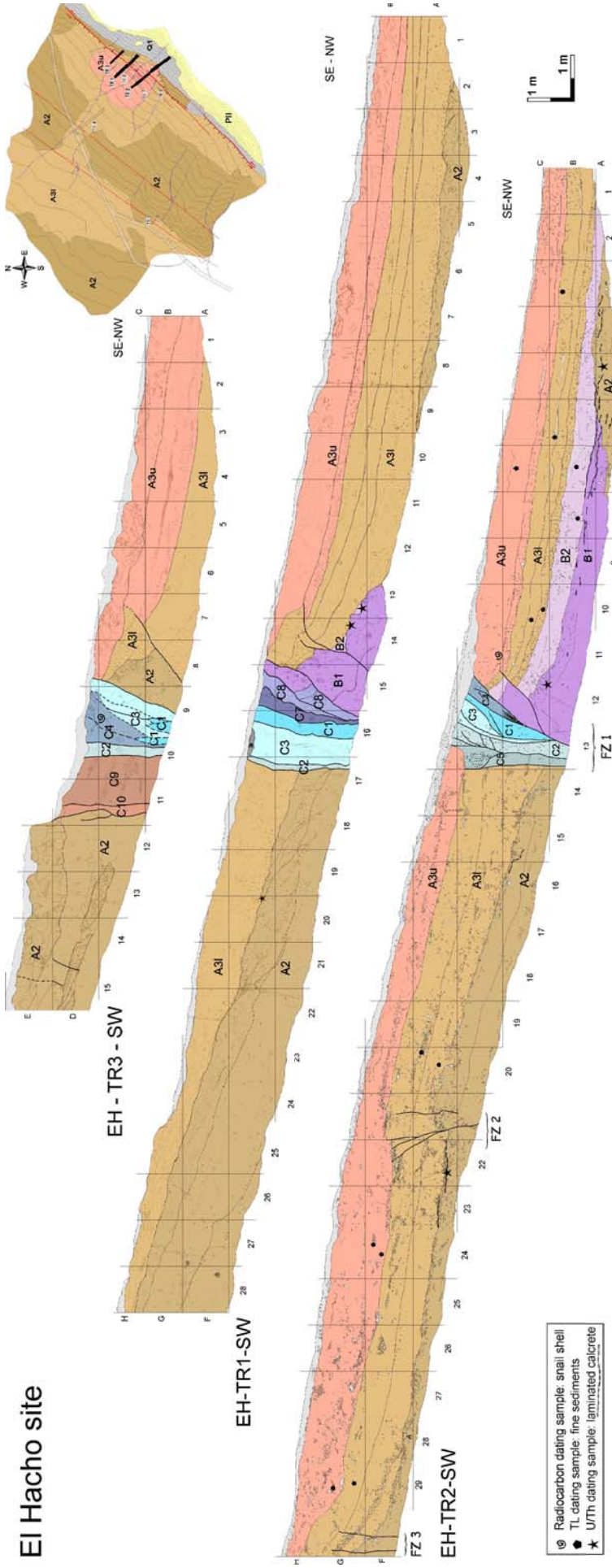

Figure 5.5. SW walls of trenches TR3, TR1 and TR2 placed successively from NE to SW along the main fault trace at the El Hacho site. Units and structures are described in the text. Dated samples are indicated (see legend). See map for relative location of trenches.

top of B2, is covered by a thin carbonatic crust formed by pisoliths and incipient millimetric laminated layers. Unit B1 onlaps A2 and unit B2 overlies B1 and extends further onlapping A2. B1 and B2 are interpreted as two colluvial wedges ascribed to sudden faulting events, originated from the degradation of a fault scarp.

The main fault zone (FZ1) is observed in all the trench walls and its upper metres correspond to a 1 m wide fault zone breaking up to the surface. This fault zone is formed by several sub-vertical stripes of crushed and fine sediments (C1 to C10 in figure 5.5). Its composition may vary depending on the origin of the sediment and the degree of crushing. Sigmoidal P-C structures are observed on the wall and on the floor of the trenches of FZ1. Sigmoids on the floor are very well defined and indicate a left-lateral motion. Sigmoids on the wall are smaller and exhibit a reverse movement, although less significant than the strike-slip movement. The scarp observed on surface (Fig. 5.2) is also observed in EH-TR3 (Fig. 5.5), where it corresponds to a fault and is therefore interpreted as a fault scarp. This is probably retrograded as the main fault zone is constrained by units C1 to C8. Units C9 and C10 have the same A2 fan composition although distorted, displaying a light vertical foliation and suggesting some kind of incipient inclusion in the fault zone. The calcrete crust on top of C9 and C10 may have been crushed by the rupture, and the scarp may have eroded backwards. FZ2 and FZ3, only observed in the longer trench EH-TR2 (Fig. 5.5), are less complicated and only affect as far as the A3ℓ lobe with less than 0.5 m apparent vertical displacement.

Trench EH-TR4 (Fig. 5.6) presents a 1.5 m thick sequence of continuous A2 alluvial fan made up of brown sands and clays with pebbles at the base and an almost 1 m thick layer of densely fragmented calcrete crust on top. Overlying this calcrete crust is a thin layer of A3ℓ that is transformed into soil. No faults were observed in this trench.

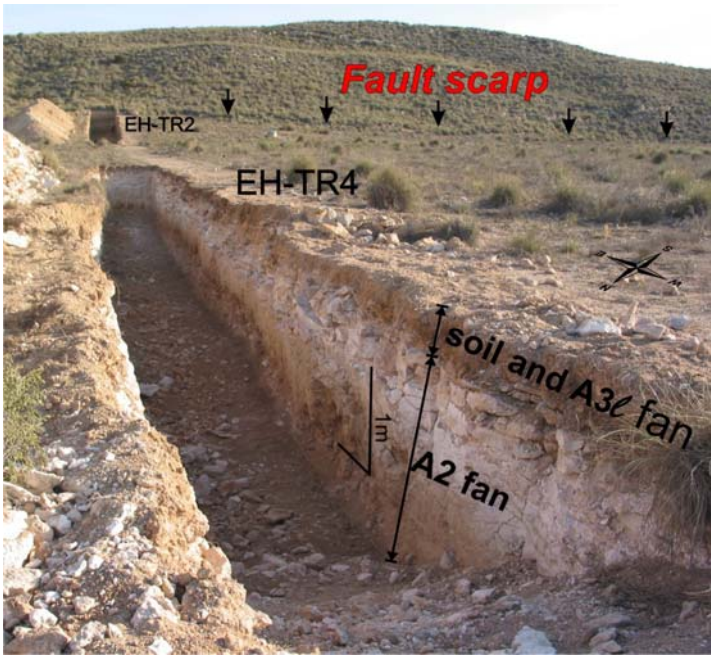

Figure 5.6. Photo of the EH-TR4 trench at the El Hacho site. This trench was not logged in detail owing to the absence of paleoseismic information. The EH-TR2 and the hill built on Pliocene Q-rich conglomerate are shown in the background of the picture.

EH-TR5 at the El Hacho site (Fig. 5.7) was not logged in detail because of the absence of exposed units and paleoseismic information. It presents a thick layer of A2 alluvial fan similar to that observed in EH-TR4. To the SW, a thin layer of A3ℓ lobe transformed into soil is observed. A flexure of the calcrete crust on top of A2 is observed in the southwestern part of the trench where the calcrete crust is tilted towards the SE. This structure resembles a fault propagation fold. The upper A3 unit does not seem to be affected by this flexure, although this should be verified by additional trenches.

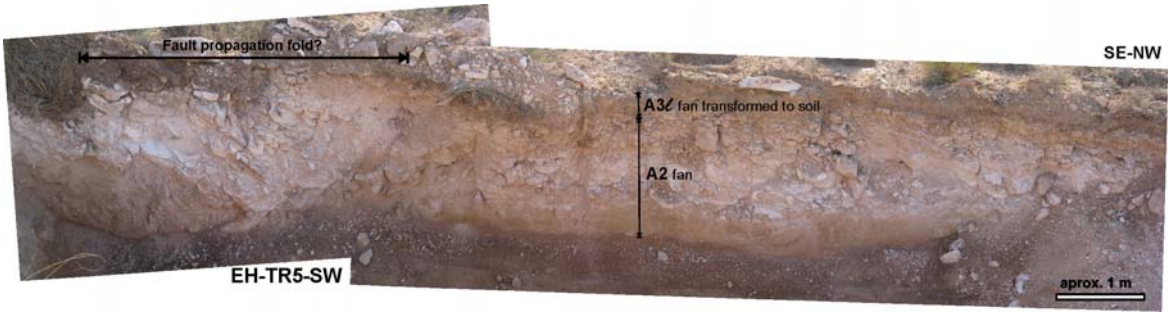

Figure 5.7. Photo-log of the SW wall of trench TR5 at the El Hacho site.

5.2.5.2. Event horizons and dating analysis

Trench EH-TR2 shows the maximum number of events, some of them also interpretable in other trench walls. The SW wall of this trench is shown in figure 5.8a as a compilation of the events observed (Fig. 5.8c) and the samples dated (Fig. 5.8b) in order to constrain the age of the events.

Units B1 and B2 are interpreted as colluvial wedges because of their local extension, chaotic texture, wedged shape and geometric relationship with the main fault zone. Although they overlap one another, they were differentiated as different wedges according to fining upward sequences of the matrix and incipient soil development on top. Colluvial wedges are formed soon after a rapid uplift of the fault scarp (seismic event) and thus, units B1 and B2 provide evidence of the seismogenic character of the CFZ. Each base of colluvial wedge delineates an event horizon, and thus B1 and B2 bases define the two older event seismic horizons observed in the trench (Fig. 5.8c): event E1 at the base of B1 and event E2 at the base of B2. The NW branch of FZ1 and the entire FZ2 affect the sedimentary units as far as the base of A3u (cells C11 and F22 in figure 5.8c), indicating a seismic event during the aggradation period of A3u. Thus, a new event horizon (event E3) is observed close to the base of A3u. Finally, the youngest event, E4, is observed at the base of the current soil, the only unit of the trenches not affected by the main fault zone.

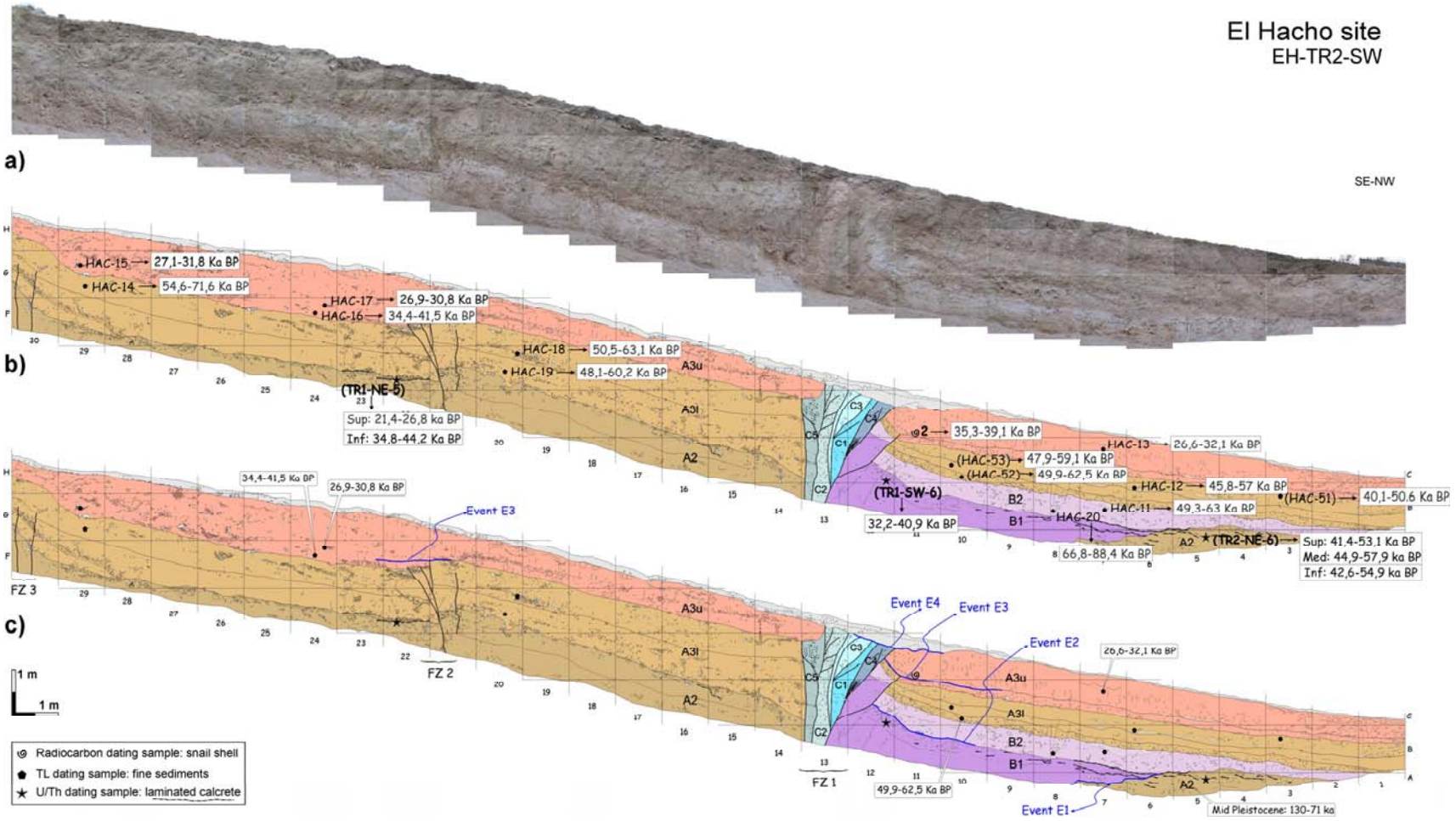

Figure 5.8. a) Photo-log of the SW wall of the EH-TR2 trench at the El Hacho site. b) Compilation of dates obtained at the El Hacho site. Most of the samples were obtained at the EH-TR2-SW wall. Samples in brackets are projected from the same position on other trench walls. c) Event horizons and ages used for constraining the paleoseismic events. See text for discussion.

An extensive analysis of all the dated samples at La Serrata is presented in Chapter 4 together with a discussion of the age of the units at La Serrata. However, units B1 and B2 are not discussed there because of their local extension. Two TL samples (HAC-11 and HAC-20) and one U/Th sample (TR1-SW-6) were obtained in this unit as a test (Fig. 5.8b). TL ages are not considered as valid ages for dating the formation of a colluvial wedge because of the uncertainty of exposure to sunlight (colluvial wedges can be formed rapidly) and because of probable calcite variation after deposition (water circulation close to the fault zone). The U/Th dates are younger than the age of the overlying units (A3 deposit) that are considered to be well constrained by the TL method. This suggests a late growth of the $CaCO_3$ probably because of the circulation of underground water in the fault zone. Thus, the age of the colluvial deposits is not constrained by radiometric dating and we can only perform a relative dating: younger than A2 and older than A3l. Moreover, the unit might be younger than the primary calcrete on top of the A2 unit (formed soon after the fan aggradation) but not necessarily younger than the secondary calcrete (formed in successive fan aggradation and stabilization phases). As discussed in Chapter 4, the calcrete dated at the El Hacho site may correspond to secondary calcrete, and the regional analysis of primary calcretes on top of this unit suggests they were formed during the Marine Isotope Stage 5: that is, 130-71 ka BP. Thus B1 and B2 are certainly younger than 130 Ka BP, although this is a minimum age constrain and they are most probably tens of thousands of years younger than 130 ka BP.

The oldest time bracket of events E1 and E2 is constrained by the age of the primary A2 calcrete and the youngest by the age of the lower sample of unit A3ℓ (HAC-52), i.e. events E1 and E2 are both constrained between 130 ka and 49.9 ka BP. Event E3 is controlled by TL samples located slightly above and below the event horizon (HAC-16 and HAC-13), and thus constrained between 41.5 ka BP and 26.6-32.1 ka BP. Event E4 can only be constrained in its lower limit by the stratigraphically upper sample of unit A3u (HAC-13). Event E4 is therefore younger than 32.1 ka BP.

5.2.5.3. Paleoseismic results

A total of 4 events were identified in the trench walls although some other events may not have been recorded. Thus, a minimum of four events have occurred since Mid Pleistocene. Using the age of the primary calcrete crust on top of A2 (130-71 ka BP) to constrain the lower age of these events, a mean recurrence period of 32.5 ka since 130 ka BP was calculated. The poor accuracy of time constraints of the two older events together with the possibility that only some of the events were recorded could result in an overestimation of the recurrence period.

A strike-slip structure, such as the CFZ, displacing laterally an irregular topography such as the A2 calcrete crust, which is assumed to be convex (covering an

alluvial fan) and irregular in a transversal cross section, can show a large variation of the apparent vertical slip along the fault trace. Despite this uncertainty, the thickness of a colluvial wedge can be used as an approach to the vertical amount of displacement. The A2 calcrete crust is considered to be the ground surface at the time of event E1. The thickness of the colluvial wedges above it was measured on the trench wall to estimate the vertical amount of displacement during E1 and E2. The base of B1 is not observed, and thus B1 is assumed to be thicker than 1.2 m. B2 is 0.37 m high (Fig. 5.8). Klinger et al., (2003) considered that the dip-slip is about twice the maximum thickness of the colluvial wedge. Thus, vertical displacements were estimated to be >2.4 for the event E1 and 0.74 m for E2. From these measurements, dip-slip rates can be estimated taking into account that they occurred later than the age of the primary A2 calcrete crust (130-71 ka BP). Thus, a minimum dip-slip rate of 0.02 mm/a since 130 ka BP was calculated from the >2.4 m of vertical displacement inferred from the B1 colluvial wedge.

Wells & Coppersmith (1994) proposed an empirical relationship relating the moment magnitude (Mw) with the maximum displacement (MD).

Mw = a + b * log (MD) where a = 6.69 +/-0.04 and b= 0.74 +/-0.07 are the coefficients obtained for an average of reverse, normal and strike slips. For this equation the standard deviation is s=0.40 and the correlation coefficient is r = 0.78.

The moment magnitude of events E1 and E2 can be estimated with the Wells & Coppersmith (1994) regression from the thickness of the colluvial wedges. Magnitudes were calculated first using the observed thickness of the colluvial wedge (minimum vertical displacement) and then assuming the vertical displacement to be twice as thick as the wedges (Table 5.1). The results range between >6.7->6.9 for event E1 and between 6.4-6.6 for event E2.

Table 5.1: Relations between the thickness of the colluvial wedges, the vertical displacement and the moment magnitudes.

Event	Unit	Thickness of the CW	Moment magnitude	Min. dip-slip rate	Moment magnitude
E1	B1	>1.2 m	>6.7	>2.4 m	> 6.9
E2	B2	0.37 m	6.4	0.74 m	6.6

However, according to the uncertainties of vertical displacements for strike-slip faults, the dip-slip rate and the moment magnitudes obtained from the measurement of the colluvial wedges have a weak paleoseisemological meaning and must be regarded as a coarse approximation.

5.2.5.4. Summary

Trenches perpendicular to the fault zone at El Hacho show a minimum of four events since 130 ka BP, suggesting a minimum mean recurrence period of 32.5 ka. Nevertheless, this value is probably larger than the real one because of the poor accuracy when constraining the age of the oldest events and the possible missing events. Two colluvial wedges provided evidence of the seismogenic character of the Carboneras Fault and were used to estimate a minimum dip-slip rate of 0.02 mm/a and preliminary moment magnitudes from 6.4 to >6.9. However, these results are weak since the CFZ is predominantly a strike-slip structure, and thus 1) its apparent vertical displacements can vary significantly along the fault trace, and 2) its net slip is probably larger. The maximum magnitude is therefore probably larger.

5.2.6. 3D trenching: parallel to the fault zone

At the El Hacho site, a present-day channel is slightly incised in the younger deposits and is slightly deflected in the fault zone (Fig. 5.2). If the fault trace was active, an offset and abandoned channel could be found buried in the opposite part of the fault to the southwest of the present-day channel (the drainage area and the flow pattern has not significantly changed over the last thousand years) in line with the left-lateral movement of the fault. In order to check this hypothesis and to localise this abandoned channel (paleo-channel), two trenches (TR6 and TR7 in Fig. 5.2) were dug parallel to and on each side of the fault zone close to the channel. On the southeastern side of the fault, a paleo-channel depocenter practically coincides with the current channel incision (TR6-NW in Fig. 5.9). On the northwestern side of the fault, a buried paleo-channel is present with its depocenter displaced to the SW with respect to the current channel (TR7-SE in Fig. 5.9). Projecting the near field strike of the channel towards the fault trace yields a 3 m offset. To ascertain whether this is a real offset or whether the channel is naturally oblique to the fault (and therefore the offset can be lower or even null), several slides parallel to the trenches were dug across the channel closer and closer to the fault zone: TR6’ and TR6’’ on the southeastern side of the fault zone and TR7’, TR7’’ and TR7’’’ on the northwestern side of the fault zone. To the SE of the fault, the channel is straight and perpendicular to the fault trace and to the NW, a slight deflection is observed. Finally, a strong deflection is observed in the last metre close to the fault zone. Smaller slides across the fault zone were open (TR6’’p and TR7’’p in figure 5.9), which provided evidence of a faulting event cutting the paleo-channel filling (Fig. 4.13b).

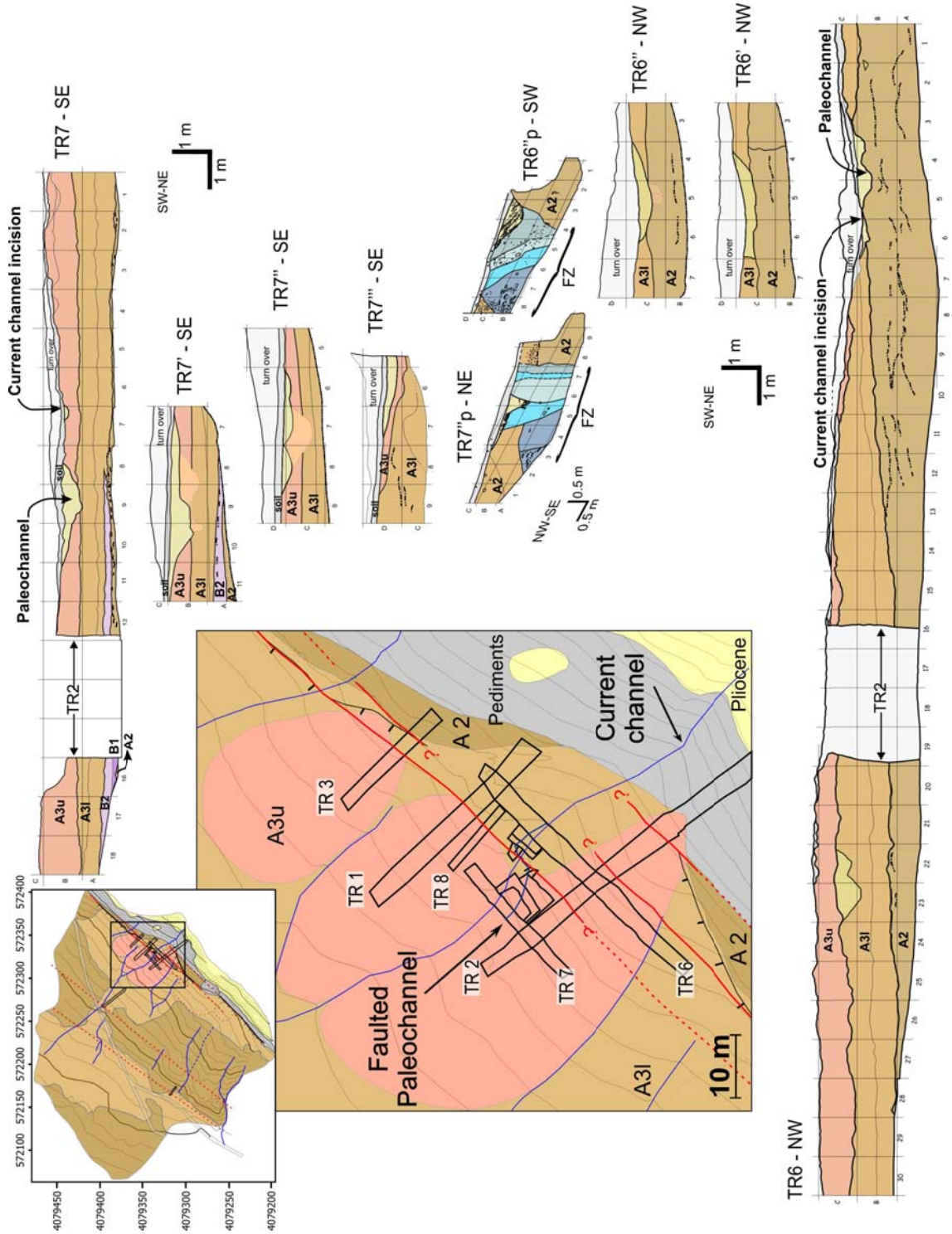

Figure 5.9. Trench logs from the 3D trenching survey at the El Hacho site. Trench slides are located schematically. Slides are termed Tr7', Tr7'', Tr7''' in successive slides parallel to TR7, and likewise for TR6. The last slides are orthogonal to the fault zone and are depicted with the letter p (Tr7"p and Tr6"p). TR7 and successive slide logs were flipped to be comparable to the TR6 logs.

5.2.6.1. *Description of trenches*

The main units observed in trenches in the 3D survey are described in section 5.2.5.1 and the same labels are used in figure 5.9. The only new deposit is the paleo-channel infilling made up of fine sediments and pebbles, removed from the upper alluvial fans, with a high percentage of organic material providing a darker aspect. Downwards the organic material penetrates the paleo-channel limits and darkens the A3 alluvial fan where it is incised. The paleo-channel width varies from 2 to 5 m of extension. In the NW part of the fault zone, it is mainly incised in the A3u fan lobe although it reaches down to the top of A3ℓ deposits. In the SE part of the fault zone it is incised directly in the A3ℓ fan and further down to the A2 alluvial fan.

5.2.6.2. Dating analysis

Several charcoal samples were obtained from the paleo-channel infilling sediments (Fig. 5.10). Three of these samples were large enough to be dated by radiocarbon and results are listed in table 5.2.

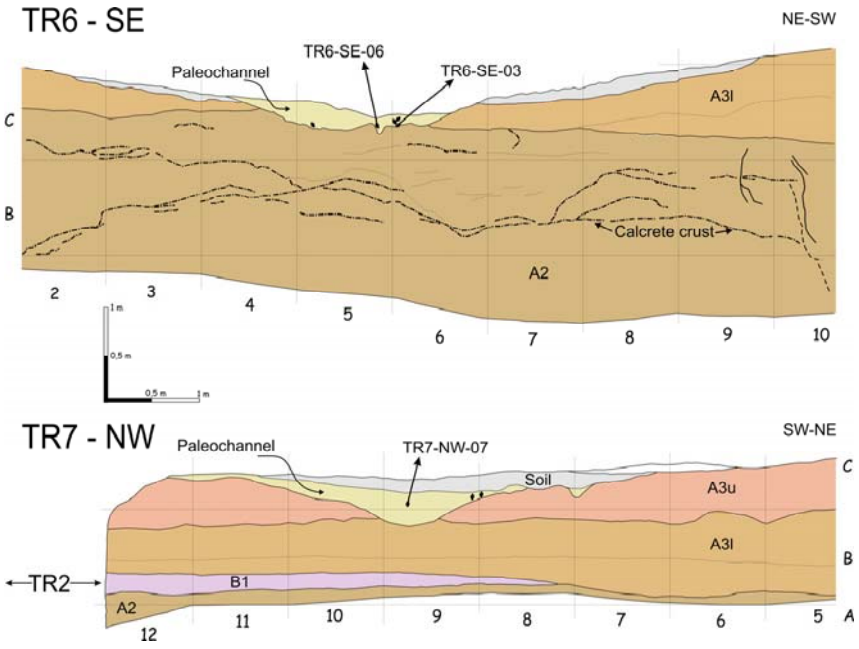

Figure 5.10. Location of dated samples from the paleo-channel found in trenches TR6 and TR7 from the El Hacho site.

The deposit filling the paleo-channel does not show any stratigraphic differentiation and is therefore considered to have filled up rapidly. Thus, the charcoal samples are interpreted to be of the same age, and the differences obtained from the radiocarbon results are interpreted as a typical deviation produced by the dating uncertainty. The weighted mean of the non calibrated Gaussian probability distributions

is calculated to obtain an average age from the three dated samples (Taylor, 1982), and the resulting age range is calibrated. The weighted mean results of 1184.8 +/-23.0 ^{14}C yrs, and its calibration yields 1016-1175 Cal yr BP (2 σ) age, i.e. AD 775-934. This age was considered for further paleoseismic analysis.

Table 5.2: Radiocarbon results for samples obtained from the paleo-channel at the El Hacho site. Calibration was done using the Calib 5.0.2 software. Pch: palochannel.

Sample	Sample type	Unit	Lab	$^{13}C/^{12}C$ (‰)	Conventional ^{14}C Age (BP)	2 σ Calibration (BP)	2 σ Calibration (AD)
TR6-SE-3	Charcoal	Pch	NOSAMS	-22,56	1190 +/-25	1013 - 1178	772 - 937
TR6-SE-6	Charcoal	Pch	NOSAMS	-25,96	1130 +/- 70	926 - 1241	709 - 1024
TR7-NW-7	Charcoal	Pch	NOSAMS	-25,07	1220 +/- 110	929 - 1313	637 - 1021

5.2.6.3. Paleoseismic results

The apparently 3 m offset paleo-channel is ascribed to two events: Ea corresponds to the older event and Eb to the younger event. More than two events could be considered but this is unlikely for such a recent channel, given that the incision may have occurred not long before the sediment infilling dated at 1016-1175 Cal yr BP. During the first event (event Ea), the channel incision was offset but not enough to abandon the path on the northwestern side of the fault. The channel geometry was subsequently smoothed in the fault zone producing a sinuous deflection. Thereafter, the channel filled with organic-rich sediments and was faulted again (event Eb) rupturing the channel infill and adding these sediments to the fault zone as observed in TR7''p (Fig. 5.9). Given that Ea affected only the channel incision and since no recent sediment was affected, dating cannot accurately assign an age to this event. We can only assume that this event is younger than the A3u alluvial fan where the paleo-channel is incised; this is younger than 32.1 ka BP (Fig. 5.8) although it is probably much younger. Eb occurred after the infilling of the paleo-channel. Thus, Ea is constrained between 32.1 ka BP and 1016 Cal yr BP, and Eb is constrained between 1175 Cal yr BP and the present day (i.e. between AD 775 and the present day). These results indicate the occurrence of an event during the Holocene and possibly coinciding with the AD 1522 Almería earthquake.

According to the unlikely probability of more than 2 large events affecting the paleo-channel, Ea and Eb can be interpreted as successive events and the time elapsed between these two events could represent a seismic cycle. The age of Ea is well constrained (AD 775-Present day) but the lower age constraining Eb (32.1 ka BP-1016 Cal yr BP) can be much older than age of the event. This uncertainty of the lower age for Eb results in a considerable overestimation of the maximum time between the two events, which is 32.1 ka BP. However, according to the age of the sediment infilling (1016-1175 Cal yr BP) the incision is interpreted to have occurred not long before, and

is probably of Holocene age. Although no numerical results can be achieved, an elapsed time of few thousand years between the two events and the occurrence of a minimum of two Holocene events are suggested. Nevertheless, a more accurate constraining of event Eb is needed to support this hypothesis.

A maximum slip per event of 1.5 m is inferred assuming 1) a characteristic behaviour of the fault 2) two events affecting the paleo-channel and 3) a 3 m maximum offset. This slip can be used to estimate a strike-slip rate. The time elapsed since the younger event (Eb) probably does not cover a whole seismic cycle. Taking this event into account yields a maximum strike-slip rate of 1.3 mm/a since AD 775. If we consider the previous event (Ea), a weak paleoseismic result is achieved because it is calculated from a) a maximum slip, and b) an overestimated lower age. However, the uncertainty derived from the age overestimation is considered to be significantly larger than the uncertainty derived from the maximum slip, and thus, a minimum strike-slip rate is inferred, resulting in 0.05 mm/a since 32.1 ka BP. In summary, although both results deals with uncertainties, it can be assumed that the strike-slip rate is constrained between 0.05 mm/a and 1.3 mm/a.

The empirical relationships of Wells & Coppersmith (1994) provide an estimation of the moment magnitude related to the maximum displacement per event with the following equation:

Mw = a + b * log (MD) where a = 6.81 +/-0.05 and b= 0.78 +/-0.06 are the coefficients obtained for lateral slips. For this equation the standard deviation is s=0.29 and the correlation coefficient is r = 0.90.

Given the 1.5 m of maximum horizontal displacement for the paleo-channel, and given the coefficients errors, the maximum moment magnitude calculated ranges between Mw 6.9 and Mw 7.0.

5.2.6.4. Summary

The observation of a faulted and buried paleo-channel has provided evidence for at least two events since the formation of the channel incision. Event Ea is constrained between 32.1 ka BP and 1016 Cal BP, and event Eb between 1175 Cal yr BP and the present day, providing evidence of the existence of at least one Holocene seismic event, which may correspond to the AD 1522 historical earthquake that destroyed the town of Almería.

Events Ea and Eb are considered to be successive with a maximum elapsed time of 32.1 ka BP. However, because of the geomorphological evolution constraints, a much lower value (about few thousand years) is yielded.

From the paleo-channel offset, a maximum slip per event of 1.5 m is inferred. This offset suggests a strike-slip rate constrained between 0.05 mm/a and 1.3 mm/a, which is the minimum value calculated for the last 32.1 ka BP and the maximum value for the last 1175 Cal yr BP. Furthermore, a maximum moment magnitude of 6.9-7.0 is obtained from the maximum slip per event.

5.2.7. El Hacho Gully trench

5.2.7.1. Description of trenches

Both walls of El Hacho gully trench show a fault zone separating Pliocene quartz-rich calcarenites to the SE from a well stratified Tp fluvial terrace of Upper Pleistocene age to the NW (Fig. 5.11). Tp is also clearly visible in a natural outcrop a few metres from the trench and along a gully (Fig. 4.13), where deeper parts of the unit are exposed. This unit is made up of millimetric pebbles with slightly cemented reddish

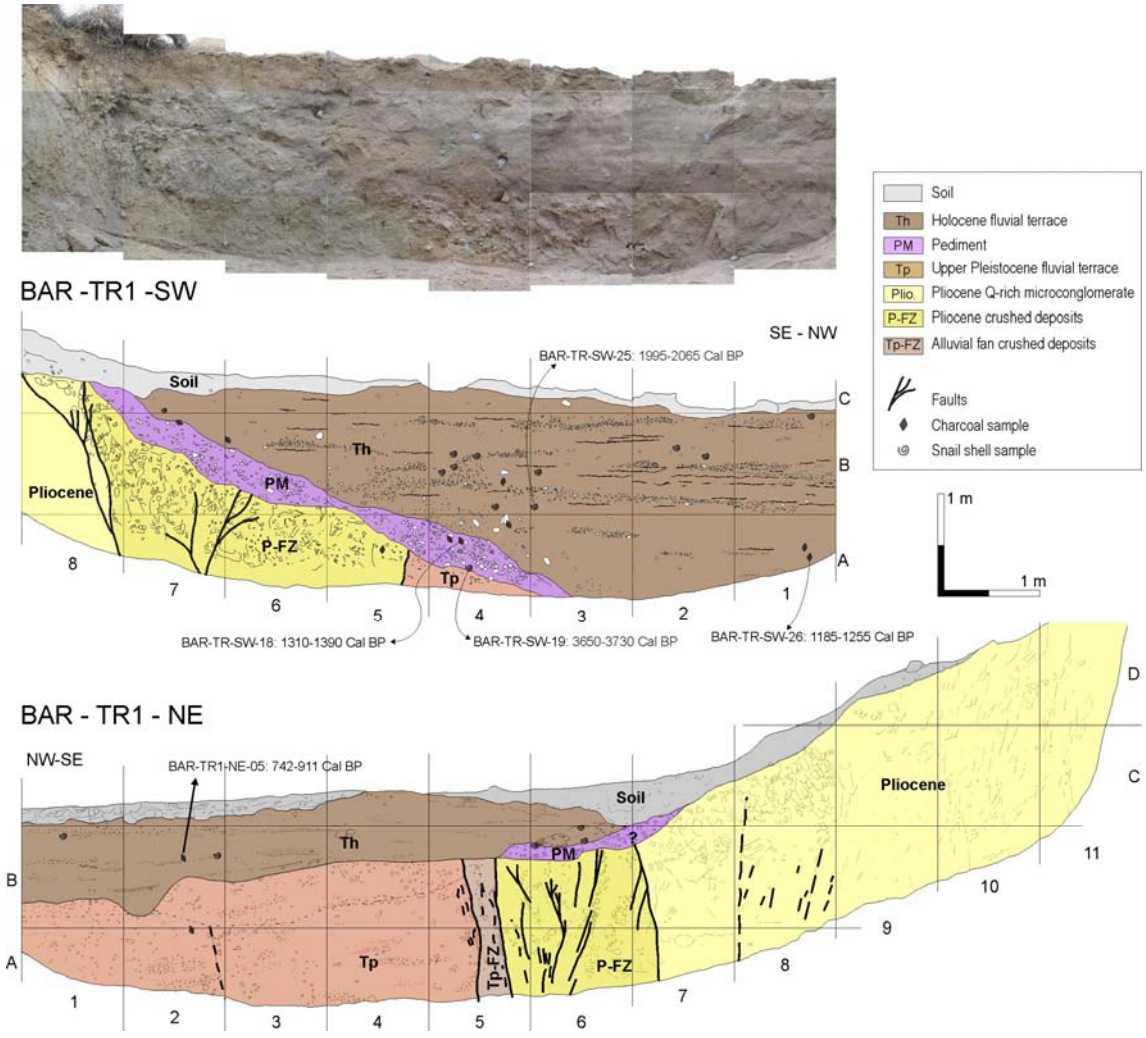

Figure 5.11. Trench logs of the two walls from the trench open at the El Hacho Gully site.

to brown fine-sandy matrix. The deposit presents interbedded sub-horizontal channel-shaped levels composed of well rounded centimetric pebbles of quartz and bioclastic composition. A local thin lentil-shaped greyish pediment deposit (PM) onlaps part of the fault zone for more than 4 m. It is formed by angular sandy, quartz and carbonatic gravels chaotically dispersed in a fine matrix. Upwards, a well stratified fluvial terrace (Th) is deposited on the pediment deposit or directly on the Tp fluvial terrace. Th is formed by a very well stratified intercalation of grey-to-black clays and silts and fining upwards sequences of very well sorted ochre sands and pebbles. Up to 3 m wide and 10 cm high interbedded channels contain abundant snail shell fragments. In the upper centimetres, a current loose soil rich in organic materials with a darkish colour is present.

The fault zone is 3 m wide in the SW wall and almost 2 m wide in the NE wall (Fig. 5.11). It is formed mainly by vertical blocks of crushed Pliocene materials, although a thin block of crushed Tp unit is observed in the NE wall. These blocks have several sub-vertical faults and vertical foliation. In the gully outcrop (Fig. 4.13), the 6 m wide fault zone mainly affects the Tp deposit with clear flower structures and well differentiated faults.

5.2.7.2. Dating analysis

Charcoal and snail shell fragments were extracted from the pediment deposit and the Th fluvial terrace. Moreover, some snail shells from the Tp deposit observed in the natural outcrop (Fig. 4.13) were also extracted for dating. As discussed in section 4.3.2.3 and given the dating results, snail shells act as open systems. This has implications for dating analysis, yielding older ages than charcoal samples. Thus, charcoal samples are preferred.

We used charcoal samples to date the Th fluvial terrace. An age of 1185-1255 Cal yr BP was assigned to the lower part and an age of 742-911 Cal yr BP was attributed to the upper part. Thus, this deposit was slowly formed during the late Holocene along several hundreds of years. Snail shells from the Tp unit have a 2 σ calibrated age of 45.7-43.4 Cal kyr BP. Despite the uncertainty of the radiocarbon method in such an old sample, this date gives an approximate age, confirming an Upper Pleistocene age. Two samples from the PM deposit were also dated and give consistent ages, slightly older than the upper Th deposit. Nevertheless, because of the chaotic character of this unit, the samples could have been re-worked, and thus the result could lead to confusion. For this reason, these ages were not considered.

5.2.7.3. *Paleoseismic results*

The aim of the trench at the El Hacho Gully site was to ascertain whether the young Th fluvial terrace was affected or not by the fault. This fluvial terrace is undeformed although it does not cover the entire fault zone and a recent activation of the SE trace cannot be ruled out. The PM deposit does not cover the entire fault zone in any of the two trench walls (Fig. 5.11). Moreover, because of its chaotic texture, a small rupture could have been overlooked, and thus this trench cannot be used to rule out a young seismic event. In summary, this trench cannot definitely confirm the lack of activity since the deposition of the Th fluvial terrace, as suggested in the natural outcrop.

However, the Tp fluvial terrace shows faulting evidence since its formation (Late Pleistocene), but the absence of truthful dating analyses prevents to give a more accurate maximum age to the fault activity along this fault trace.

5.2.8. *Paleoseismic results obtained at El Hacho: Integration and discussion*

A summary of the events observed in the trenching surveys at El Hacho, and the samples used to constrain their ages is given in figure 5.12. Events E1 and E2 coincide in time but are defined as two different events since they correspond to two superimposed colluvial wedges. The ages of events E3 and E4 overlap, but correspond to two different events observed in different levels on the trench walls. Events Ea and

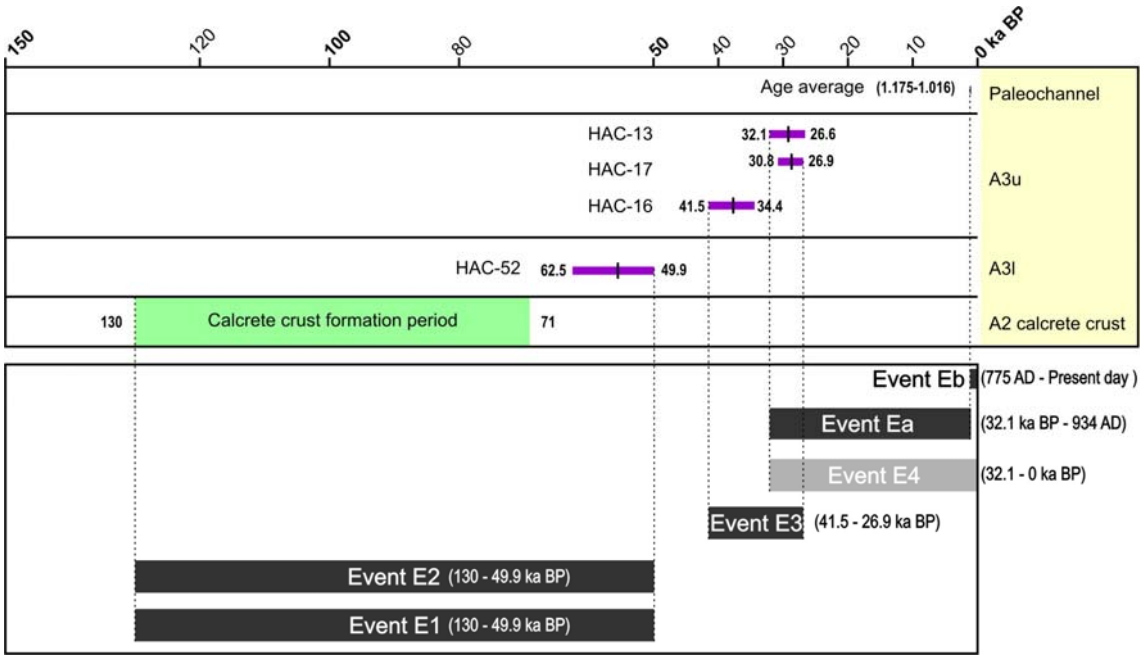

Figure 5.12. Dated samples used to constrain the age of the event horizons defined at El Hacho during the two trenching surveys. Event E4 (in grey) is not considered in the total amount of events observed at El Hacho (see text for discussion).

Eb overlap in time with events E3 and E4 and because they were inferred from different trenches, they could be interpreted as the same events. However, event E3 (Fig. 5.8) clearly occurred in the early stages of the A3u fan aggradation, and event Ea is interpreted to have occurred as soon as A3u was completely formed because of the incision of the paleo-channel in this A3u fan. Thus, a good understanding of the geomorphological evolution in the area allows us to interpret events E3 and Ea as two separate events. On the other hand, events Ea and Eb both coincide in time with event E4. No evidence suggests that they are separate events and thus event E4 might be interpreted as a multiple event including events Ea and Eb.

In summary, at the El Hacho site evidence of four events was found in the trenches perpendicular to the fault (E1, E2, E3 and E4), and evidence of two events in the 3D trenching analysis (Ea and Eb). Event E4 could represent the same event as Ea or Eb with the result that event E4 is not taken into account in the total number of events at El Hacho. Thus, there is evidence for at least 5 events since 130 ka BP at El Hacho, suggesting a mean recurrence period of 26 ka. However, the lower age of the oldest events (E1 and E2) is poorly constrained and could significantly extend this recurrence period. The three youngest events (E3, Ea and Eb) are better constrained and if we take them into account the mean recurrence period falls to 13.8 ka since 41.5 ka BP, which is consistent with the results from the northern Alhama de Murcia fault (Martínez-Díaz et al., 2001; Masana et al., 2004).

As stated in section 5.2.6.3, events Ea and Eb could be successive with a maximum elapsed time of 32.1 ka BP. The time elapsed between Ea and Eb could thus be interpreted as a seismic cycle, which would be no longer than 32.1 ka BP. However, because of the geomorphological evolution constraints, a much shorter elapsed time is interpreted, about few thousand years, which contrasts with the 13.8 ka mean recurrence suggested above. Although further numerical analyses are needed to confirm this, Ea and Eb suggest: a) a much shorter recurrence period than that previously calculated for the CFZ, or b) that Ea and Eb are cluster events forming part of the same seismic cycle.

Slip rates were obtained from the analysis of deposits observed in trenches. From the paleo-channel offset, a maximum slip per event of 1.5 m is inferred. Although the ages constraining this event consider large uncertainties (see section 5.2.6.3) they suggest a strike-slip rate between 0.05 mm/a and 1.3 mm/a (which is the minimum value calculated for the last 32.1 ka BP and the maximum value for the last 1175 Cal yr BP). Given the thickness of the colluvial wedges, an approximation to the dip-slip rate resulted in a minimum value of 0.02 mm/a since 130 ka BP. This result is consistent with values obtained using geomorphological indicators discussed in Chapter 4 (min. dip-slip rate of 0.02 mm/a since the Early Pleistocene, and 0.15-0.28 mm/a since 130-71 ka). However, according to the uncertainties of vertical slips observed along a dominantly strike-slip structure (see section 5.2.5.3), these results are coarse estimates

and the strike-slip rate is considered to have a more significant paleoseismic meaning for this study.

Mean recurrence periods were also estimated from the analysis of deposits in the trenches. A maximum slip per event of 1.5 m was inferred from the paleo-channel offset, and a maximum moment magnitude between Mw 6.9 and Mw 7.0 was calculated (see section 5.2.6.3). From the thickness of colluvial wedges, vertical slips were inferred and in turn moment magnitudes ranging from 6.4 to >6.9 were calculated (see section 5.2.5.3). Although the results from the two analyses are consistent, the magnitudes obtained from the colluvial wedges are thought to have a weak meaning given the dominantly strike-slip component of the CFZ. This strike-slip component results in: 1) an apparent vertical displacements that can significantly vary along the fault trace, and 2) a larger net slip and therefore a larger maximum magnitude. Thus magnitudes from strike-slip observations were used.

5.2.9. Summary

The colluvial wedge deposits observed at the El Hacho trench walls provided evidence of the seismogenic behaviour of the Carboneras Fault during the Quaternary. A minimum of five events were observed:

E1: 130 – 49.9 ka BP
E2: 130 – 49.9 ka BP
E3: 41.5 – 26.6 ka BP
Ea: 32.1 ka BP – AD 934
Eb: AD 775– Present day

The last event suggests Holocene seismic activity and could correspond to the historical AD 1522 Almería earthquake. A mean recurrence period of 26 ka is inferred from the five events since 130 ka BP, although this recurrence is probably overestimated because of the poor constraining of the two first events. If we consider the three last events (best constrained ones), the mean recurrence period decreases to 13.8 ka. Geomorphological observations on the last two events suggest a shorter recurrence, although these two events could also be interpreted as cluster events.

A maximum slip per event of 1.5 m is inferred from the paleo-channel offset. These results suggest a strike-slip rate between 0.05 mm/a (for the last 32.1 ka BP) and 1.3 mm/a (since 1175 Cal yr BP), and a maximum Mw 6.9-7.0. Coarse dip-slip rates of >0.02 mm/a since 130 ka BP and Mw 6.4->6.9 were estimated from the thickness of the colluvial wedges. Nevertheless, slip-rates and maximum Mw calculated from the horizontal slip observation were preferred because of the dominantly strike-slip behaviour of CFZ.

5.3. Los Trances area

5.3.1. Geographic and geological setting

Los Trances site is located in the central part of the NW Serrata boundary, northeast of the village of Atochares. Here, the fault bounding La Serrata splits into two main fault traces delimiting a pressure ridge (Fig. 5.13) made up of Pliocene quartz-rich calcarenites and conglomerates. To the southeast, the La Serrata is constitued by volcanic rocks (polygenic tuffs and conglomeratic breccias). To the northwest of the pressure ridge, the Quaternary alluvial fans cover the surface. The thick calcrete crust on top of the A1 alluvial fans crops out locally at the bottom of a channel. A2 alluvial fans are in linear contact with the pressure ridge except in the northeast of the area (Fig. 5.13) where a group of apexes have been preserved and overlie the fault zone. A3.1 alluvial fans are mostly deposited downhill from the pressure ridge, although in some cases their apexes go beyond the north-western fault trace.

5.3.2. Overview

In the last decades, farming with greenhouses has drastically changed the geomorphology at the foot of La Serrata. This has involved large excavations to flatten the land to facilitate agriculture. The introduction of greenhouses commenced in the low-lying areas close to the main river but the high demand for agricultural produce led to an increase in the number of greenhouses upslope as far as the foot of the hill and in places across the fault zone. At Los Trances the excavations for a greenhouse development ascended up to the pressure ridge exposing the fault contact between Pliocene and Quaternary deposits in a 5 m high wall (picture in figure 5.13). This was an exceptional opportunity to observe a deep cross section showing the lower A1 alluvial fans being thrusted by Pliocene rocks, and thus to observe event horizons older than the ones previously observed. The greenhouse wall was cleaned and logged as a trench, called LT-TR2 (Fig. 5.13). Nevertheless, evidence of faulting of the uppermost deposits at the greenhouse wall was not clear and, to offset this, a 2.5 m deep trench, known as LT-TR1 (Fig. 5.13), was opened parallel to the outcrop of the greenhouse wall. These two trenches showed the northwestern fault trace bounding the pressure ridge. To obtain evidence of recent faulting at the southeastern fault trace, a third trench (LT-TR3 in figure 5.13) was opened where the fault trace is covered by a young alluvial deposit of unknown age.

5.3.3. Description of trenches

The three trenches at Los Trances show very different situations and are discussed separately although the units maintain the same description.

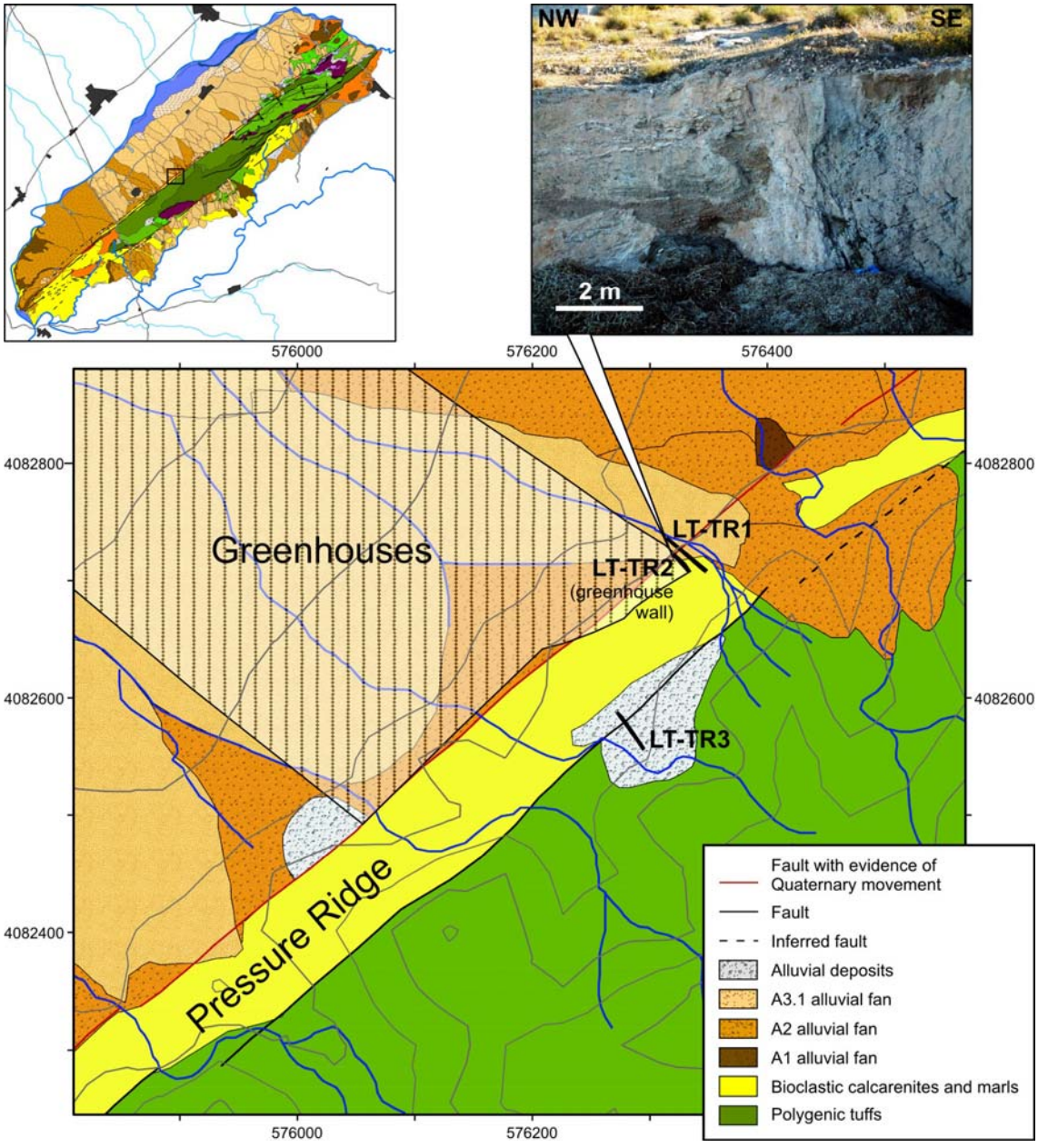

Figure 5.13. Zoom of the geomorphological map of La Serrata in its central section and location of Los Trances trenches. The dashed area is currently covered by greenhouses. Inset: location of Los Trances in the geomorphological map of La Serrata. Picture: aspect of the greenhouse wall (later LT-TR2) showing the fault contact between Pliocene rocks to the SE and Quaternary sediments to the NW.

The NE wall of trench LT-TR1 (Fig. 5.14) shows a 5 m wide fault zone. To the SE the quartz-rich Pliocene calcarenites show interbedded calcium micro-conglomerates of well-rounded quartz pebbles and abundant marine shell fossils. The Tp fluvial terrace onlaps the Pliocene rocks and is faulted and uplifted in the fault zone showing a flower structure. This deposit is made up of light brown sandy matrix-supported conglomerates with millimetric to decimetric pebbles showing a good but irregular internal

stratification, which suggests a fluvial process of formation. Pebbles are mainly of volcanic nature and define layers of alternating different sizes and cementation degree. Locally, some channel-shaped bodies of matrix-supported sand and clay orangey levels are observed inside the Tp unit. The A3.1 Upper Pleistocene alluvial fan overlies the Tp unit and extends to the SE directly overlying the Pliocene rocks. It is absent in the fault zone where it was probably faulted, uplifted and eroded. Here, the A3.1 alluvial fan shows a high calcification process that has completely bleached the sediment and replaced its internal texture by a more homogenous white deposit. On top of the trench wall and unaffected by the fault zone, the current soil is constituted by a dark brown unit with pebbles, roots and high organic content. The area bounded by faults contains units C10, C11 and B3 (picture in figure 5.14). C10 has a chaotic aspect made up of rounded cobbles (up to 25 cm) with smaller pebbles and sand filling the interstitial spaces. C11 is also composed of rounded cobbles but with a good internal stratification, representing a slightly deformed fluvial unit. Both units probably correspond to lower layers of a deformed Tp fluvial terrace. Overlying the fault contact between C10 and C11 is a loose and chaotic deposit, labelled B3, which is made up of angular volcanic pebbles of different sizes. This deposit is interpreted as the rest of a colluvial wedge associated with the fault zone.

Trench LT-TR2 (Fig. 5.14) shows a superimposition of the three alluvial fan units described at La Serrata: A1 in the lower parts, A2 in the middle and A3.1 in the upper parts. A1 unit is a matrix supported conglomerate made up of a brown to ochre sandy matrix with dispersed quartz and volcanic pebbles, the later up to 30 cm in size. Quartz pebbles are sub-rounded and the volcanic ones are sub-angular containing abundant hornblende crystals. Towards the top, this unit presents an up to 50 cm calcrete crust with different phases of laminated layers. The base of the A2 conglomerates is erosive. It has paleo-channels that are filled with decimetric well-rounded boulders of volcanic origin at the base grading upwards to centimetric-size pebbles. The upper parts of the channels are made up of a hardened clay-sandy pink matrix and contain well-rounded quartz pebbles changing into volcanic gravels upwards. A densely fractured calcrete crust covers the unit with variable thickness, from centimetric to half a metre. A1 and A2 alluvial fans are in reverse fault contact with the Pliocene quartz-rich calcarenites and microconglomerates, and in the NW part of the trench wall these units are eroded and filled with the Tp fluvial terrace deposits. A3.1 alluvial fan overlies either Tp or A2 deposits and does not reach the fault zone. A fault zone strip labelled C12 shows sands and clays with dispersed pebbles of quartz and volcanic lithologies, and probably corresponds to a deformed A2 (and A1?) strip.

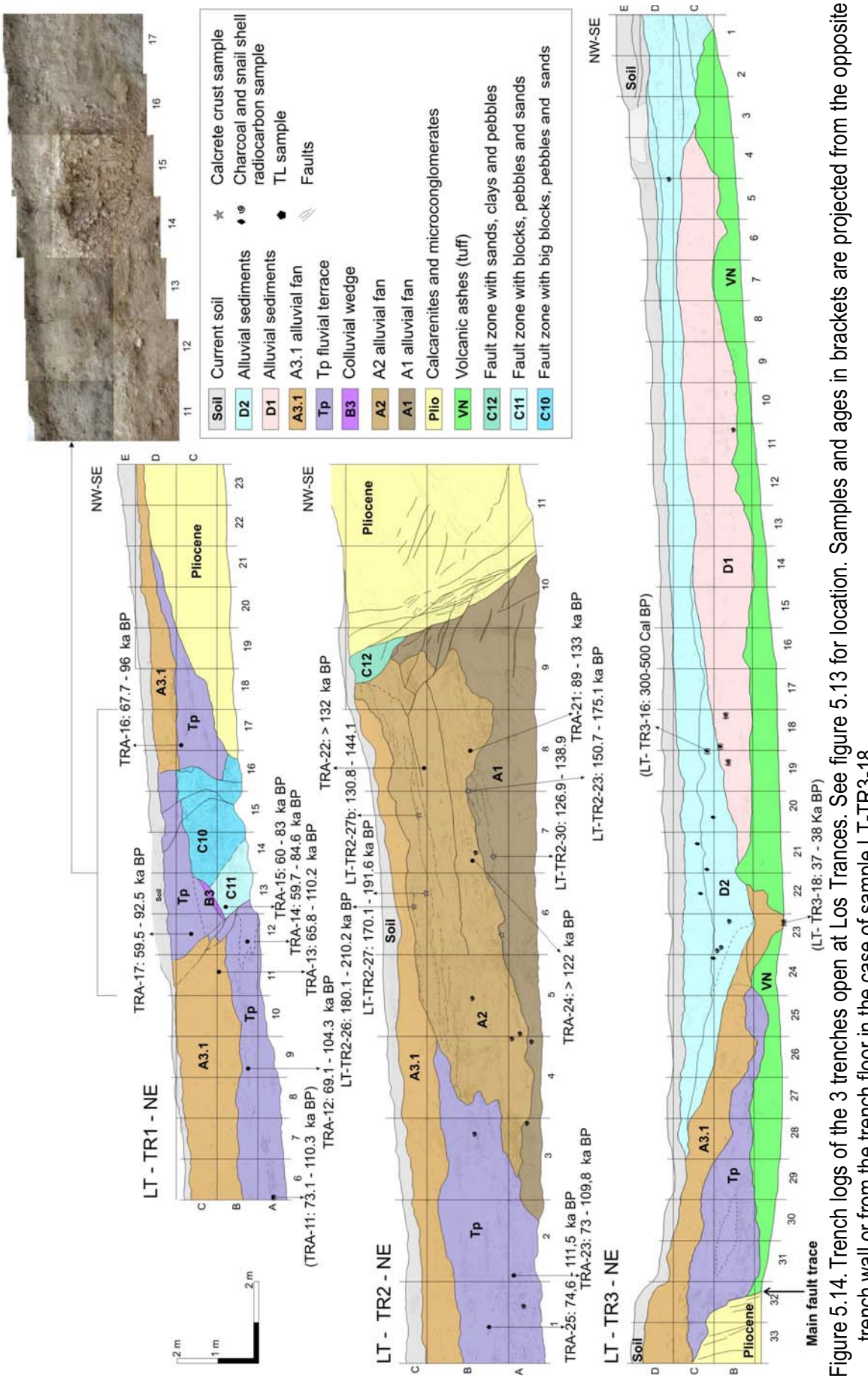

Figure 5.14. Trench logs of the 3 trenches open at Los Trances. See figure 5.13 for location. Samples and ages in brackets are projected from the opposite trench wall or from the trench floor in the case of sample LT-TR3-18.

Trench LT-TR3 (Fig. 5.14) shows the southeastern fault trace delimiting the Pliocene rocks of the pressure ridge with light green to white tuffs from the Neogene volcanism. This volcanic deposit has some interbedded light orange layers containing millimetric hornblende crystals. The main fault zone is covered by an apparently underformed Tp deposit, which is covered by the A3.1 alluvial fan (north-western edge of the trench log). About 9 m to the SE of the main fault trace (column 23 in the log), an open crack tracing a N50º strike is observed in the irregular volcanic unit and filled by A3.1 sediments. To the SE of this crack and onlapping the A3.1 unit, two superimposed alluvial units labelled D1 and D2 are described. At the bottom, D1 is made up of sands, clays and pebbles of different shapes and sizes. At the base of D1, millimetric and well-rounded pebbles form channels. In the middle of the unit, up to 10 cm long angular pebbles are dispersed in a slightly cemented clay to sandy matrix, with interbedded well rounded pebbles. Towards the top, D1 unit becomes well consolidated. This unit seems to be an intercalation of chaotic and low energy levels. Overlying D1 and A3.1, unit D2 is a double channel shaped unit filled with a loose dark brown to grey sandy matrix with plenty of millimetric to centimetric pebbles mainly of volcanic origin. The entire trench is covered by an undeformed current soil constituted by a dark brown sandy matrix with pebbles and fine roots.

5.3.4. Dating analysis

In the trenches at Los Trances, U/Th was used to date calcrete crusts from A1 and A2 deposits, TL was employed to date fine grained sediments from A2, Tp and A3.1 deposits, and radiocarbon was used to date a charcoal fragment and a snail shell from the A3.1 and the D2 deposits (Fig. 5.14). In line with the discussion on the development of calcrete crust (section 4.3.2.1) and given the overlying disposition of A1, A2 and A3 fans, calcrete crust sampled on top of A1 and A2 fans may be secondary calcretes (formed long after the aggradational phase of each unit). These calcrete crusts were sampled and dated because, even if they do not provide an age approximation of the alluvial fans, they predate the age of the calcrete crust rupture.

A radiometric age of the A1 alluvial fan was not achieved and only an Early Pleistocene age can be assumed. A2 unit was dated by TL and this method yields two reliable ages (TRA-22 and TRA-24 in Fig. 5.14), whose upper ages are 132 ka BP and 122 ka BP, respectively, and whose lower ages are beyond the method limits. The A2 aggradational phase must be close to the upper TL ages, suggesting a MIS 6 age. Thus, A2 deposits are considered to have ages between 191-130 ka BP. The Tp fluvial terrace was dated with TL and the results are consistent, suggesting a Late Pleistocene (MIS 5) age constrained between 111.5-59.5ka BP. One TL sample in the A3.1 alluvial fan was analysed in order to test the method. As expected from the calcification process observed in the trench wall, the TL results are older than those expected for this unit and

thus not reliable. Nor is the dating of the snail shell sample extracted from the A3.1 deposits because of problems of dating old snail shells (see section 4.3.2.3). Nevertheless, it gives a broad Late Pleistocene (MIS 4-2) age of the unit. This is consistent with the discussion of the unit ages (section 4.3.3) where A3.1 deposits were considered to have a MIS 4-2 age (14-71 ka BP). Finally, the D2 alluvial deposit was dated by a charcoal sample that yielded a 300-500 Cal yr BP age, i.e. late Holocene.

5.3.5. Event horizons and mean recurrence period

Three event horizons are observed in trench LT-TR2 (L1, L2 and L3) (Fig. 5.15). The first event, event L1, is defined because it delimits faulted A1 and A2 deposits below the event horizon with non-faulted A2 deposits above the event horizon. In the same way, the second event, event L2, also limits faulted and non-faulted A2 deposits below and above the event horizon. Both events must have occurred when the A2 alluvial fan was in its aggradation phase, as only the lower half of this unit is faulted. According to the MIS 6 age for this aggradational phase, L1 and L2 events are constrained by the MIS 6 boundary ages, i.e. between 191 ka BP and 130 ka BP. In the same trench (LT-TR2) the last event, event L3 is located at the base of the undeformed current soil covering the fault zone (Fig. 5.15). Nevertheless, the time span between the soil and the underlying faulted units is too long to constrain the age of the event.

Trench LT-TR1 shows younger units involved in the fault zone and allows us to differentiate two events (L3 and L4), postdating the A2 alluvial fan, which coincides with the younger event observed in LT-TR2 (Fig. 5.15). Event L3 is represented at the base of B3 colluvial wedge (B3) which confirms the seismogenic character of the CFZ in this area. The age of this event is constrained by the age of the TL samples TRA-15 in the C11 unit (which corresponds to the lower part of Tp unit) and TRA-17 in the Tp unit. In other words, event L3 has an age between 83-59.5 ka BP. Finally, event L4 is located at the base of the current soil, the only undeformed unit in LT-TR1 and LT-TR2 trenches. The immediately younger faulted unit is A3.1 and it can therefore only be assumed that this event is younger than the age of this unit, dated between 14-71 ka BP at La Serrata. Thus, event L4 is constrained between 71 ka BP and the present day.

In trench LT-TR3, the fault crack observed in the volcanic materials is filled by A3.1 deposits (Fig. 5.14), suggesting an opening of the crack after the deposition of A3.1, this is after 71 ka BP. However, this is weak evidence for a paleo-earthquake as other processes like terrain adjustments may account for it

In summary, four events (L1, L2, L3 and L4) since 191 ka BP are observed at Los Trances trench walls, suggesting a mean recurrence period of 47.7 ka. As in most paleoseismic studies, this mean recurrence is a maximum value because in trenches, a minimum number of events are detected. However, in such cases, where the dates

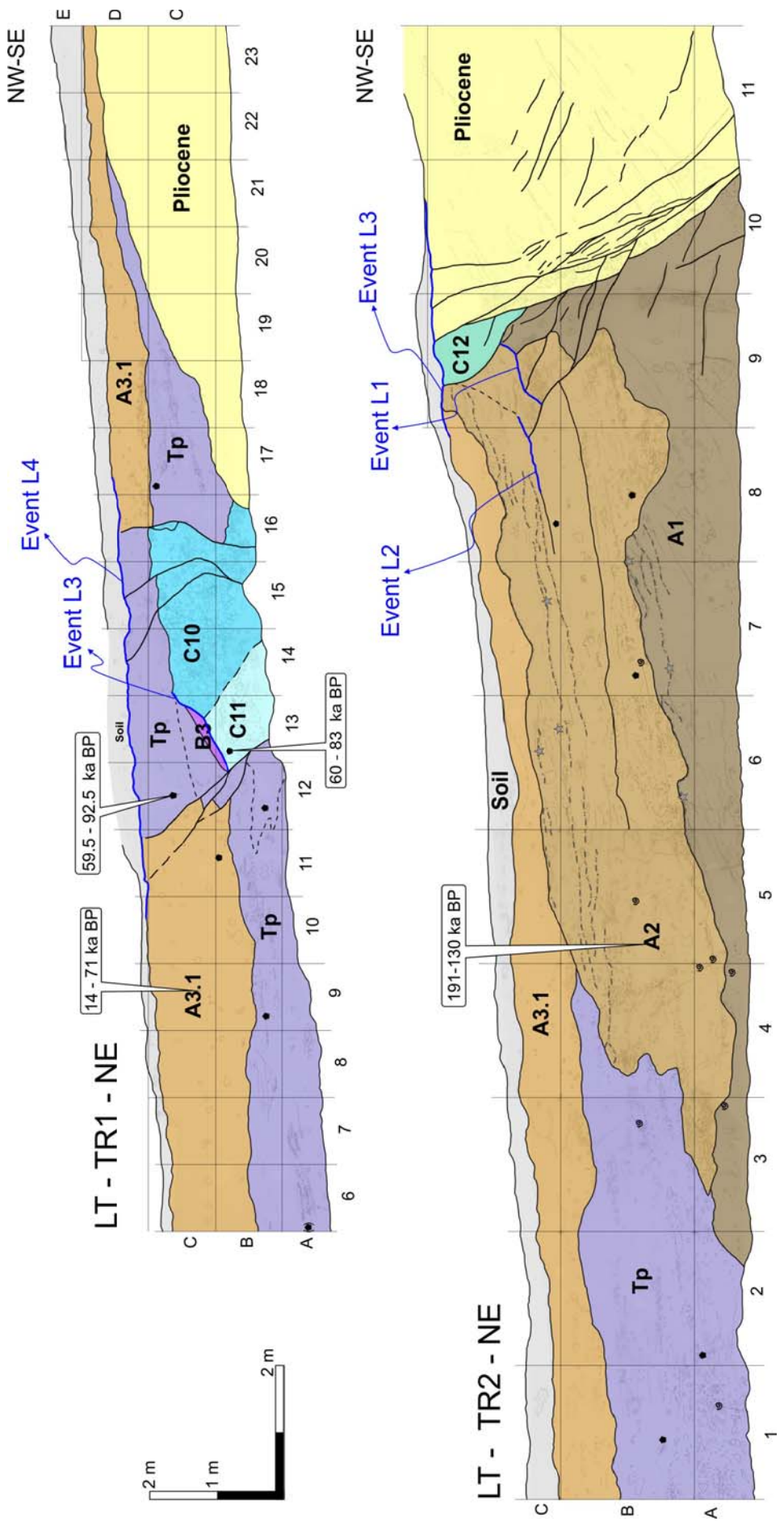

Figure 5.15. LT-TR1 and LT-TR2 northeastern wall showing the four event horizons and dates used to constrain the age of these horizons. See figure 5.14 for legend. Note that the dates indicating a sample are obtained from this sample but ages indicating the unit name or calcrete crust are relative ages discussed in Chapter 4.

constraining the events present such a large uncertainty, the overestimation of the recurrence may be strengthened and the fault mean recurrence may be considerably shorter than those calculated from trench observations.

5.3.6. Summary

The presence of a colluvial wedge deposit at Los Trances reinforces the seismogenic behaviour of the Carboneras Fault during the Quaternary. Moreover, a minimum of four events are evidenced:

L1: 191 - 130 ka BP
L2: 191 - 130 ka BP
L3: 83 - 59.5 ka BP
L4: 71 - 0 ka BP

These four events have occurred since 191 ka BP, suggesting a 47.7 ka mean recurrence period. Nevertheless, this value is probably overestimated because of the large uncertainty of constraining the age of the events.

5.4. Other trenching sites

5.4.1. Pecho de los Cristos site

5.4.1.1. Geographic and geological setting

The Pecho de los Cristos site is located in the central part of the NW boundary of La Serrata, and NW of the Pecho de los Cristos hill. The La Serrata is formed here by volcanic rocks (polygenic tuffs and conglomeratic breccias), and at its base, a band of Pliocene quartz-rich calcarenites and conglomerates forms the NE-SW pressure ridge bounded by two parallel N050º fault traces (Fig. 5.16a). At the foot of La Serrata and partially covering the pressure ridge, A2 and A3.1 alluvial fans currently display a linear contact with the pressure ridge or with the base of the range. The A2 alluvial fans covering the pressure ridge towards the SW are slightly folded in contrast to the A3.1 alluvial fans covering the pressure ridge towards the NW that apparently maintains their original slope. The youngest deposits in the area are a 100 m long and narrow fluvial terrace (Th) formed along the southwestern gully, and some superficial alluvial sediments (pediment-like).

5.4.1.2. Motivation for the study

A wide and highly incised arcuate gully exposes Pliocene rocks thrusting on an A1 alluvial fan (Fig. 5.16b,c), providing evidence of the Quaternary activity of this fault trace. Some fault planes in A1 deposits show a calcrete re-growth sheet with 20/060º pitch slickensides (Fig. 5.16d), suggesting a predominant strike-slip movement. The A2 alluvial unit overlaps the A1 fan although it is not clearly affected by the fault zone observed along the gully. To the SW, the fluvial terrace is deposited across the fault trace and PC-TR1 trench (Fig. 5.16a) was dug there in order to confirm or rule out its most recent movement. To the NE, A3.1 alluvial fans overlie the A2 unit and are not deformed according to surface observations. The PC-TR2 trench was dug on top of the A3.1 alluvial fan to ascertain whether the fault trace affected these deposits.

5.4.1.3. Description of trenches and discussion

Trench PC-TR1 (Fig. 5.17) was dug on a young fluvial terrace with a maximum thickness of 2 m in the SW wall. This trench is made up of sands, clays and well-rounded pebbles with a good internal stratification and channel-like structures. The terrace is not deformed and discordantly overlies the older deposits and the fault zone. The 4 m wide fault zone, which is only observed in the NE wall, raises the Pliocene quartz-rich conglomerates to the level of the A2 alluvial fan underlying the terrace. The fault zone includes two vertical and chaotic units: unit C13 incorporates decimetric blocks of volcanic origin in a red matrix, and unit C14 is more massive with few centimetric pebbles in a white to pink calcic matrix. The reddish colour and the

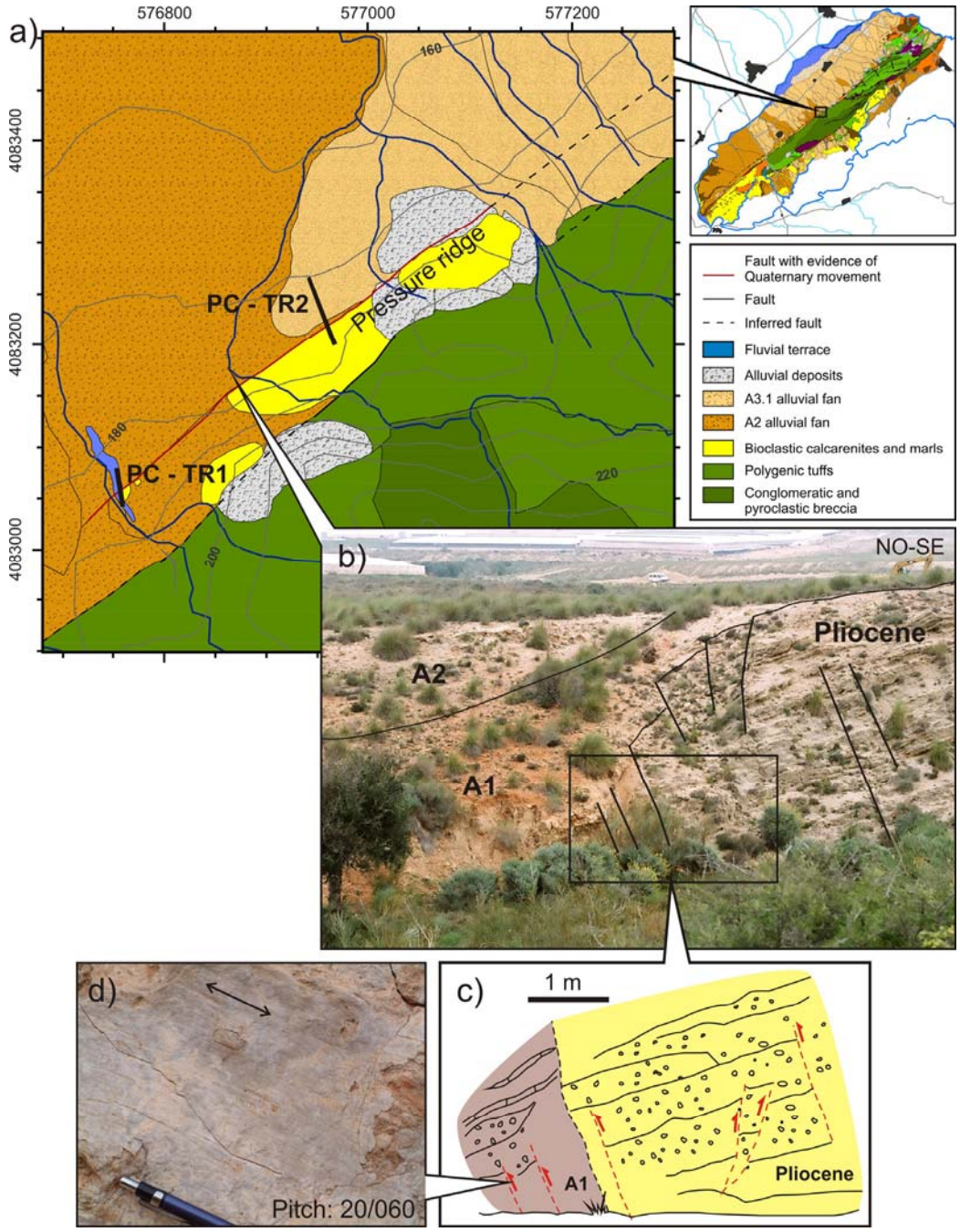

Figure 5.16. a) Zoom of the geomorphological map of La Serrata at Los Trances site. Trenches PC-TR1 and PC-TR2 are located. Inset: location of the area in La Serrata geomorphological map. b) Landscape picture and line drawing of the fault contact between Pliocene rocks thrusting on the A1 alluvial fan. c) Sketch of the fault zone at the contact between the Pliocene rocks and the A1 alluvial fan. d) Slickensides observed on a calcrete crust re-growth at the fault plane in the A1 alluvial fan (modified from Prada, 2008).

presence of volcanic pebbles suggest that they belong to the A1 alluvial fan that underlies the A2 alluvial fan in the area. Unit C14 underwent a strong calcification probably as a result of water circulation in the fault zone, turning the red colour into

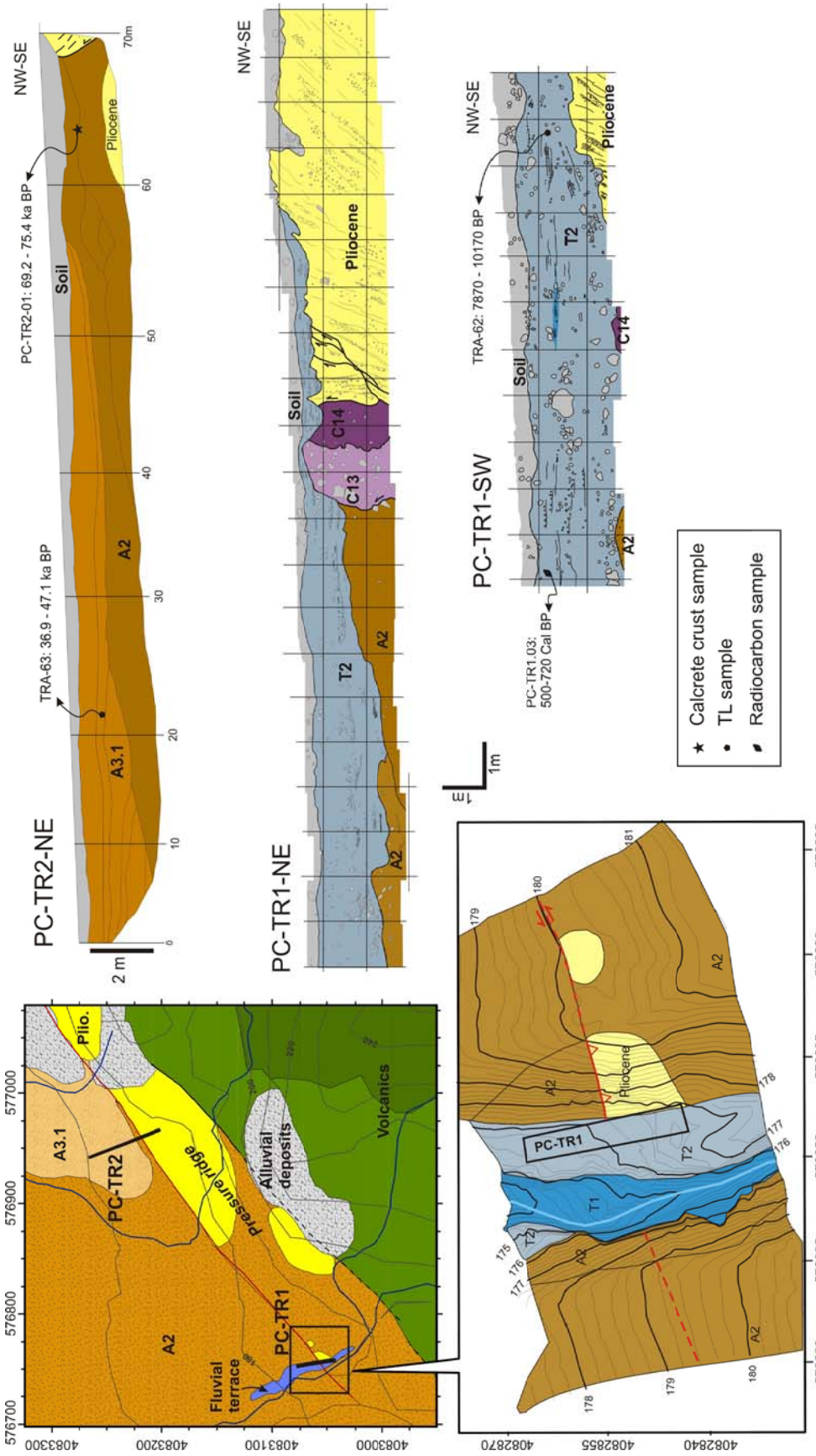

Figure 5.17. Pecho de los Cristos trench logs and location of trenches in a zoom of the geomorphological map of La Serrata (Fig. 5.1) and in a microtopographic map specially built for the paleoseismic survey. Dated samples are located and results are summarized in the logs (modified from Prada, 2008).

white or pink. A few centimetre-thick soil with a high content of organic material is present along the upper part of the trench.

Trench PC-TR2 (Fig. 5.17) shows the fault contact of the Pliocene quartz-rich micro-conglomerates thrusting on the A2 alluvial fan. The A2 unit displays different sub-levels and a continuous decimetric calcrete crust. A3.1, which consists of three upper thinning sequences with an erosive base, is made up of volcanic gravels, reddish sands and clays. The three A3l levels concordantly onlap the A2 unit but do not reach the fault zone. From bottom to top at the trench wall, the A3.1 sub-units are increasingly larger, with the southeastern end located further to the SE. A loose and organic-rich soil is present along the trench.

In both trenches, the Mid Pleistocene A2 alluvial fan is the youngest unit clearly affected by faulting. Following the dating analysis in Chapter 4, the calcrete crust in PC-TR2-NE is probably a secondary re-growth calcrete and thus its U/Th age is not conclusive. Using geological and climatic data, A2 alluvial deposits are assumed to be of Mid Pleistocene age, probably of MIS 6 age. Trench observations show faulting dating back to Mid Pleistocene on this fault trace. The T2 fluvial terrace overlies the fault zone in trench PC-TR1 and is not deformed, suggesting seismic silence since its formation. Two samples were analysed in this unit with surprisingly different ages. The TL method (TRA-63) yields a 7870-10170 yr BP age, and the ^{14}C method (PC-TR1-03) a 500-720 Cal yr BP age (Fig. 5.17). The aspect of the fluvial terrace suggests the Late Holocene deposits observed at other sites (e.g. El Hacho, Los Trances sites), which is consistent with the ^{14}C result. The TL date could be overestimated if the sample presented a lack of bleaching, but this is unlikely according to the fluvial nature of the unit. Thus, there are no apparent reasons to dismiss the TL date, and an uncertain Holocene age can be estimated for the T2 fluvial terrace with an approximate age between 10170 and 500 yrs BP. However, the younger age of this unit suggests that no fault activity has occurred on this fault trace since AD 1450, which rules out the historical 1522 Almería earthquake. Nevertheless, other fault traces in the area, such as the fault trace bounding the pressure ridge to the SE (Fig. 5.17) can be considered for this event.

5.4.2. La Pared Alta site

5.4.2.1. Geographic and geological setting

La Pared Alta site is located in the northern part of the NW boundary of La Serrata range, north of Cerro de las Bichas and close to a country house called *Cortijo de la Pared Alta* (Fig. 5.18). At the range, Maláguide and Alpujárride metamorphic rocks crop out between the volcanic units, suggesting a stronger uplift of the range in this area with respect to southern areas. The NE-SW pressure ridge at the base of La Serrata is mainly formed here by volcanic rocks bounded by N050º trending faults. The

pressure ridge is less evident in this area and loses continuity because the same volcanic rocks crop out to the NW and because E-W trending elongated mounds, interpreted as push-ups, coincide with the pressure ridge. The well exposed volcanic rocks at the foot of the range suggest that the stronger uplift evidenced by the metamorphic rocks at the range is a regional uplift, not restricted solely to the range. A parallel fault depicts a sharp contact between volcanic and Miocene and Pliocene outcrops 600 m further to the NW. A3.1 deposits partially cover the surface from the base of the range downwards. Fluvial terraces are formed at the sides of current incised channels, and superficial alluvial deposits (pediment-like) are also present.

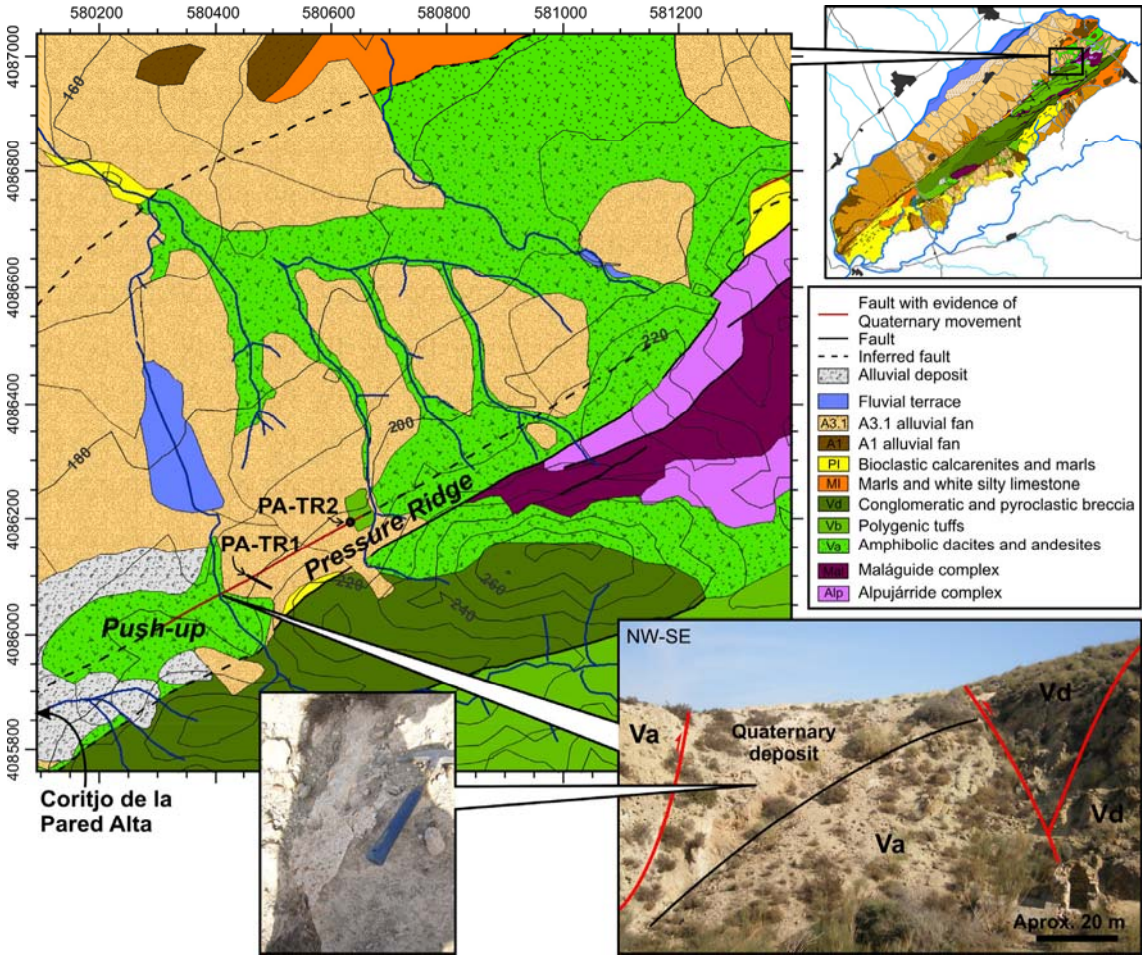

Figure 5.18. Location of la Pared Alta site in a zoom of the geomorphological map of La Serrata (Fig. 4.2). The large picture shows the natural outcrop across the channel exposing the fault zone with trapped Quaternary deposits. The small picture shows the fine calcite crusts re-growth at the fissures of the Quaternary deposits.

5.4.2.2. Motivation for the study

A wide gully crossing the fault zone exposes recent (Quaternary) deposits thrusted and trapped between volcanic rocks (Fig. 5.18). These deposits are made up of

sands and clays with dispersed volcanic pebbles, suggesting the Quaternary alluvial fans observed in the area although with considerable deformation. Along the channel, the deposits present a net of fractures with thin re-growths of calcite crusts (usually less than 1 mm) (Fig. 5.18). Trench PA-TR1 was planned to be parallel to the gully outcrop and orthogonal to the fault zone 60 m to the NE, where the Upper Pleistocene A3.1 alluvial fans cover the surface. However, because of the morphological conditions and the presence of anthropological features such as a path and agricultural fields, the trench was finally dug with approximately 20º of obliquity. A second smaller trench (PA-TR2), 2 m long, was opened to the NE, following the fault trace at the foot of a small hill that is interpreted as a small push-up.

5.4.2.3. Description of trenches and discussion

Trench PA-TR1 (Fig. 5.19) shows two Quaternary units (Q1 and Q2, lithological description in legend of figure 5.19) overlying volcanic deposits (V1 and V2) to the SE and in vertical fault contact with the deformed materials of the NW part of the trench. The fault zone is about 5 m wide and contains three sub-vertical deformed units (C15, C16 and C17). Units C15 and C16 are deformed Quaternary deposits (alluvial units) and C17 is probably composed of Pliocene marls trapped in the fault zone. C17 unit is overthrusted by volcanic deposits (V3) and delimits the fault zone to the NW.

The SE part of the fault zone is covered by an undeformed paleosoil (S1) dated by a bulk soil sample as 5000 +/-85 yr BP. Bulk soil samples yield average ages of the material recovered and thus provides a less precise result than other ^{14}C samples, such as charcoal. However, because of the absence of other datable materials along the trench it was only possible to obtain an age estimation for the Holocene S1 soil.

A3.1 alluvial unit covers the area and is locally very thin. In some places A3.1 has been completely transformed into (S2) soil. The top of trench PA-TR1 corresponds to this soil mapped as A3.1 on the geomorphological map of figure 5.19.

Trench PA-TR2 was dug in the fault zone and shows a fault contact between Pliocene and volcanic rocks covered by a thin layer of current soil (S2). Pliocene rocks do not crop out on surface at the trench site. They could be related to the fault zone, as occurs further to the SW (see the geomorphological map of figure 5.19).

Observations at the La Pared Alta site show that the trenched fault trace has been active during the Quaternary since Q1 and Q2 deposits are clearly faulted. Unit S1 covers only part of the fault zone in trench PA-TR1 and thus a seismic event after the age of the unit cannot be ruled out, as the deformation could have been concentrated along the NW trace. The S2 soil on top of both trenches seems to be undeformed and thus it is the only unit that postdates the age of the fault activity. This unit was not dated and it can only be assumed that it is younger than the S1 unit. However, this does not contribute to the constraining of the upper age of the fault activity.

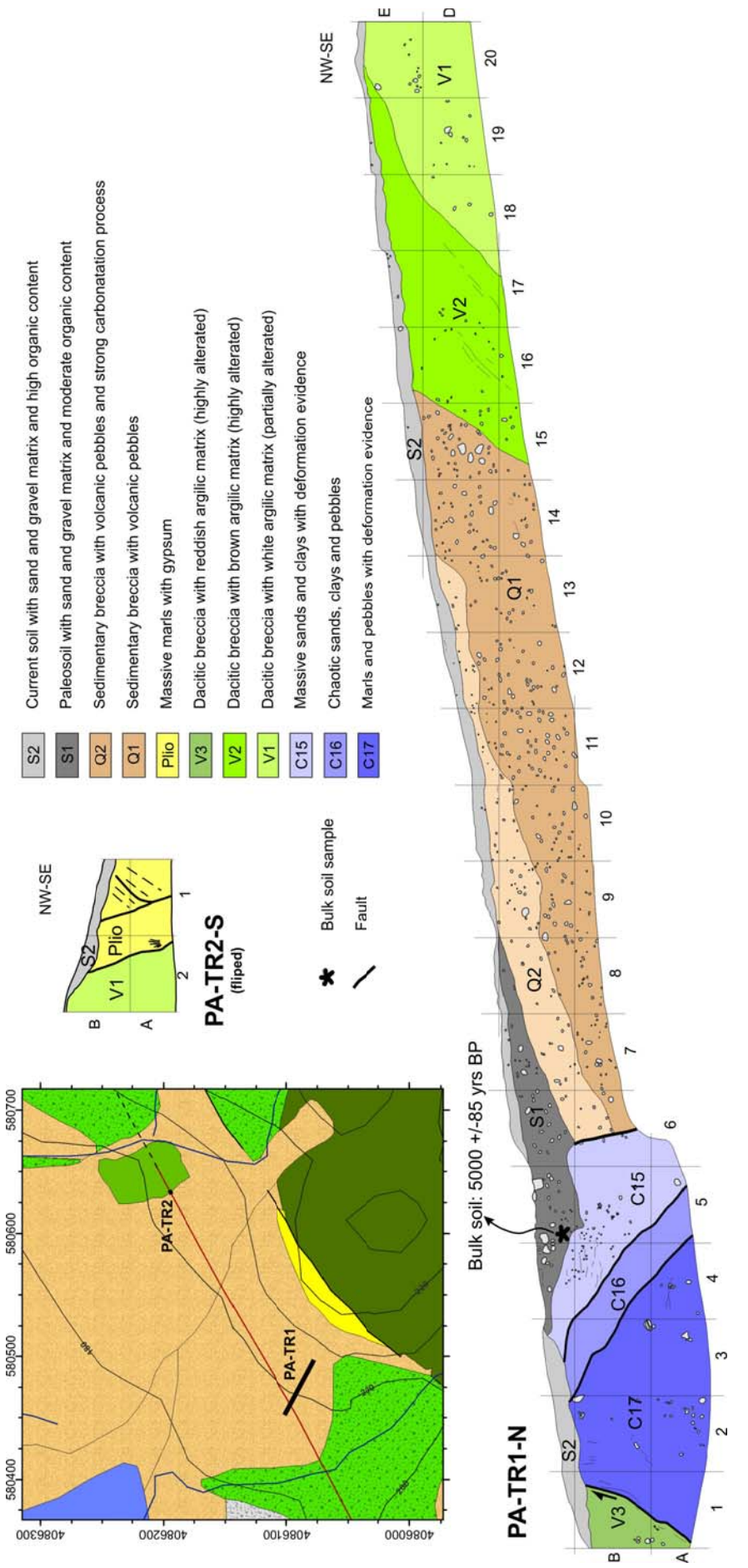

Figure 5.19. Detail of the geomorphological map of the Pared Alta site (Fig. 5.18) where the two trenches are located and trench logs with lithological legend above (modified from Echevarría, 2007).

5.4.3. The Cerro Blanco site

5.4.3.1. Geographic and geological setting

The Cerro Blanco site is located in the southern part of the NW boundary of La Serrata, north of the Cerro Blanco hill and west of Las Yeseras (Fig. 5.20). The range is mainly made up of Miocene and Pliocene rocks, suggesting a lower uplift in this part. The constant band of Pliocene rocks forming the NE-SW pressure ridge ends sharply in the area. However, the structure continues towards the SW and folds the A2 alluvial fans that cover it. A2 alluvial fans at the foot of the range have a linear contact with the pressure ridge or with the range. A1 alluvial fans locally crop out along the channel or are uplifted in the fault zone. Narrow fluvial terraces are formed along the gullies of the area and alluvial deposits are present.

5.4.3.2. Motivation for the study

At the SW end of the pressure ridge made up of Pliocene rocks, an incised gully shows a sharp deflection of 6.6 m coinciding with a linear A1-Pliocene contact (Fig. 5.20b). The linearity and orientation of the A1-Pliocene contact suggest that it is a fault contact although this is not evidenced in the natural outcrop across the gully. On the SW side of the gully, a narrow fluvial terrace follows the deflection of the channel. A 35 m long trench was dug along the fluvial terrace and across the inferred fault trace (Fig. 5.20c) to ascertain whether the gully deflection responded to a fault offset or just to an adaptation to a paleo-relief.

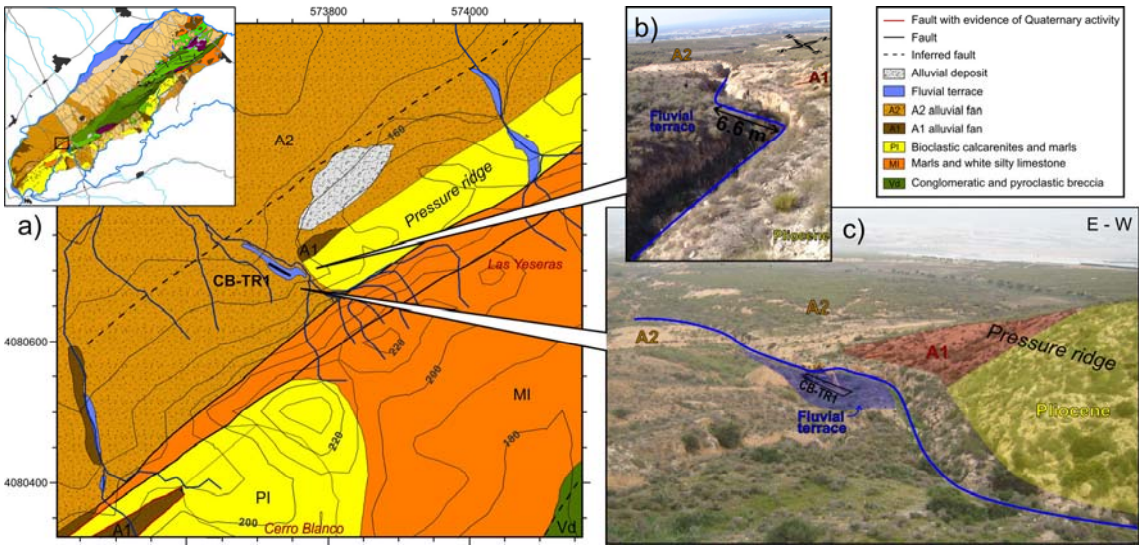

Figure 5.20. a) Zoom of the geomorphological map of La Serrata at Cerro Blanco and location of trench CB-TR1. Inset: location of this site in the geomorphological map of La Serrata. b) Image of the sharp deflection of the gully. c) Image of the deflected channel and the contact between units at the pressure ridge.

5.4.3.3. Description of trenches and discussion

Trench CB-TR1 shows no clearly deformed sedimentary units, and thus was not logged. However, the sketch presented in figure 5.21 shows the oldest A1 units overlain by A2, F1 and F2 deposits. The A1 alluvial fan is made up of red sands and clays with volcanic pebbles and presumably overlies the Pliocene, but the trench was not deep enough to reach this contact. The A2 alluvial fan is formed by poorly sorted sands and gravels with angular pebbles topped by a hardened white (calcified) layer (although no laminar calcrete crust was formed). Above it, two units of loose sands and gravels are differentiated by their different colour. F1 is constituted by ochre sands and gravels and shows an irregular base. F2 is composed of poorly sorted sands and gravels with some layers of centimetric well-rounded pebbles. This unit is dark brown because of its high organic content.

The upper part of the A2 unit presents a vertical irregularity (Fig. 5.21) that may be interpreted as a vertical offset. Below this irregularity, a sharp colour change occurs in the A2 sediments although the same texture is observed on both sides. More evidence is needed to ascertain whether this corresponds to a fault contact or to a lateral change in the unit. A deeper trench would probably resolve this question. The overlying F1 and F2 units are undeformed. One radiocarbon age is obtained from the F2 fluvial terrace. Owing to the small amounts of datable material, three samples closely collected in the same stratigraphic level were mixed to obtain an age of 1420-1300 Cal yr BP. Thus, it may be concluded that the fluvial terrace (AD 530-650) is not faulted and that the deflection observed in the gully is an adaptation to a paleo-relief.

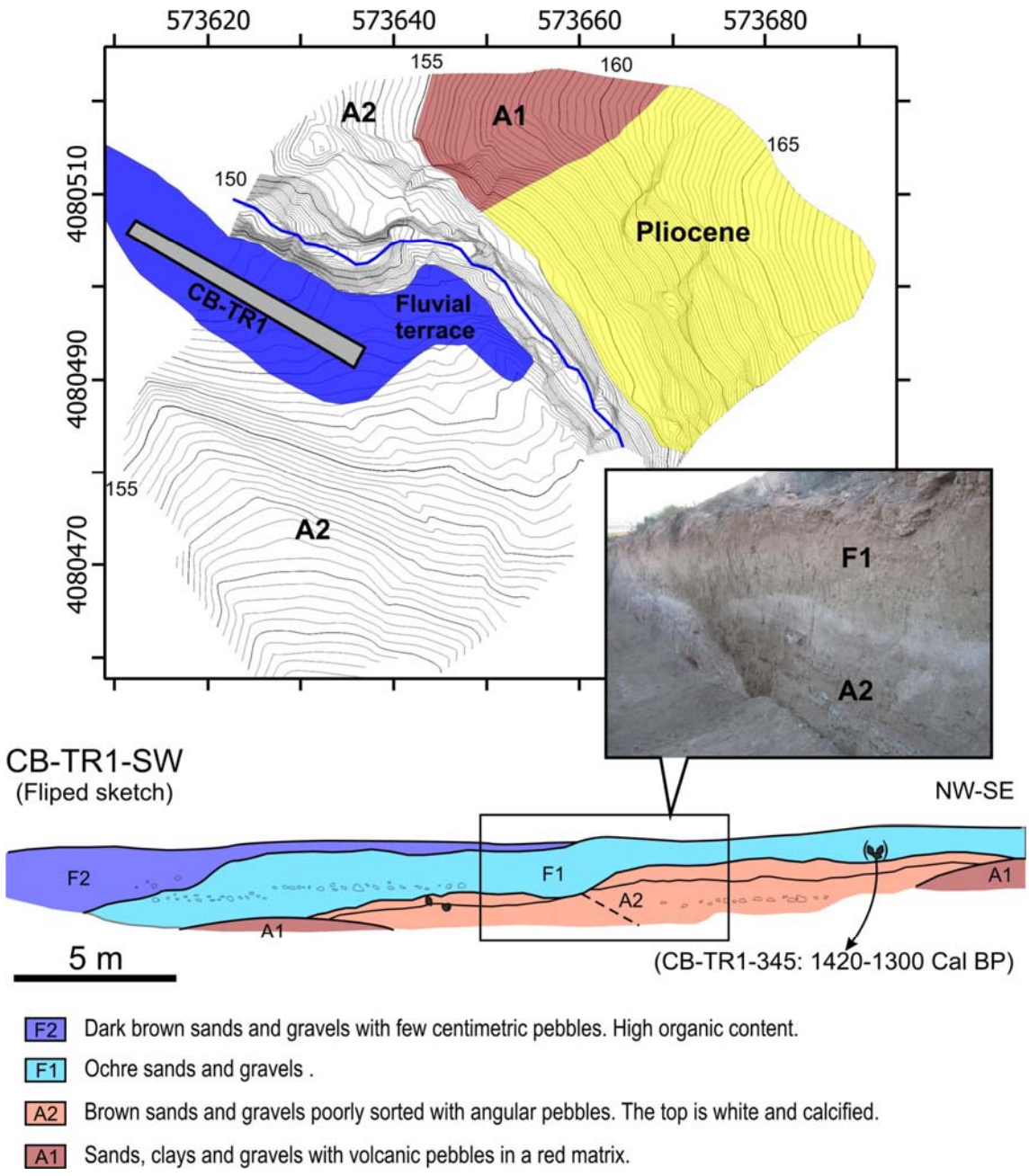

Figure 5.21. Microtopographic map and sketch of the trench opened at the Cerro Blanco. The sample location (in brackets) is projected from the opposite trench wall (modified from Echevarría, 2007).

5.5. Imaging the depth structure at La Serrata using magnetotelluric methods

5.5.1. Overview

The paleoseismic study carried out at several sites of La Serrata provides paleoseismic numerical results of the activity of the fault traces where the observations were made. These results were assumed to be minimum values for the fault zone that bound the range to the northwest given that all the traces observed along this side (e.g. the two traces bounding the pressure ridge) converge at a seismogenic depth. However, an analysis of the structure at depth is needed to confirm this convergence and the possible convergence with the fault trace bounding La Serrata to the SE. For this reason, a magnetotelluric survey was conducted (Queralt et al., In prep.) in collaboration with the EXES geophysics team from the *Universitat de Barcelona*.

Previous broadband magnetotelluric surveys had been conducted in the area and across La Serrata by Pedrera et al. (2010). These authors describe the CFZ as a conductor in the uppermost part of the MT model, constrained between the stations on each side of the fault zone. Moreover, MT information together with seismic receiver function, Bouger anomaly data and geological observations allowed them to observe the CFZ crossing crustal discontinuities at least up to about 15 km. Downwards they observed a small flexure at the Moho discontinuity coinciding with the CFZ, which suggested that the fault deformation could reach down to the mantel. These observations are of great interest to the discussion about the deep structure of the CFZ and its possible nucleation at the base of the crust. However, a greater resolution is required to observe the convergence of individual fault traces, which is the aim of the present study.

In our study, a total of 24 audiomagnetotelluric (AMT) soundings were acquired across the range with an average distance between soundings of approx. 100 m. Moreover, in order to better determine the regional deeper structure, 10 broadband magnetotelluric (BBMT) soundings were acquired and added to the dataset.

To mesure the strike of the regional structures and the regional impedance tensor, the distortion decomposition method of Groom and Bailey (1989) was applied following the scheme of McNeice and Jones (2001). Figure 5.22 displays the strike directions estimated from the MT impedance tensors at each site for the period band of 10^{-5} – 10 s. The site estimates of strike are weighted by the error misfit to the GB distortion model; misfits with an RMS less than 1.7 are considered reliable, whereas larger misfits are indicative of three-dimensional (3D) effects or of errors that are too small. The best-fit average multi-site, multi-frequency GB regional strike is N45ºE, which is consistent with the strike of the main surface geological structures.

Simultaneous 2D regularized inversions of the TM and TE apparent resistivities and phases were undertaken using the algorithm of Rodi and Mackie (2001). This algorithm simultaneously searches for the model that trades off the lowest overall RMS

misfit with the smallest lateral and vertical conductivity gradients in a regularized manner. On average, the logarithm of the apparent resistivity data fit to within 5%, and the phases to within 1.4º. During the inversions, neither structural features nor conductivity discontinuities were imposed, and the start model was a uniform half space. The final model is shown in figure 5.23.

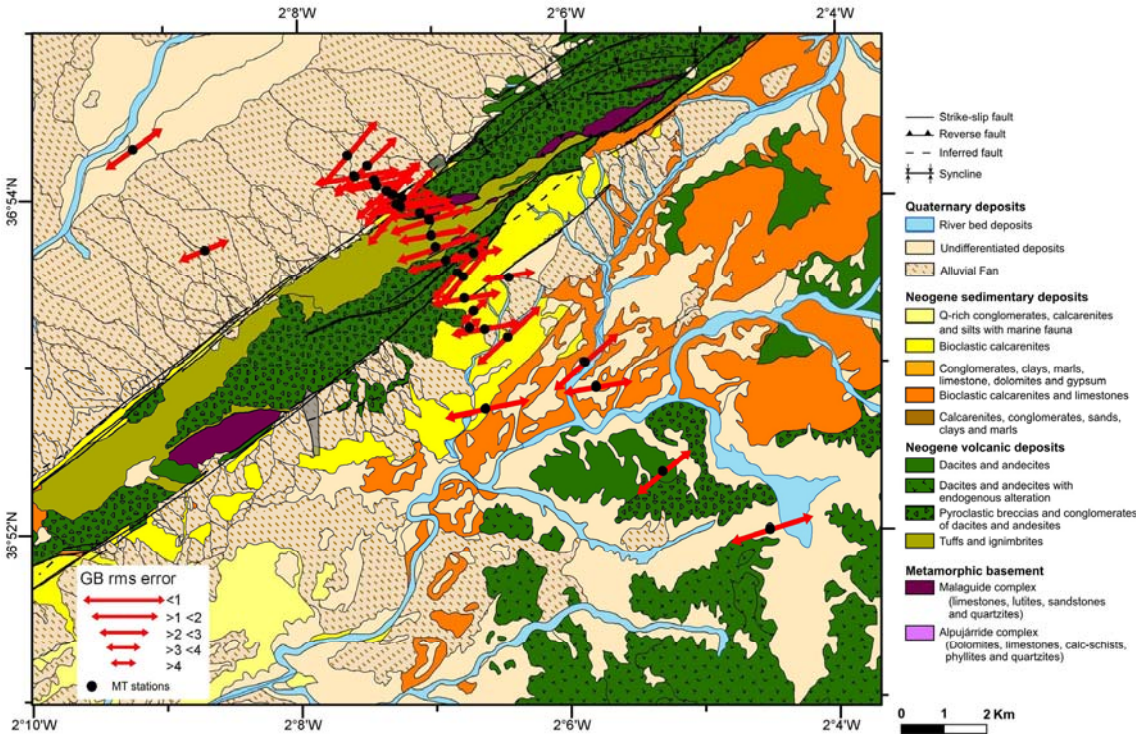

Figure 5.22. Geological map of the area across La Serrata where the MT profile was obtained and location of the MT sites. Red arrows show the strike direction of the regional structures estimated from the MT impedance tensors for the period band of 10^{-5}-10 seconds.

5.5.2. Description and interpretation of the resistivity inversion model

The resistivity inversion model presented in figure 5.23b shows a series of conductors and resistivity zones and two scales of resolution can be defined. The highest resolution covers the upper 500 m below the surface and was achieved by the dense distribution of AMT stations across La Serrata. Below this, the more scattered BBMT stations allow us to extend the model to the NW below the Nijar Basin, to the SE below the Gata Basin and to a greater depth down to 1800 m. However, to the NW of km 2500 and to the SW of km 8500, to lateral resolution is very low and in consequence, these boundaries of the model were not used for the structural interpretation (Fig.5.23a).

The part of the profile with the highest resolution is defined by a few hundred metre wide bodies delimited by sharp vertical conductivity boundaries. This dense distribution of sub-vertical bodies is consistent with field observations represented on

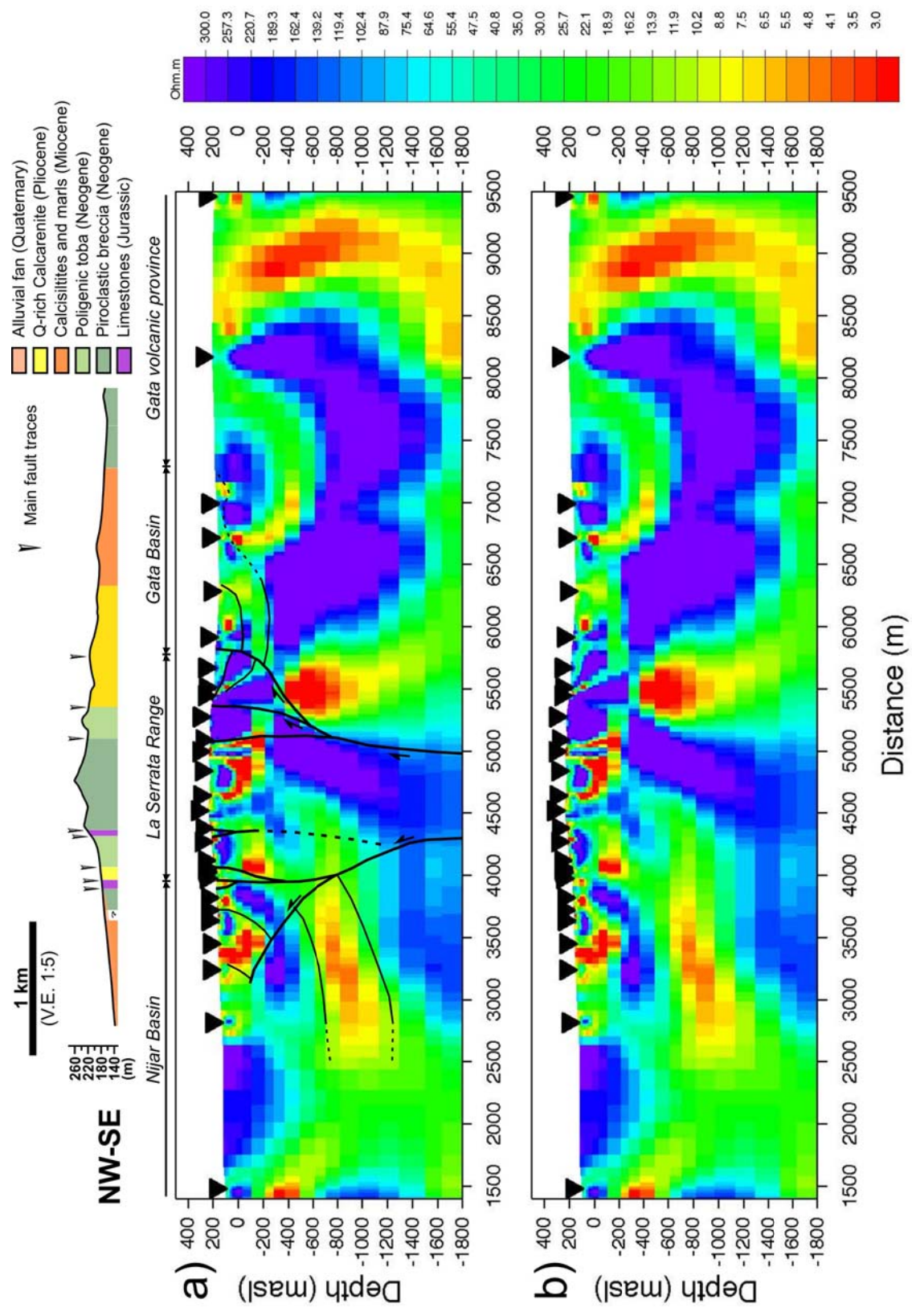
Ohm.m
300.0
257.3
220.7
189.3
162.4
139.2
119.4
102.4
87.9
75.4
64.6
55.4
47.5
40.8
35.0
30.0
25.7
22.1
18.9
16.2
13.9
11.9
10.2
8.8
7.5
6.5
5.5
4.8
4.1
3.5
3.0
Alluvial fan (Quaternary)
Q-rich Calcarenite (Pliocene)
Calcisilitites and marls (Miocene)
Poligenic toba (Neogene)
Piroclastic breccia (Neogene)
Limestones (Jurassic)
Main fault traces
1 km
(V.E. 1:5)
NW-SE
260
220
180
140
(m)
Nijar Basin
La Serrata Range
Gata Basin
Gata volcanic province
a)
b)
Depth (masl)
Distance (m)
400
200
0
-200
-400
-600
-800
-1000
-1200
-1400
-1600
-1800
1500
2000
2500
3000
3500
4000
4500
5000
5500
6000
6500
7000
7500
8000
8500
9000
9500

Figure 5.23. (previous page) 2D Magnetotelluric model and geological interpretation. MT sites (black triangles) are located. The topographic profile shows the lithologies observed on surface.

the geological cross section (topographic profile on top of Fig. 5.23a) where about 100-500 m wide bands of different lithologies are separated by faults.

To the NW of La Serrata, a layered structure with a more resistive layer on top and a more conductive layer at the base is identified as the Miocene to Quaternary infilling of the Níjar Basin, reaching down to 1200 m. These depths are consistent with drillings in the Nijar Basin (Marín-Lechado, 2005) in which the Miocene-volcanic contact was achieved. To the SE of the basin, a highly variable domain with conductive and resistive zones is interpreted as tilted Miocene and Pliocene deposits, whose limits coincide with the field observations, deformed by a blind (inactive?) SE dipping fault.

To the SE, a concave-shaped layered area is limited at their base by highly resistive bodies. The area next to the La Serrata range is identified as the Miocene to Quaternary infilling of the Gata Basin. To the NW, the basin is affected by a sub-vertical fault observed on surface which is inferred to dip to the NW at depth in the MT model.

The main fault traces depicted on the geomorphological map (Fig. 5.22 and 4.2) across La Serrata are correlated with some sharp vertical conductivity boundaries in the MT model and extended at depth following the highest resistivity gradient. Thus, the faults located at each side of La Serrata seem to converge at depth in two main structures, one located at the NW boundary of La Serrata, and one located at the SE boundary. Moreover, these two structures seem to converge at depth narrowing the deformation zone to about 700 m at 1.8 km depth. However, a complete convergence of the structures on a single fault trace is not proved, probably owing to the limited penetration of the model. Despite this, the deformation zone is inferred to display a flower structure, with a narrow fault deformation at depth and divergent fault traces towards the surface.

5.5.3. Discussion and conclusions

Magnetotellurics enables us to characterize the electrical structure of the upper kilometres below La Serrata. The resistitvity inversion model was used to interpret the structure of the fault zone and the adjacent basins. The deformation zone, which is located between the Nijar and Gata basins, coincides on surface with the topography of La Serrata. This deformation zone is 2 km wide with vertical faults in the central part and faults on the sides that converge towards the central part of the deformation zone. At depth, the limits of the fault zone tend to converge with the narrowing of the deformation zone to 700 m (at 1.8 km depth). The model was not deep enough to

confirm a final convergence of the limits of the fault zone. To study deeper parts, a larger broad band would be needed. However, deeper penetration implies a lower resolution (i.e. the MT survey presented by Pedrera et al. (2010)), and this would prevent us from ascertaining whether the deformation converged on a single fault trace or on several traces in a relatively narrow deformation zone. However, the fault traces inferred from the resistivity model presented in this study is interpreted as a flower structure of which evidence on a smaller scale was found at La Serrata (e.g. outcrop along El Hacho gully site, or along the NE-SW pressure ridge on the NW boundary of La Serrata). Thus, it is inferred that at depth, the fault traces converge being a single seismic source.

5.6. Integration of paleoseismic results obtained along the NW boundary of La Serrata

5.6.1. Synthesis of paleoseismic results

The main paleoseismic results obtained at the trenching sites analysed along the NW boundary of La Serrata are listed in table 5.3.

Table 5.3: Synthesis of the main paleoseismic results obtained at the trenching sites analysed along the NW boundary of La Serrata

	El Hacho	**Los Trances**	**Pecho de los Cristos**	**La Pared Alta**
Evidence for seismic events	E1: 130 – 49.9 ka BP E2: 130 – 49.9 ka BP E3: 41.5 – 26.6 ka BP Ea: 32.1 ka BP – AD 934 Eb: AD 775– Present day	L1: 191 - 130 ka BP L2: 191 - 130 ka BP L3: 83 - 59.5 ka BP L4: 71 - 0 ka BP	Evidence of faulting activity between the Mid Pleistocene and AD 1450	Quaternary movements were observed, but the age of events was not constrained
Mean recurrence period	13.8 ka since 41.5 ka BP according to the last 3 events (E3, Ea and Eb)	47.7 ka since 130 ka BP		
Maximum slip per event	1.5 m based on the paleo-channel offset			
Moment magnitude	Min. Mw: 6.4-6.9 based on the thickness of the colluvial wedges			
	Max. Mw: 6.9-7.0 based on the paleochannel offset			

Other results obtained at the trenching site are as follows:

1) The presence of colluvial wedge deposits at El Hacho and Los Trances strongly suggest the seismogenic behaviour of the CFZ.

2) Evidence of Holocene seismic activity in the CFZ was found at El Hacho. This Holocene event, younger than AD 775, may correspond to the historical AD 1522 Almería earthquake.

3) At the Pecho de los Cristos, the undeformed deposits suggest an absence of faulting activity since AD 1450, ruling out the AD 1522 Almería earthquake on the fault trace analysed. However, other fault traces in the area could be considered.

5.6.2. Discussion and conclusions

The paleoseismic analysis carried out by micro-topography, trenching and dating at selected sites along the NW boundary of La Serrata provided numerical paleoseismic results (table 5.3) to the geomorphological observation of faulted Early-to-Late Pleistocene and Holocene deposits described in Chapter 4. Moreover, the presence of colluvial wedge deposits associated with the fault zones analysed in trench walls at El Hacho and Los Trances strongly suggests the seismogenic character of the fault. An increasing degree of deformation of the Quaternary deposits was observed by the

geomorphological study. This was corroborated by further detailed paleoseismic analyses, suggesting that the activity of the CFZ has been constant throughout the Quaternary.

A minimum of 5 events were identified at El Hacho (E1, E2, E3, Ea and Eb) and 4 events at Los Trances (L1, L2, L3 and L4) (Fig. 5.24). Some events at the two sites can be correlated. L1 and L2 at Los Trances are the oldest events and were observed thanks to the 5 m high trench wall. L3 is within the time range of E2 and E1 and thus could represent any of the events observed at El Hacho. Likewise, L4 at Los Trances coincides in time with E3, Ea and Eb at El Hacho, and thus could correspond to any of these events or to the three of them simultaneously.

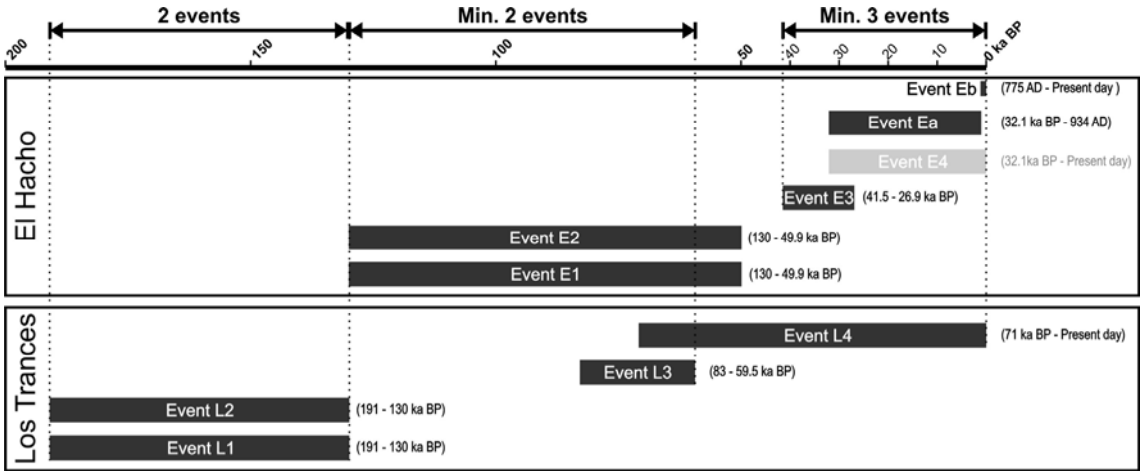

Figure 5.24. Summary of the events defined at El Hacho and Los Trances. The events were correlated between sites. See text for discussion.

In summary, a minimum of 7 events occurred since 191 ka, suggesting a mean recurrence period of 27.3 ka. However, the age of the older events (L1, L2, E1 and E2) is very poorly constrained with the result that the calculated mean recurrence could be overestimated. Considering only the last three events defined at El Hacho (E3, Ea, Eb) since 41.5 ka BP, the mean recurrence period decreases to 13.8 ka, which is a value similar to that of the mean recurrence obtained in the northern Alhama de Murcia Fault (Martínez-Díaz et al., 2001; Masana et al., 2004). Furthermore, geomorphological observations of the last two events (Ea and Eb) suggest a shorter interval of few thousand years between two successive earthquakes, which can be interpreted as a) evidence for a shorter mean recurrence period for the CFZ, or b) evidence of Ea and Eb being a cluster.

According to this data, the longer the period of time observed, the longer the mean recurrence period obtained. This is due to a decrease in resolution when observing older events. A single event horizon can also reflect several seismic events and thus only a minimum number of events are detected. Moreover, the older the events, the

more difficult it is to accurately constrain their ages and a large age uncertainty contributes to enlarge the mean recurrence value. At El Hacho, the two younger events (Ea and Eb) were recorded in a young feature (probably of Late Holocene age), and according to geomorphological interpretation, two events were distinguished. However, with time, as more events occur and the offset increases, these two events will probably not be discernible.

Holocene fluvial terraces were trenched at La Serrata in order to confirm or rule out the most recent fault activity. The terrace trenched at the El Hacho gully did not cover the entire fault zone, and the trench dug at Cerro Blanco did not show a clear fault zone. Thus, neither of the two trenches provided conclusive evidence of Holocene activity. At Pecho de los Cristos the trench exposed the fault zone overlain by the undeformed fluvial terrace. This constrained the last movement of the fault in AD 1450 with the result that it can be deduced that the 1522 Almería earthquake was not produced by this fault trace. Other parallel traces, however, may be considered for this historical earthquake although these traces lack young deposits to support such a young event. The search for recent events at La Serrata becomes restricted to the analysis of very local young sedimentary features that do not usually cover more than one fault trace with the result that information could be overlooked, giving rise to paleoseismic uncertainty.

The youngest event identified at El Hacho, event Eb, occurred after AD 775 and, although it was not possible to numerically constrain its upper age, it could correspond to the AD 1522 Almería earthquake. Moreover, the last event observed at Los Trances, event L4, which coincides in time with Eb, could also lend support to this historical earthquake. However, L4 covers a very long time span (71 ka) and probably reflects several Late Pleistocene and Holocene events.

Dip-slip offsets in a dominantly strike-slip fault that displaces an irregular surface yield large uncertainties. Paleoseismic results based on the horizontal offsets are more reliable (see section 5.2.8). Accordingly, the results obtained from the paleo-channel offset (maximum slip per event of 1.5 m, min. strike-slip rate of 0.05 mm/a for the last 32.1 ka BP, max. strike-slip rate of 1.3 mm/a since 1175 Cal yr BP, and max. Mw 6.9-7.0) are preferred to those obtained from the thickness of the colluvial wedges (dip-slip rates of >0.02 mm/a since 130 ka BP and Mw 6.4->6.9). These slip-rate results are consistent with the slip-rates obtained from the geomorphological analysis (section 4.5.3): a) a minimum left-lateral strike-slip rate of 1.1 mm/a since 130 was obtained from the deflected drainage along La Serrata boundaries, and b) minimum dip-slip rates of 0.05 mm/a since the Early Pleistocene and 0.15 mm/a since 130 ka were obtained from folded and faulted alluvial fans. The poorly constrained strike-slip rate obtained from the offset paleo-channel (0.05-1.3 mm/a) can be enhanced with the results obtained from the deflected drainages at La Serrata, resulting in a left-lateral strike-slip

rate between 1.1 mm/a and 1.3 mm/a (calculated since 130 ka BP and 1175 Cal yr BP, respectively).

The paleoseismic results discussed in this chapter are concerned (Fig. 5.23) with the fault zone bounding La Serrata to the northwest. The interpretation of the MT model across La Serrata shows that the fault traces located on each side of La Serrata converge at depth in a narrower deformation zone. Furthermore, the two structures delimiting the deformation zone under the range are interpreted to converge on a single structure at the seismogenic depth, depicting a flower structure. Thus, the paleoseismic results are considered to be minimum values on the assumption that the recent deformation may be distributed over the entire deformation zone. In order to obtain a more realistic idea of the paleoseismic parameters at La Serrata, all the fault traces should be taken into account and should be analysed from a paleoseismic point of view.